PHOSPHOTYROSINE-MEDIATED SIGNAL TRANSDUCTION PATHWAYS ESSENTIAL FOR RET/PTC-1-INDUCED TUMOR FORMATION

DISSERTATION

Presented in Partial Fulfillment of the Requirements for

the Degree Doctor of Philosophy in the Graduate

School of The Ohio State University

By

Tara Lynne Furminger Buckwalter, B.S.

*****

The Ohio State University

2000

Dissertation Committee:

Professor Sissy M. Jhiang, Adviser

Professor James DeWille

Professor James Lang

Professor George Marzluf

Approved by

_____

Adviser

Ohio State Biochemistry Program

UMI Number: 9994844

UMI

UMI Microform 9994844

Copyright 2001 by Bell & Howell Information and Learning Company.

All rights reserved. This microform edition is protected against unauthorized copying under Title 17, United States Code.

Bell & Howell Information and Learning Company
300 North Zeeb Road
P.O. Box 1346
Ann Arbor, MI 48106-1346

ABSTRACT

The *PTC1* oncogene is a rearranged form of the *RET* proto-oncogene detected in human papillary thyroid carcinomas (PCs). The tumorigenicity of PTC1 in thyroid tumors has been demonstrated in transgenic mice with thyroid-targeted expression of *PTC1* using the bovine thyroglobulin (Tg) promoter. Previous signal transduction studies using cultured cells suggest that the phosphotyrosine residues (pY), pY294, pY404, and pY451, play important roles in PTC1-induced transformation via signaling pathways mediated by signaling molecules Grb10, PLCγ, or Enigma and Shc, respectively. In this study, transgenic mice expressing thyroid-targeted PTC1 mutants, abolishing the signaling pathways mediated by one or three of these three pY, were generated to investigate which signaling pathways are essential for PTC1-induced thyroid tumor formation *in vivo.* Furthermore, other studies have shown PTC1-induced activation of the ras/MAPK pathway. Thus, MAPK activation was evaluated in the thyroid glands of these transgenic mice to investigate whether MAPK activation correlates with tumor formation in these transgenic mice.

Site-directed mutagenesis generated three single mutants of PTC1-Y294F, PTC1-Y404F, or PTC1-Y451F, as well as a triple mutant PTC1-3Y/F carrying

mutations Y294F, Y404F, and Y451F. Transient expression studies in Cos-7 cells showed proper expression of all 4 mutants, but tyrosine phosphorylation of only the 3 single mutants, indicating that the combination of three Y/F mutations disables PTC1 kinase activity.

Transgenic mice lines were established from each of the four Tg-PTC1-Y/F transgenes (Y294F: 6 lines, Y404F: 4 lines, Y451F: 12 lines, 3Y/F: 1 line). Low iodine diet supplemented with propylthiouracil (LID/PTU) was fed to a portion of the mice, to promote thyroid stimulating hormone (TSH)-induced stimulation of the thyroid, leading to increased thyroid size, and potentially accelerated PTC1-induced phenotypes, via TSH stimulation of the transgene promoter, thyroglobulin (Tg). While LID/PTU treated thyroids were larger than their normal diet counterparts, Western blot analysis (WB) indicates no increase in transgene expression while on LID/PTU. This may result from PTC1-induced de-differentiation of the thyroid follicular cells, leading to non-responsiveness to TSH.

Both macroscopic and microscopic analyses of mouse thyroid tissues were performed to evaluate tumor formation. Thyroid glands with normal histology were graded as "1", with distorted follicles as "2", and with tumor formation as "3". Consistent with our previous studies, every Tg-PTC1 transgenic mouse developed thyroid tumors (grade 3, 100%). The non-transgenic (NTG) mice had an average histological grade of 1.1 (normal diet), or 1.2 (LID/PTU diet), with 1.8% of mice

forming tumors. The triple mutant transgenic mice, Tg-PTC1-3 Y/F, had an average histological grade of 1.3 (normal diet), or 1.0 (LID/PTU diet), with 0% tumor formation. Despite intra- and inter-line variations, the three single mutant Tg-PTC1-Y/F transgenic mice groups (Y294F, Y404F, or Y451F) had lower average histological grades on either normal diet (1.4, 1.9, or 1.8), or on LID/PTU diet (1.5, 2.3, or 1.9), and lower total rates of tumor formation (6%, 41%, or 30%) than Tg-PTC1 transgenic mice. LID/PTU diet resulted in slight increases in average histological grades, predominantly contributed to an increase in the percentage of grade 2 tissues. Further, one line from the Y451F mutant group presented more aggressive tumors on LID/PTU than on normal diet, as indicated by a greater amount of spindle cells.

Statistical analysis was performed comparing the thyroid histological grade with age, sex, diet and different types of transgene. The data showed that the type of transgene, diet, and the age of the mice significantly affected histological grades of the thyroid glands. In contrast, the sex of the mouse had no impact upon the histological grade. Comparison of the frequency of tumor formation among the six groups of mice (NTG, Tg-PTC1, Tg-PTC1-Y294F, Tg-PTC1-Y404F, Tg-PTC1-Y451F, and Tg-PTC1-3 Y/F) showed no significant difference between NTG and Tg-PTC1-3 Y/F mice groups, and no significant difference between Tg-PTC1 and Tg-PTC1-Y404F mice. These data indicate the overall essential nature of kinase activity (3Y/F), as well

as the variable contributions of different signaling pathways (pY294 > pY451 > pY404), towards PTC1-induced tumor formation.

While radioiodine-concentrating activity is normally heterogeneous among different follicles in NTG mice, radioiodine-concentrating activity was always severely decreased in regions of the thyroid containing either distorted follicles or tumors in transgenic mice carrying PTC1 or a PTC1Y/F mutant. Reduced radioiodine-concentrating activity and distorted follicles detected in the thyroid glands of Tg-PTC1 transgenic embryo thyroids as early as embryological day 16 (Cho, 1999) suggest that PTC1-induced signaling pathways may have direct effects on reduced radioiodine-concentrating activity and distorted follicles preceding tumor formation. However, this study showed that abolishing signaling pathways mediated by pY294, pY404, or pY451 alone, does not abolish the PTC1-induced signaling pathways leading to reduced radioiodine- concentrating activity and distorted follicles.

To investigate whether the histological grades of transgenic mice thyroid glands correlate with the expression levels of transgene and/or the extent of MAPK activation, Western blot analysis was performed comparing transgene expression, MAPK, pMAPK, and tubulin within mouse thyroids. For Tg-PTC1-Y294F transgenic mice, the histological grade appears to correlate with pMAPK and MAPK (predominantly), but not with the expression levels of the transgene. For Tg-PTC1-Y404F transgenic mice, tumor formation appears to correlate with the expression

levels of transgene and the extent of MAPK activation, as indicated by increased pMAPK but not MAPK. For Tg-PTC1-Y451F transgenic mice, histological grades do not appear to correlate with the levels of transgene expression, pMAPK, MAPK, or tubulin. Taken together, the expression levels of transgene and the extent of MAPK activation can not serve as general indicators for thyroid tumor formation in these transgenic mice.

In conclusion, this study has shown a decrease in the rate of tumor formation in mice expressing thyroid-targeted expression of the Tg-PTC1-Y(294, 404, or 451)F transgene, compared to the Tg-PTC1 transgene. The lack of tumor formation in the triple mutant is most likely due to the kinase inactive status of PTC1-3Y/F, as determined by transient expression studies in Cos-7 cells. The decrease of tumor formation in the single mutant PTC1 Y/F transgenic groups indicates that signaling pathways mediated by pY294 (Grb10), pY404 (PLCγ), and pY451 (Enigma and Shc) do play a role in PTC1-induced tumor formation in the thyroid. Among these signaling pathways, the one mediated by pY404 (PLCγ) perhaps plays the least important role, and the one mediated by pY294 (Grb10) appears to have the most significant impact on PTC-1 induced tumor formation. However, as tumors are still able to form in some mice of these three single mutant transgenic lines, it indicates that none of the signaling pathways mediated by pY294, pY404, or pY451, are solely essential for PTC1-induced tumor formation. It is most likely that multiple PTC1 phosphotyrosine residues and multiple signaling pathways, respectively, mediate

PTC1-induced tumor formation *in vivo*. Further, the intra-line and inter-line variations in the observed histological spectrum suggest that additional factors are needed to cooperate with the signaling pathways induced by the single PTC1 Y/F mutants to form thyroid tumors. Finally, the lack of correlation between histological grades and the expression levels of transgene or the extent of MAPK activation, suggest that while both transgene expression and MAPK activation may play roles in inducing tumor formation, they are not required to maintain tumor formation in the thyroid gland.

Dedicated to Harry C. Furminger, in loving memory

ACKNOWLEDGMENTS

Firstly, I would like to thank my adviser, Dr. Sissy M. Jhiang. I appreciate the opportunity to work in her lab, learning about the mechanisms of thyroid disease, cancer and molecular biology. I would also like to thank my dissertation committee, Dr. Ross Dalbey, Dr. James Lang, Dr. George Marzluf, and Dr. James DeWille for their advice and support towards the completion of this project.

I would like to acknowledge the assistance of those who contributed to this work. Following the production of the original Tg-PTC1 transgene by Dr. Qiang Tong, *in vivo* characterization studies were performed by Drs. Qiang Tong, John Sagartz and Je-Yoel Cho. Dr. Shunhua Xing performed expression and tyrosine phosphorylation studies of the PTC1-Y/F single mutants in Cos-7 cells. Both Dr. Jan Parker-Thornberg and Dr. Michael Robinson produced Tg-PTC1-Y/F founder mice for this project. Animal care was provided by the Ohio State University animal vivariums at Rightmire Hall, Wiseman Hall, Biological Sciences Building and Postle Hall. Dr. Charles Capen and his graduate student, Dr. Krista La Perle, helped in histological evaluation of mouse thyroid tissue sections. Dr. Stacy Hoshaw-Woodard

of the Biostatistics Program was instrumental in statistical analysis. Further, this work was supported by a grant to Dr. Sissy Jhiang, from the National Institutes of Health.

I would like to acknowledge the former and current members of the Jhiang lab: Dr. Patricia Smanik, Dr. Qiang Tong, Dr. Shunhua Xing, Dr. Je-Yoel Cho, Kwon-Yul Ryu, Dr. Krista La Perle, Dr. Daniel Shen, Ruey Kao, Anjli Venkateswaran, Xiaoqin Lin, Linda Fithian, Don McHugh, Marc Lavender, and Danielle Westfall. I am grateful to those who taught me molecular biology techniques and strategy, as well as patience in research. Further, I am thankful for the opportunity to teach others that which I have learned.

Lastly, I would like to thank my family, for their support. I am particularly grateful for the support provided by my loving husband, Damon Buckwalter. When confronted with hard times, his strength and compassion provided for me when my own driving force faltered.

VITA

1992	B.S. Biochemistry, The State University of New York at Geneseo
1993 - present	Graduate Research Associate, The Ohio State University
1995	Ph.D. candidate

PUBLICATIONS

1. Smanik, P.A., Furminger, T.L., Mazzaferri, E.L., and Jhiang, S.M. (1995). Breakpoint characterization of the RET/PTC1 oncogene in human papillary thyroid carcinoma. *Human Molecular Genetics* 4 (12): 2313-2318.

2. Smanik, P.A., Liu, Q., Furminger, T.L., Ryu, K., Xing, S., Mazzaferri, E.L., and Jhiang, S.M. (1996). Cloning of the Human Sodium Iodide Symporter. *Biochemical and Biophysical Research Communications* 226: 339-345.

3. Xing, S., Furminger, T.L., Tong, Q., and Jhiang, S.M. (1998). Signal transduction pathways activated by RET oncoproteins in PC12 pheochromocytoma cells. *Journal of Biological Chemistry* 273 (9): 4904-4914.

4. Jhiang, S.M., Cho, J.-Y., Furminger, T.L., Sagartz, J.E., Tong, Q., Capen, C.C., and Mazzaferri, E.L. (1998). Thyroid carcinomas in RET/PTC transgenic mice. *Recent Results in Cancer Research* 154: 265-270.

5. Cho, J.-Y., Xing, S., Liu, X., Buckwalter, T.L.F., Hwa, L., Sferra, T.J., Chui, I.-M., and Jhiang, S.M. (2000). Expression and Activity of Human Na+/I- Symporter in Human Glioma Cells by Adenovirus-mediated Gene Delivery. *Gene Therapy* 7:740-749.

FIELDS OF STUDY

Major Field: Biochemistry

TABLE OF CONTENTS

Page

LIST OF TABLES

LIST OF FIGURES

Page

LIST OF ABBREVIATIONS

Ab	antibody
AC	anaplastic carcinoma
bp	base pair
cAMP	cyclic adenosine monophosphate
CC	coiled-coil dimerization domain
cDNA	complementary deoxyribonucleic acid
CMV	cytomegalovirus
DNA	deoxyribonucleic acid
E	PTC1-Y451F mutation; site of Enigma & Shc binding
EC	extracellular domain
EGF	epidermal growth factor
EGFR	epidermal growth factor receptor
F	phenylalanine amino acid residue
FC	follicular carcinoma
G	PTC1-Y294F mutation; site of Grb10/7 binding
gDNA	genomic deoxyribonucleic acid

GDNF	glial cell line derived neurotrophic factor
GPE	PTC1-Y(294, 404, & 451)F mutation; binding sites for Grb10/7, PLCγ, Enigma and Shc
H & E	hematoxylin and eosin
HER/RET	human epidermal growth factor receptor – RET
IC	intracellular domain
Kb	kilobase pair
KDa	kilodaltons
LBD	ligand binding domain
LID/PTU	low iodine diet supplemented with propylthiouracil
MAPK	mitogen-activated protein kinase
MEN2	multiple endocrine neoplasia type 2
mRNA	messenger ribonucleic acid
MTC	medullary thyroid carcinoma
MW	molecular weight
NIS	sodium iodide symporter
nt	nucleotide
NTG	non-transgenic
P	PTC1-Y404F mutation; PLCγ binding site
PI3K	phosphatidyl inositol 3 kinase
PLCγ	phospholipase C gamma
PC	papillary thyroid carcinoma

PTC1-3Y/F	PTC1-Y(294, 404 & 451)F
RIA	radioiodide accumulation
RTK	receptor type tyrosine kinase
RT-PCR	reverse transcription – polymerase chain reaction
SP	signal peptide
T3	triiododthyronine
T4	thyroxine
Tg	thyroglobulin
TG	transgenic
TK	tyrosine kinase domain
TM	transmembrane domain
TPO	thyroid peroxidase
TSH	thyroid stimulating hormone
WB	western blot
Y	tyrosine amino acid residue

CHAPTER 1

INTRODUCTION

The normal thyroid gland

The function of the thyroid gland is two fold: production of thyroid hormone and calcitonin. In order to complete these tasks, the thyroid is comprised of two types of cells: follicular cells and C-cells. Thyroid hormone produced by the follicular cells is necessary for proper development and maintenance of metabolism. Calcitonin, on the other hand, is produced by the C-cells (calcitonin-secreting cells), and plays a role in proper calcium homeostasis within the body (Fox, 1990).

Follicular cells make up the majority (95-98%) of the thyroid gland, and are organized into spherical structures known as follicles. Thyroid hormone biosynthesis in follicular cells is a multi-step process (Fig. 1.1). In order for follicular cells to produce this hormone, expression of several important proteins is required. The sodium iodide symporter (NIS) is expressed on the basolateral membrane of follicular cells, enabling uptake of iodine from the blood, while the pendrin transporter enables

iodine transport across the apical membrane. Further, thyroglobulin (Tg) iodination and coupling by thyroid peroxidase (TPO) at the apical membrane of follicular cells results in the production of thyroid hormone precursor, which is then stored in the lumen of the follicle and referred to as colloid. When the organism requires more thyroid hormone, colloid is endocytosed into the cell and hydrolyzed in lysosomes. The resulting products, thyroid hormones thyroxine (T4) and triiodothyronine (T3), are then released into the blood stream for systemic circulation (Taurog, 1991).

The body has a natural feed-back mechanism in place to ensure the proper amount of thyroid hormone synthesis. The hypothalamic-pituitary-thyroid axis is stimulated in the event of abnormally low levels of thyroid hormone (Fig. 1.2). The hypothalamus releases thyrotropin releasing hormone (TRH) which induces the pituitary to produce more thyroid stimulating hormone, TSH. TSH binding to the TSH receptor (TSHR), on the surface of the thyroid follicular cell, stimulates increased expression of NIS, Tg and TPO, all as a means of increasing output of T4 and T3 (Kohn, 1995; Ajjan, 1998). In the event that normal thyroid hormone levels are reestablished, excess amounts of thyroid hormones are able to inhibit the further release of TSH from the pituitary (Johnson, 1999).

Thyroid neoplasias

Thyroid cancer accounts for approximately 1.1% of the cancer diagnosed in the U.S., with 55 new cases per million people diagnosed with thyroid cancer annually

(Parker, 1996; Ries, 1999). There are several forms of thyroid cancer (Fig. 1.3). Neoplasias of the thyroid follicular cells include follicular (FC), papillary (PC) and anaplastic (AC) carcinomas. Among FC, PC and AC, AC is the least likely to occur (2-10% of all thyroid tumors). However, it is the most aggressive of the three follicular neoplasias, with thyroid follicular cell dedifferentiation (and subsequent loss of iodide uptake in the thyroid), high metastatic potential, and a much shorter time course of tumor formation leading to death. In contrast, FC and PC are both slow growing, well-differentiated tumors. PC is the most common form of thyroid cancer, with a rate of approximately 60-85%. FC is the second most common form (5-20%), seen at a higher rate in countries where dietary iodide is insufficient (Gleich, 1999).

Neoplasias of the thyroid C-cells include medullary thyroid carcinomas (MTC) seen in either sporadic or inherited forms, such as multiple endocrine neoplasia type 2 (MEN2A or MEN2B). Medullary tumors occur at a fairly low rate (3-10%) among thyroid tumors (Gleich, 1999) (Fig. 1.3).

Papillary thyroid carcinoma

Clinical overview

The majority of papillary thyroid carcinoma diagnoses occur within the third or fourth decade of life, with a 10-year survival rate of 80-90%. Further, it appears that women are two to three times more likely to be affected than men (Mazzaferri, 1991; Gleich, 1999; Wartofsky, 2000).

Clinical symptoms

PC patients present with clinical symptoms such as palpable hard neck masses, neck tenderness, vocal hoarseness and frequently, reduced iodide uptake in the thyroid gland. Upon surgical removal, the neck mass is frequently observed as a solid tumor, although cystic regions can be present. Further, the mass can be either a single nodule or multi-nodular, and is usually of irregular size (Daniels, 1991; Wartofsky, 2000).

Histology

Histological analysis of PC tumor tissue shows distortion of the normally round follicle structure. Instead, the follicles are collapsed and the follicular cells line up in a ribbon-like fashion, separated from adjacent rows of cells by fibrous stroma. Colloid amounts and iodide accumulation in PC thyroids are usually reduced compared to a normal thyroid. Common PC features include multifocal tumors, variable amounts of fibrosis surrounding the tumor, and unique nuclear features, such as nuclear grooves, cytoplasmic pseudo-inclusions and nuclear "ground glass" appearance (Gleich, 1999).

Genetic rearrangements

Development of some PC's has been associated with chromosomal rearrangement between a gene encoding for a receptor type tyrosine kinase (RTK) and another gene, usually ubiquitously expressed and containing an N-terminal dimerization domain. The breakpoint in the RTK occurs between the transmembrane

(TM) and tyrosine kinase (TK) domains. The resulting chimeric protein contains a foreign N-terminal dimerization domain fused to the TK domain. The resulting chimera's TK activity is now subject to regulation of expression, localization and enzymatic activity as dictated by the 5' sequence of the ubiquitously expressed gene. Chromosomal rearrangements of *RET* and *TRK* have been found in PC (Pierotti, 1998). *RET* rearrangements have been found in approximately 0-59% of adult PC's, 30-71% of childhood PC's, and 38-87% of post-Chernobyl childhood PC's (reviewed in Pacini, 2000).

The RET proto-oncogene

Identification and molecular characterization

The *RET* proto-oncogene was first reported in 1985. Following transfection of human T cell lymphoma gDNA into NIH3T3 cells, the cells became transformed, exhibiting increased focus formation in cell culture and tumor formation in nude mice, compared to parental cells (Takahashi, 1985). Genomic DNA analysis showed that the transformants contained a recombinant DNA not seen in either the parental NIH3T3 or human T cell lymphoma gDNA. This rearrangement resulted in the fusion of two novel genes: *RET* and *rfp* (Fig.1.4). The names *RET* and *rfp* referred to "rearranged during transfection" and "RET finger protein", respectively. Further transfection assays identified two other *RET* rearrangements: RET II upon rearrangement with *rfg* ("*ret* fusion gene") following transfection with human sigmoid

colon carcinoma gDNA (Ishizaka, 1989), and RET III upon rearrangement with *urf* upon transfection with human stomach carcinoma gDNA (Kunieda, 1991) (Fig. 1.4).

Upon cloning of the entire *RET* gene, sequence homology analysis revealed it to be a member of the receptor tyrosine kinase (RTK) family (Takahashi, 1987). The gene, found on chromosome 10q11.2 in an approximately 55 kilobase (Kb) sequence, encodes a single open reading frame spanning 20 exons (Ishizaka, 1989; Sozzi, 1991; Ceccherini, 1993; Pasini, 1995). The last exon, number 21, does not contain any coding sequence (Kwok, 1993). The resulting RET protein contains three general regions: an extracellular domain (EC), a single transmembrane domain (TM) and an intracellular domain (IC) (Takahashi, 1988). The EC domain has a signal peptide (SP) sequence, a cadherin-like sequence, calcium binding sites, a cysteine-rich ligand binding domain (LBD), and several potential N-linked glycosylation sites. The IC is primarily composed of a tyrosine kinase (TK) domain. This TK sequence shows 40 – 50% homology to other RTKs, with a conserved adenosine triphosphate (ATP) binding sequence (Takahashi, 1987). Interestingly, the tyrosine kinase domain was shown to have a 27 amino acid insertion, separating the TK domain into two parts.

The presence of multiple sizes of *RET* mRNA, 3.9, 4.5, 4.6, 6.0 and 7.0 Kilobases (Kb), indicates alternative splicing of the *RET* gene. (Takahashi, 1988; Ikeda, 1990; Tahira, 1990; Lorenzo, 1995). Three different isoforms of RET proteins have been identified, p9, p43 and p51, differing only in the sequence following a c-

terminal splice site (Takahashi, 1988; Ishizaka, 1989; Tahira, 1990; Myers, 1995; Ishiguro, 1999). RET (p9) has a 9 amino acid c-terminal sequence following the splice site, and a total of 1072 amino acids. RET (p43), with a unique sequence of 43 amino acids following the c-terminal splice site, has a total of 1106 amino acids. Lastly, RET (p51) has a unique 51 amino acid c-terminal sequence, and a total of 1114 amino acids.

All three RET protein isoforms are subject to glycosylation during post-translational modification, resulting in an apparent molecular weight (MW) of one of two approximate sizes: 140-155 kilodaltons (KDa) (immature, intracellular form), or 160-190 KDa (mature form found at plasma membrane) (Takahashi, 1991). The exact MW varies, depending on cell type-specific glycosylation patterns. For example, in the mouse neuroblastoma cell line, Neura-2, RET has MWs of 140/160 KDa, versus 150/190 KDa in leukemia cells, opposed to 150-155/170-175 KDa seen in most other cell types (Takahashi, 1991; Iwamoto, 1993; Miyazaki, 1993).

RET Ligands

The ligands for RET have been identified as members of the glial cell line-derived neurotrophic factor (GDNF) family: GDNF, neurturin (NTN), Persephin (PSP) and Artemin (ART) (reviewed in Rosenthal, 1999) (Fig. 1.7). The ligands bind to RET via one of four glycosyl-phosphatidyl inositol-linked co-receptors, GFRα (1-4). GDNF was first identified as a potent survival factor for motor neurons in cell

culture, when researchers were searching for a potential therapeutic agent for Parkinson's Disease (reviewed in Robertson, 1997). Interestingly, knock-out mice studies looking at the developmental role of RET, GDNF and GFRα1 show similar phenotypes, confirming the cell culture interaction studies (reviewed in Airaksinen, 1999).

Developmental expression

The function of the RET protein has been shown to be essential for proper development of the kidney and parts of the nervous system. *RET* expression studies showed that it was expressed at a higher rate in developing rat embryos than in adult rats, supporting the role of RET in development (Tsuzuki, 1995). Further, when proper *RET* expression is prevented in RET knock-out mice, the result is kidney agenesis, improper development of the enteric and sympathetic nervous systems, and mortality shortly after birth (Schuchardt, 1994). In addition, studies looking at RET expression, either at the RNA or protein level, indicate that RET is normally expressed during development in tissues of the neural or excretory systems in zebrafish, drosophila, mice, rats, chickens, and humans (Pachnis, 1993; Avantaggiato, 1994; Sugaya, 1994; Tsuzuki, 1995; Schuchardt, 1995; Marcos-Gutierrez, 1997; Widenfalk, 1999). Lastly, mutations knocking out the TK enzymatic activity of the *RET* gene product have been found in Hirschsprung's disease (HD), associated with insufficient development of the enteric nervous system (ENS) of the colon and subsequent aganglionic megacolon in these patients (Romeo, 1994; Edery, 1994).

RET mutations in human disease

Point mutations

RET mutations have been associated with several forms of human disease underlying either a developmental defect or cancer. Point mutations in *RET* can have either a loss-of-function effect, as in Hirschsprung disease (HD), or a gain-of-function effect, as in sporadic medullary thyroid carcinoma (MTC), familial medullary thyroid carcinoma (FMTC), or multiple endocrine neoplasia types 2A or 2B (MEN2A or MEN2B).

HD mutations have been found in locations spanning the entire *RET* sequence. The result of these RET mutations is usually either tyrosine kinase inactivation or a failure to transport the mutant protein to the cell surface, thus causing an overall loss-of-function in cell culture studies. In contrast, *RET* mutations found in sporadic MTC, FMTC, MEN2A or MEN2B lead to constitutive tyrosine kinase (TK) activity of the RET oncoprotein. While both sporadic MTC and FMTC consist of only the development of medullary thyroid carcinoma, MEN2A and MEN2B present with MTC, as well as additional clinical phenotypes. MEN2A patients present with MTC, in conjunction with pheochromocytoma and/ or hyperparathyroidism. In contrast, the disease spectrum for MEN2B patients includes MTC, pheochromocytoma, mucosal neuromas, ganglioneuromas, and/or skeletal abnormalities (marfanoid habitus).

The majority of *RET* mutations in MEN2A have been found in the cysteine-rich extracellular domain (EC), at cysteine residues 609, 611, 618, 620, and 634 (Eng, 1996) (Fig. 1.6). In contrast, the majority of MEN2B mutations occur within the intracellular domain (IC), resulting in either the M918T mutation, or less frequently, the A883F mutation (Hofstra, 1994; Smith, 1997). Interestingly, mutations leading to the development of FMTC or sporadic MTC have been found in either the EC at residues 609, 611, 618, 620, 630, or 634, or in the IC at residues 766, 768, 804, 883, 891, 918, or 919 (Uchino, 2000).

Chromosomal rearrangements

As the first studies of the *RET* gene suggest, the gene is frequently involved in chromosomal rearrangements. This event appears to be common among RTKs, as it has been documented to also occur in others such as EGFR, MET, and TRK (Downward, 1984; Park, 1986; Martin-Zanca, 1986).

The oncogenes resulting from *RET* rearrangements found exclusively in human PCs are referred to as *PTC* oncogenes (papillary thyroid carcinoma). To date, eight different *PTC* oncogenes have been identified, *PTC* (1-7) and *ELKS-RET*. The eight different oncogenic versions refer to the N-terminal donor genes, with which *RET* rearranges to form a novel *PTC* chimeric oncogene (Fig. 1.5). Each of the resulting PTC fusion products contain an N-terminal dimerization domain (coiled-coil domain or cysteine residues for di-sulfide bonding), fused to the RET TK domain.

PTC1 involves the fusion of the *RET* C-terminus to the N-terminus of another gene called *H4*, or D10S170, found on chromosome 10q21 (Fusco, 1987; Donghi, 1989; Bongarzone, 1989; Grieco, 1990; Pierotti, 1992). *PTC2* results from fusion of *RET* to the regulatory subunit *R1α* of cyclic adenosine monophosphate-dependent protein kinase A, found on chromosome 17 (Bongarzone, 1993; Sozzi, 1994). Both *PTC3 r(1,2 or 3)* and *PTC4* are created following chromosomal rearrangements between *RET* and *Ele1* (Jhiang, 1994b; Minoletti, 1994; Santoro, 1994a; Klugbauer, 1996; Klugbauer, 1998a; Fugazzola, 1996). Like *RET* and *H4*, *Ele1* was shown to be located on chromosome 10 (Bongarzone, 1994; Minoletti, 1994). *PTC5* is a recombination between *RET* and *rfg*, the same two genes involved in the creation of *ret* II *in vitro* (Klugbauer, 1998b). Chromosomal localization for *rfg* has yet to be reported. *PTC6* involves a fusion between *RET* and the transcription coactivator *htifI*, while *PTC7* involves a fusion between *RET* and another protein with homology to *htifI*, named *rfg7* (Klugbauer, 1999). Lastly, *ELKS-RET* consists of a fusion between *RET* and a novel gene called *ELKS*, named as such due to the high concentration of glutamic acid, leucine, lysine and serine (Nakata, 1999).

For PC patients with no previous radiation exposure, *PTC1* is the most frequent form of *PTC*. However, areas of the world affected by radiation, such as eastern Europe following the Chernobyl nuclear reactor explosion, show a greater frequency of *PTC3* in childhood PC than any other form of *PTC* (Fugazzola, 1995; Klugbauer, 1995; Nikiforov, 1997).

RET/PTC1*: oncogenicity*

Transforming activity in cell culture

Once *PTC1* was correlated with the existence of human PC, investigators began exploring the biochemical nature and oncogenic potential of the fusion gene. *PTC1* is a fusion gene comprised of the *H4* N-terminal coding sequence, containing a coiled-coil motif, fused to the C-terminal coding sequence of *RET*, containing a TK domain. The resulting protein is 520 amino acids and has a MW of 64 KDa (p51), or 477 amino acids and has a MW of 57 KDa (p9) (Fusco, 1987; Bongarzone, 1989; Grieco, 1990; Ishizaka, 1990; Pierotti, 1992; Ishizaka, 1992). In transfection assays in cell culture this fusion protein has been shown to be located in the cytoplasm, able to form homodimers, constitutively tyrosine phosphorylated, and able to induce a transformed phenotype in cells expressing the oncogene (Ishizaka, 1992; Lanzi, 1992; Santoro, 1993; Tong, 1995; Tong, 1997).

Transgenic mice models

Several transgenic mouse models expressing *PTC1*, under the control of one of several different promoters, have been reported with varying results. Jhiang et al (1996) reported 100% thyroid tumor formation among three different lines of transgenic mice expressing the *PTC1* oncogene under the control of the bovine thyroglobulin (Tg) promoter. However, Santoro (1996) reported that expression of the same *PTC1* cDNA, under the control of the rat Tg promoter, resulted in 20-30%

penetrance for thyroid tumors among the three lines investigated. The difference in penetrance of the tumors may be due to the species difference in Tg promoter activity.

Promoters seem to play quite an important role in transgene expression, as seen in a study by Portella et al (1996). In the Portella study, expression of the PTC1 transgene under the control of the physiologically relevant H4 promoter did not result in thyroid tumors. However, incomplete penetrance for development of mammary and skin tumors was observed. Interestingly, neither mammary nor skin tissue is involved in naturally occurring PC's. This is due, in part, to the somatic nature of the chromosomal rearrangements leading to the creation of *PTC*, occurring only in the thyroids of patients with PC. Further, the absence of thyroid tumor formation in H4-PTC1 transgenic mice may be due to the H4 promoter DNA fragment used to drive PTC1 expression. It may not contain all the necessary sequences or chromosomal structure necessary to drive PTC1 expression in thyroid glands.

RET *signal transduction studies*

Signal transduction studies: cell culture vs. animal models

Normal and oncogenic RET signal transduction pathways have been of keen interest to many investigators in recent years. Towards this aim, many different groups have worked on elucidating the signal transduction pathways *in vitro*, or in a wide variety of cell cultures. While the animal model system allows for a more physiologically relevant environment, the value of the cell culture or test tube

environment lies in the ease of manipulation and control of interference from unknown sources.

While cell culture studies are flexible, the limitation of choice of cell line exists. To date, studies looking at RET signaling have used NIH3T3 mouse fibroblasts, Cos-7 monkey kidney epithelium, 293 human embryonic kidney cells, PC12 rat pheochromocytoma cells, Hela human ovarian carcinoma cells, or one of many different neuroblastoma cell lines (NB). It is interesting to note that normally *RET* is only expressed in cells of neuroendocrine origin. In such a case, the only cell lines of physiological relevance are PC12 and NB. The benefit of using physiologically relevant cell lines is the assumption that all the cellular machinery necessary for signal transduction is available. However, it is unclear what impact upon RET signal transduction studies will exist when working with immortalized cell lines derived from tumors. Furthermore, *PTC* is expressed in tissue that doesn't normally express *RET*, thyroid follicular epithelial cells. In this case, Cos-7 cells are the closest match, also being epithelial cells. However, Cos-7 cells are known to be infected with the SV40 T antigen, and thus, are not quite the same background (Gluzman, 1981). Along these same lines, it is well established that immortalized cell lines do not necessarily reflect the same properties of cells *in vivo*. Despite all of these potential limitations, some key pieces of information regarding RET signal transduction have begun to emerge.

Receptor tyrosine kinase activation: overview

As RET is a member of the receptor tyrosine kinase family (RTK), it is believed to act like other RTK's upon ligand-induced activation and signaling. It is commonly held that RTK activation commences upon ligand binding to the extracellular (EC) receptor (reviewed in Schlessinger, 1992). Ligand binding induces a conformational change leading to homodimerization of RTKs. The net effect of protein conformational changes and dimerization is the activation of TK domains and phosphorylation of tyrosine residues within and outside of the TK domain. Phosphorylated tyrosine residues then act as docking sites for intracellular (IC) proteins containing Src homology 2 (SH2) domains. The docked proteins then become tyrosine phosphorylated, and can then act as docking sites for other SH2 containing molecules, or as adaptor molecules to link the RTK to IC protein substrates lacking SH2 domains, via other protein interaction domains such as Src homology 3 domains (SH3). The phosphorylation of IC substrates begins the signal transduction cascade(s), where phosphorylation appears to modulate activity of several downstream effectors in the relay of the EC signal from the plasma membrane to the cell nucleus.

RET variants: overview

In the past decade, RET's signaling pathways have been studied in cell culture. Prior to identification of the RET ligands, it was necessary to use activated forms of RET to study signaling. This was accomplished using either artificial fusion gene constructs, such as *HER/RET*, or constitutively active forms of RET found in human

cancer syndromes, such as *RET/MEN2A*, *RET/MEN2B*, or the *RET/PTC* oncogenes, as the enzymatic domains are identical between wild type (WT) RET and RET/PTC's. However, with the identification of the RET ligands, WT RET proto-oncoprotein signaling pathways in cell culture are beginning to be reported.

HER/RET

The *HER/RET* construct is the result of the fusion of the EC and TM domains of the RTK human epidermal growth factor receptor (EGFR) to the IC domain of RET, containing the TK domain. It enabled inducible activation of RET TK, with the addition of epidermal growth factor (EGF) to the cell culture media. Comparing biological properties and biochemical behavior of cells expressing activated HER/RET versus EGFR, lead investigators to suggest a RET specific signaling pathway (Santoro, 1994b). Early response to HER/RET activation was shown to correspond with mitogen-activated protein kinase (MAPK) pathway activation, as seen by Shc phosphorylation, complex formation between MAPK signaling molecules (Shc, Grb2 and Sos), p21ras activation and sustained ERK2 activation in SK-N-MC neuroblastoma cells (van Weering, 1995). Longer periods of HER/RET activation in SK-N-MC cells lead to sustained ERK2 activation, and subsequently, a differentiated cellular response consisting of cell scattering, growth inhibition and loss of anchorage independent growth (van Puijenbroek, 1997).

RET/MEN2A or RET/MEN2B

Expression of either RET/MEN2A or RET/MEN2B oncoprotein leads to a transformed phenotype in cell culture, to tumor formation in nude mice, and to hyperplasia in transgenic mice (Santoro, 1995; Xing, 1996; Michiels, 1997; Sweetser, 1999; Smith-Hicks, 2000). The RET/MEN2A mutation results in the loss of one cysteine residue in the ligand binding domain (LBD), a cysteine that would normally form an intramolecular disulfide bond (Mulligan, 1993). However, this loss leaves the RET/MEN2A monomer with one free cysteine, which is now able to form an intermolecular disulfide bond with another RET/MEN2A monomer (Fig. 1.8). Such dimerization in the absence of ligand, is sufficient to induce the TK activation and autophosphorylation (Santoro, 1995). On the other hand, MEN2B mutants do not require dimerization to be activated. In contrast, a mutation in the TK domain causes constitutive activation and a change in substrate specificity (Songyang, 1995; Santoro, 1995) (Fig. 1.8).

As there are two groups of clinical symptoms, genetic mutations, and mechanisms of activation, it appears that there may also be some signaling differences between these two RET mutants. Both RET/MEN2A and RET/MEN2B have been associated with activation of the MAPK, PI3K, and JNK pathways, as well as Src activation (Lorenzo, 1997; Arighi, 1997; Asai, 1996). However, RET/MEN2A has been shown to have a higher autokinase activity than RET/MEN2B (Marshall, 1997). Interestingly, a study analyzing autophosphorylation patterns showed that WT RET

and RET/MEN2A had six out of six identical autophosphorylation sites (Liu, 1996). In contrast, RET/MEN2B had only five of these same six sites autophosphorylated. Further, as a part of the RET/MEN2B mutation process, one autophosphorylation site was destroyed while another was created (Liu, 1996). This may have some impact on the change in substrate specificity seen in RET/MEN2B.

Site-directed mutagenesis assays looking at the role of each tyrosine residue within the TK domain of MEN2A and MEN2B also showed some mutation-specific selectivity. Phosphotyrosine (pY) residue pY905 was shown to be critical for MEN2A transforming activity. In contrast, MEN2B's oncogenic behavior required residues pY864 and pY952 (Iwashita, 1996). In these assays the tyrosine is selectively mutated to a phenylalanine (F), identical in structure to tyrosine except for the lack of a hydroxyl group which is necessary to undergo phosphorylation. Thus the mutant protein is unable to be phosphorylated at the site of the Y/F mutation. Should this Y residue be crucial for signal transduction and subsequent activation of a particular biological function, the Y/F mutant should not display this biological function.

While both 2A and 2B have been shown to activate the ras/MAPK, the PI3K and the JNK-1 pathways, as well as c-Src activity, it appears there are detectable differences in the 2A- or 2B-mediated activation. In NIH3T3 and NB cells, both mutants have been shown to activate the ras/MAPK pathway by inducing complex formation between RET, Shc and Grb2, at RET pY1062 (Asai, 1996; Arighi, 1997;

Lorenzo, 1997; Ohiwa, 1997; Alberti, 1998; Ishiguro, 1999). Mutating this residue to Y1062F caused an 80% reduction in transforming activity. However, it appears that 2A had greater affinity than 2B, for Grb2 binding (Liu, 1996). Further, while it appears that both 2A and 2B are able to stimulate the P13K pathway, with the PI3K regulatory subunit p85 binding to pY1062, 2B showed higher levels of PI3K activation and phosphorylation of downstream effectors (Murakami, 1999b; Segouffin-Cariou, 2000). In terms of JNK-1 signaling, both 2A and 2B were able to induce JNK-1 activation (Marshall, 1997; Chiarello, 1998). This activity was shown independent of RET Y1062, as Y1062F mutants abolished MAPK activity but did not affect JNK activity, and was mediated by Rho/rac related small GTPases and Cdc42 (Chiariello, 1998). However, another report indicated that RET signaling via the JNK-1 pathway lead to altered biological properties seen more in 2B than in 2A. For example, 2B expressed in NB cells showed an increase in JNK-1 activity, anchorage independent growth, and metastatic tumor formation when these NB cells were injected into nude mice, compared to 2A or parental cells (Marshall, 1997). Finally, it appears that both 2A and 2B are able to activate c-Src, in a tyrosine phosphorylation dependent manner (Melillo, 1999). In conclusion, it seems that all 4 signaling mediators are important for 2A and 2B's ability to alter cellular activity. However, while 2B binds Grb2 less than 2A, 2B activates PI3K and JNK-1 more than 2A.

Ligand stimulation of WT RET

As the ligands for RET have been discovered, researchers are trying to identify pathways activated by the normal proto-oncoprotein. GDNF stimulation of RET has shown to lead to activation of the ras/MAPK, JNK-1, and PI-3K pathways, as well as c-Src activation, in NIH3T3 or NB cell lines (Worby, 1996; van Weering, 1997; Ohiwa, 1997; Chiariello, 1998; Melillo, 1999; Murakami, 1999a, Murakami, 1999b).

RET/PTC

For the most part, the majority of signal transduction studies looking at PTC oncoproteins and their respective signaling pathways deal with the PTC2 oncoprotein. PTC2 Y586 has been shown to bind Enigma, which relocates the cytoplasmic PTC2 protein to the cell periphery (Durick, 1995; Durick, 1996). Once PTC2 is located at the cell membrane and becomes activated by dimerization, PTC2 pY residues (429, 586 and 620) act as docking sites for Grb10/7, Shc, and Grb2, respectively (Durick, 1996; Borrello, 1994; Durick 1995, Arighi, 1997; Alberti, 1998; Durick, 1998). These correspond to RET phosphotyrosine residues 905, 1062 and 1095 respectively (Table 1.1). Further, PTC2 binding and phosphorylation of Shc and Grb2 has shown to lead to increased mitogenic activity (Shc) or transforming activity (Grb2) of cell cultures (Durick, 1995; Durick, 1998; Alberti, 1998). PLCγ has also shown to bind to PTC2, at PTC2 pY539, leading to activation of the PLCγ pathway and to transforming activity (Borrello, 1996; Durick, 1996). Furthermore, while PI3K has yet to be formally implicated in PTC2 signaling, studies of SH2 domains that bind to PTC2 show that

Crk and Nck are able to bind PTC2 (Bocciardi, 1997). These two proteins have been shown to be phosphorylated in a PI3K dependent fashion in cells expressing RET/MEN2A or RET/MEN2B, or upon GDNF stimulation of RET (Murakami, 1999a; Murakami, 1999b).

PTC1 has been shown to induce the ras/MAPK pathway (Borrello, 1994; Grieco, 1995). While little has been published in the literature regarding specific PTC1 phosphotyrosine docking sites, it has been shown that PTC1 interacts with Shc, Grb2, and PLCγ (Borrello, 1994; Borrello, 1996). Further, PTC1 has been shown to activate JNK-1 in a manner dependent upon Rho/rac/cdc42 (Chiariello, 1998). Along those lines, PTC1 expression was shown to correlate with an increase in both c-*jun* mRNA and jun protein phosphorylation levels (Ishizaka, 1991). Lastly, PTC1 was also shown to activate c-Src (Melillo, 1999).

As all the RET variants contain the same RET TK sequence, alignment studies show that the RET, RET/MEN2A, and RET/MEN2B tyrosine residues 905, 1015, 1062, and 1095 correspond to PTC2 residues 429, 539, 586, and 620, respectively (Table 1.1). Interestingly, the same relationship between respective pY docking sites and interacting intracellular proteins exists between these RET variants, at each of these corresponding pY residues (Fig. 1.9). For example, PLCγ has been shown to bind pY 1015 of RET or RET/MEN2 mutants, as well as pY539 of PTC2. In light of this relationship, it can be inferred that the corresponding PTC1 pY residues may also

mediate signaling of the corresponding signaling pathway. For example, PTC1 pY 294 corresponds to PTC2 pY429, and may mediate Grb10 binding and signaling via ras/MAPK in PTC1 expressing cells, as it does in PTC2 expressing cells. Likewise, PTC1 pY 404 corresponds to PTC2 pY 539, and may be the crucial PTC1 phosphotyrosine residue leading to the activation of PLCγ seen in PTC1 (Borrello, 1996). Lastly, PTC1 pY 451 corresponds to PTC2 pY 586, and may play a pivotal role in Enigma relocation to the cell periphery, as well as Shc activation, as has been detected for PTC2 residue 586.

Objectives of this study

Based on the current knowledge, it appears that pY residues within RET and RET variants play a key role in mediating signal transduction cues to the intracellular signaling machinery. Studies suggest RET or RET/MEN2 mutants' phosphotyrosine residues 905, 1015, 1062, and 1095, or corresponding PTC2 pY residues 429, 539, 586, and 620 play a key role in signaling via Grb10, PLCγ, Shc, and Grb2, respectively. Further, these signaling pathways appear to be important for mitogenic or transforming activity in cell culture. In consideration of 1) the conserved relationship among pY residues within RET variants, 2) their role in activating the same spectrum of signaling molecules and pathways, 3) the ability of PTC1 to activate several of the same signaling molecules, and 4) the ability of PTC1 to form tumors in transgenic mice, it is the goal of this study to determine if the PTC1 tyrosine residues (Y294, 404, and/or 451) play an essential role in tumor formation *in vivo*. To this end,

transgenic mice expressing Tg-PTC1-Y(294, 404, and/or 451)F will be characterized for thyroid histology, iodide uptake, and MAPK activation by phosphorylation.

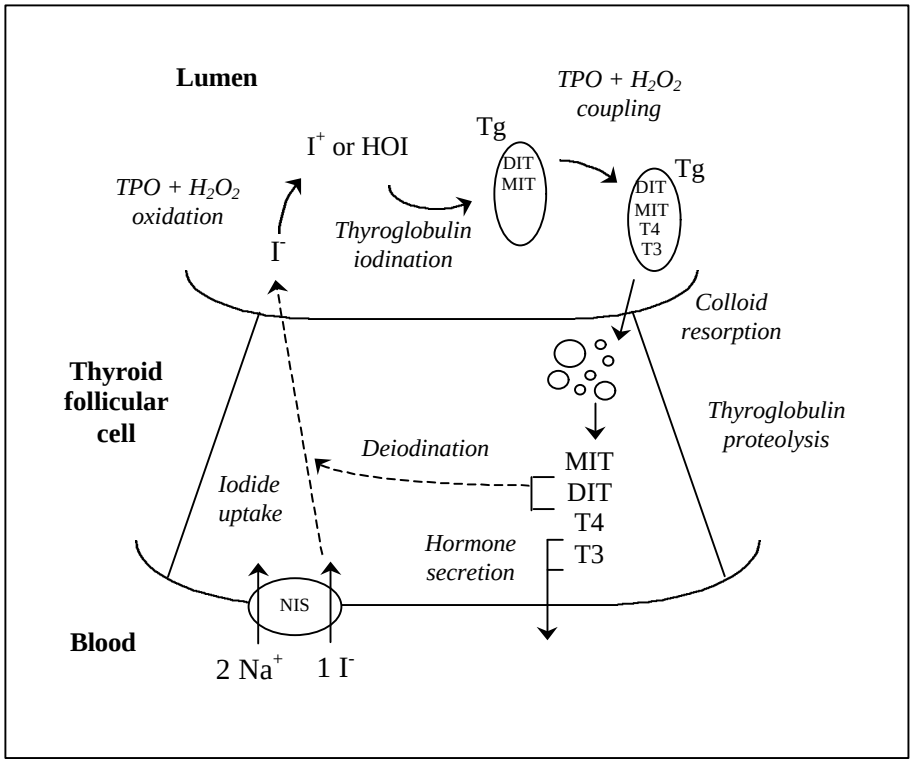

Figure 1.1: Thyroid hormone biosynthesis within a thyroid follicular cell. Iodide uptake from the bloodstream by the sodium iodide symporter (NIS), thyroglobulin (Tg) iodination and coupling by thyroid peroxidase (TPO), and proteolysis of thyroid hormone precursors are necessary for the production of thyroid hormones, T4 and T3. (modified from Taurog, 1991) (Na: sodium, I: iodine, H_2O_2: hydrogen peroxide, MIT: monoiodotyrosine, DIT: diiodotyrosine.)

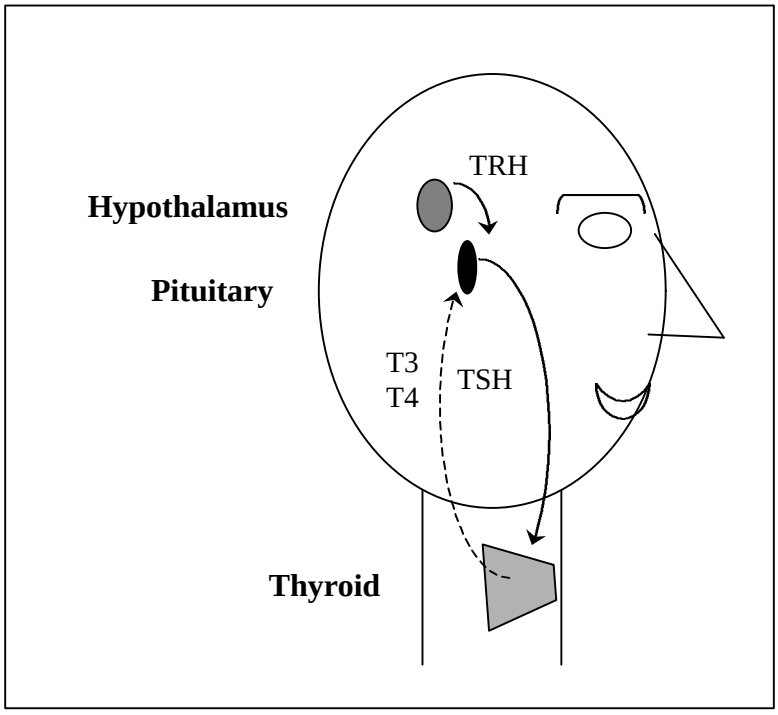

Figure 1.2: Diagram of the hypothalamic-pituitary-thyroid axis. The release of thyrotropin releasing hormone (TRH) from the hypothalamus, and subsequently, thyroid stimulating hormone (TSH) from the pituitary leads to thyroid hormone secretion (T3, T4) from the thyroid. Acting by negative feed-back regulation, T4 and T3 inhibit further production of TSH. (Solid lines, stimulatory pathway; dashed lines, inhibitory pathway). (modified from Johnson, 1999)

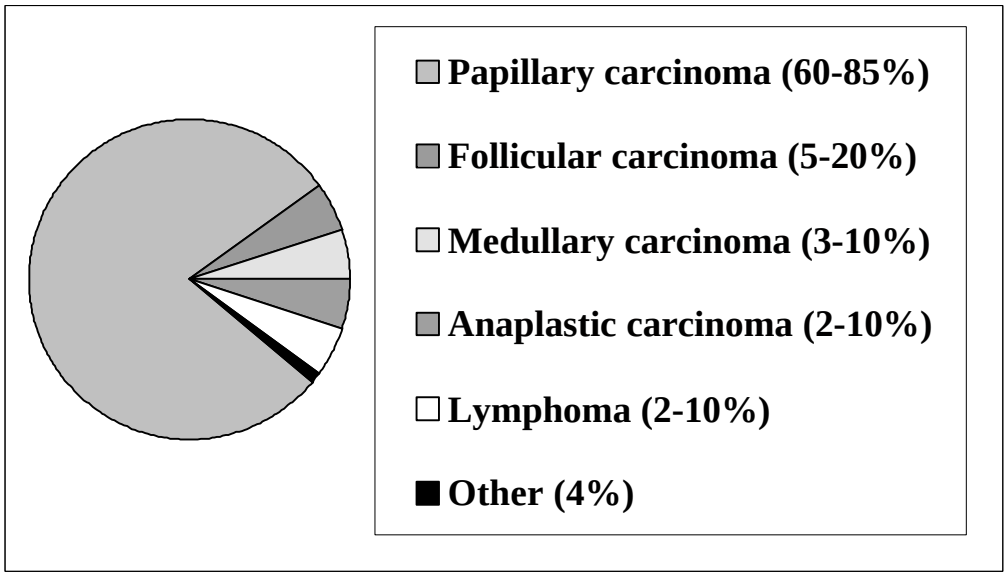

Figure 1.3: Incidences of thyroid neoplasias. (modified from Gleich, 1999)

***RET* proto-oncogene**

***RET* oncogenes activated during gene transfer**

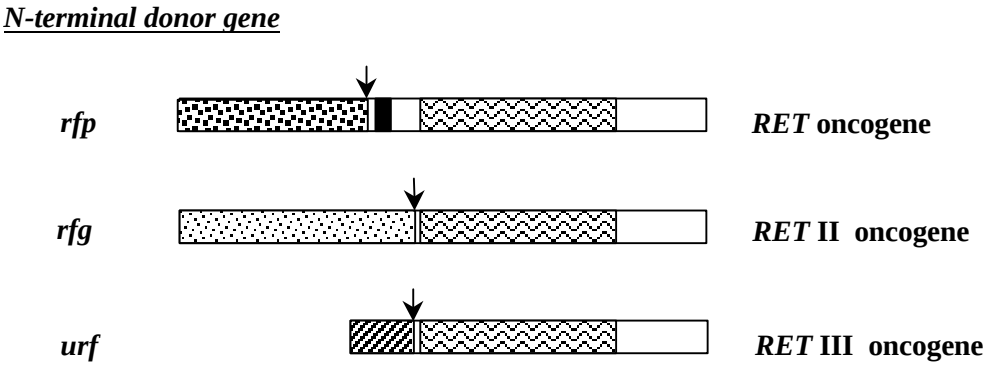

Figure 1.4: Diagram showing the *RET* proto-oncogene and *RET* oncogenes created by chromosomal rearrangement during *in vitro* experiments (modified from Jhiang, 1994a). (SP: signal peptide; EC: extracellular domain; TM: transmembrane domain; TK: tyrosine kinase domain; *rfp*: ret fusion protein; *rfg*: ret fusion gene; *urf*: unnamed ret fusion gene).

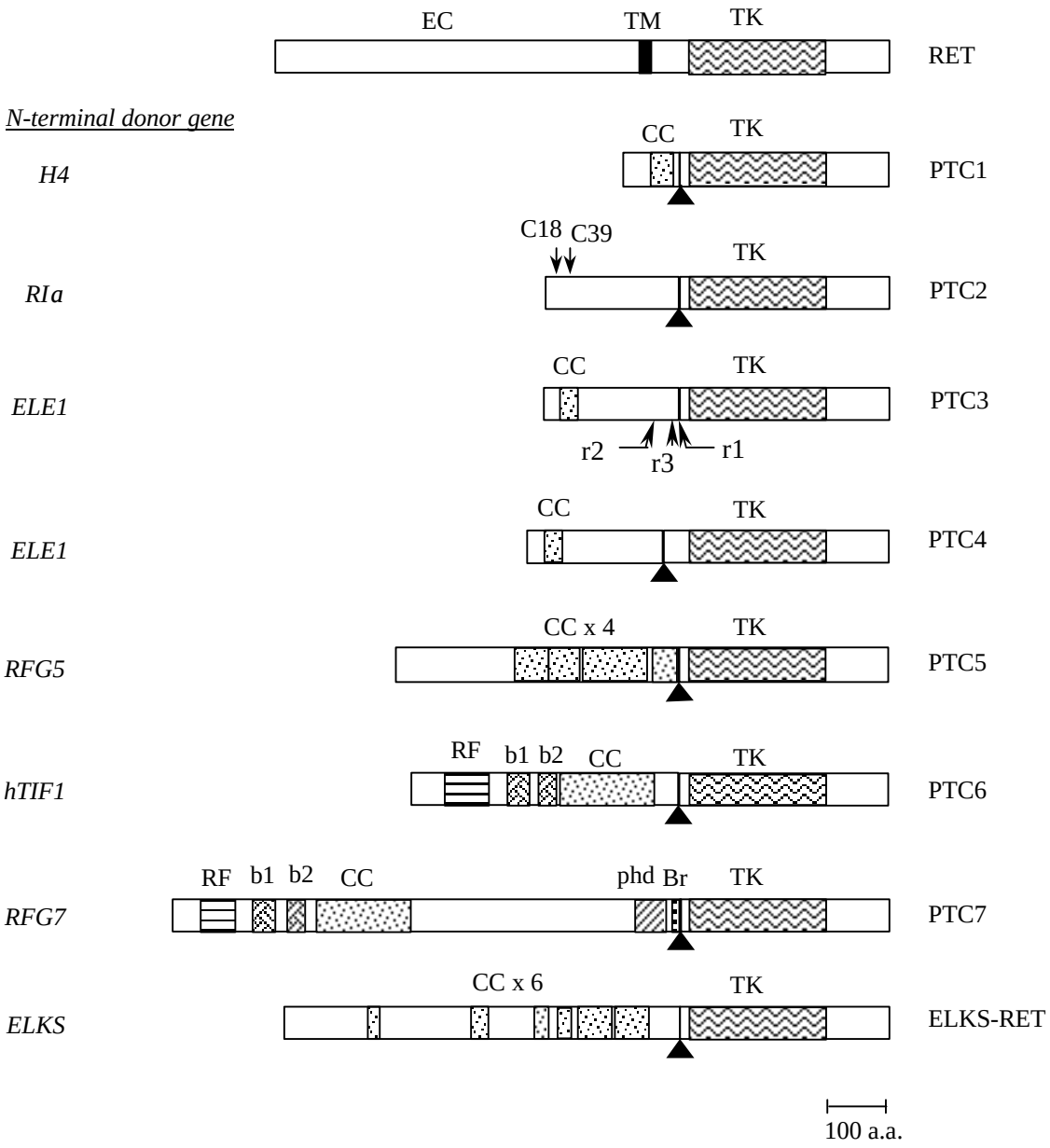

Figure 1.5: Schematic representation of the wild-type RET protein and RET/PTC chimeric oncoproteins found in human papillary thyroid carcinomas. The breakpoint location is indicated by a black arrow. The N-terminal donor genes and corresponding PTC names are listed. The extracellular domain (EC), transmembrane domain (TM), tyrosine kinase domain (TK), coiled-coil domain (CC), cysteine residues involved in disulfide bonds in PTC2 dimerization (C18, C39), ring finger domain (RF), b1 and b2 box domains (b1, b2), phd finger domain (phd), and the bromodomain (Br) are indicated.

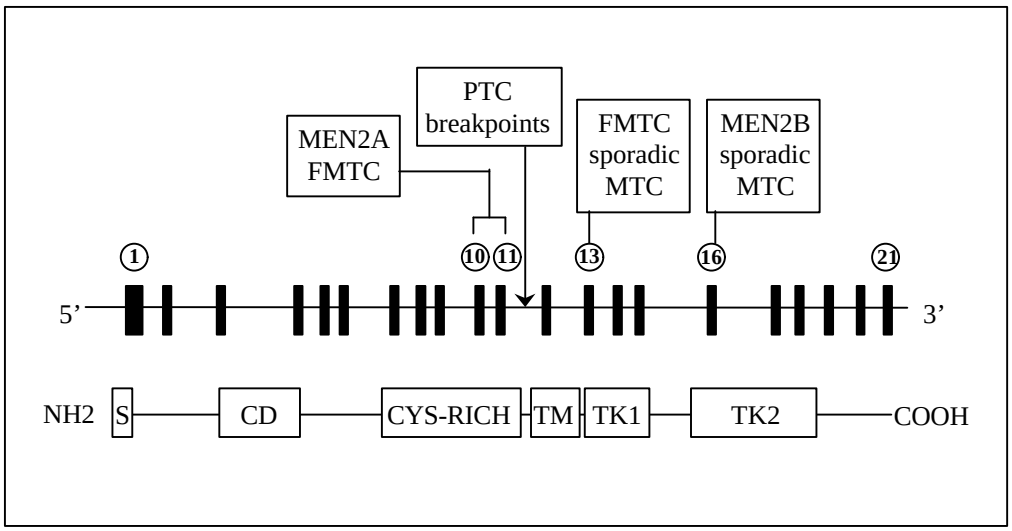

Figure 1.6: RET structure and oncogenic mutation hot spots. The schematic representation shows the intron/exon structure of the c-*ret* proto-oncogene, the protein domains of the RET protein, and the relative sites of mutations found in human thyroid cancers. FMTC: familial medullary thyroid carcinoma; MEN2A: multiple endocrine neoplasia type 2A; MEN2B: multiple endocrine neoplasia type 2B; MTC medullary thyroid carcinoma; PTC: papillary thyroid carcinoma; arrow: site of PTC breakpoint; circled number: exon number; CD: cadherin domain; Cys-rich: cysteine-rich ligand binding domain; TM: transmembrane domain; TK1, TK2: tyrosine kinase domain. (modified from De Lellis, 1995)

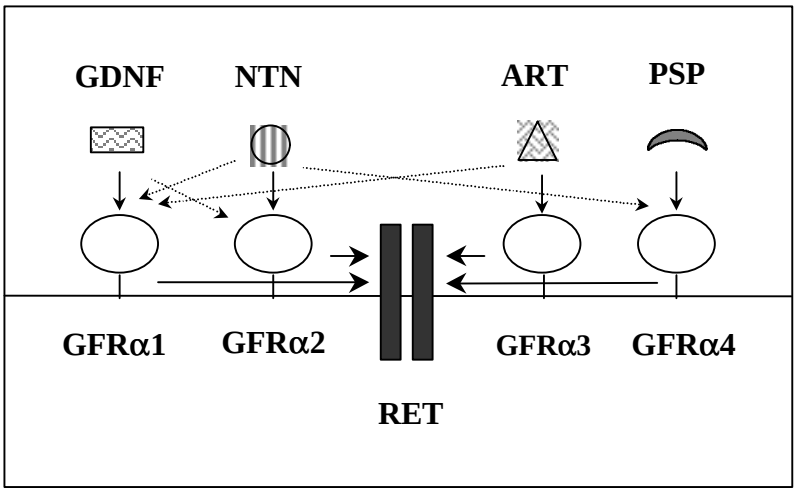

Figure 1.7: The RET protein and its ligands. In order for RET to become activated, one of the four RET ligands binds to its respective co-receptor. The co-receptor/ligand complex then binds to RET to induce dimerization and activation. The horizontal arrows indicate the direction of complex formation. Studies suggest that there is promiscuity among the ligand/co-receptor complexes, as indicated by the dashed lines. GDNF: glial cell-line derived neurotrophic factor; NTN: neurturin; ART: artemin; PSP: persephin; GFRα (1-4): glial cell-line derived neurotrophic factor receptor alpha (1-4) (modified from Airaksinen, 1999).

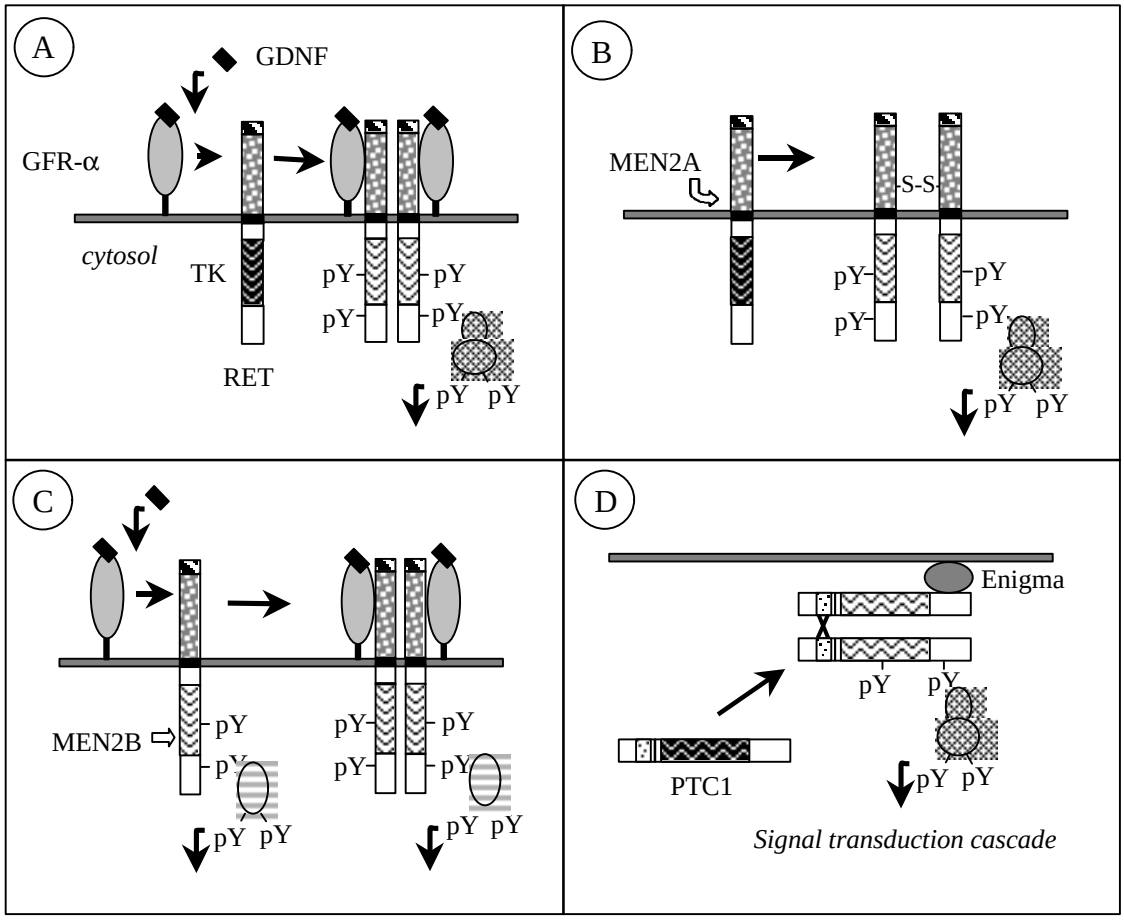

Figure 1.8: Activation of RET and RET mutants. **A:** The RET extracellular ligand binding domain interacts with the complex containing GDNF and it's membrane bound receptor, GFR-α, to induce RET dimerization and tyrosine kinase (TK) activation (hatched TK box: black=inactive; white=active). **B:** RET/MEN2A ligand-independent dimerization due to intermolecular disulfide bonding (S-S) activates the TK domain (mutation site indicated by open arrow). **C:** RET/MEN2B TK activation, in the absence or presence of ligand, is due to altered TK catalytic activity and substrates. **D:** Following recruitment to the cell periphery via binding to Enigma, RET/PTC dimerization is mediated by either coil-coiled motifs or intermolecular di-sulfide bonding, resulting in TK activation.

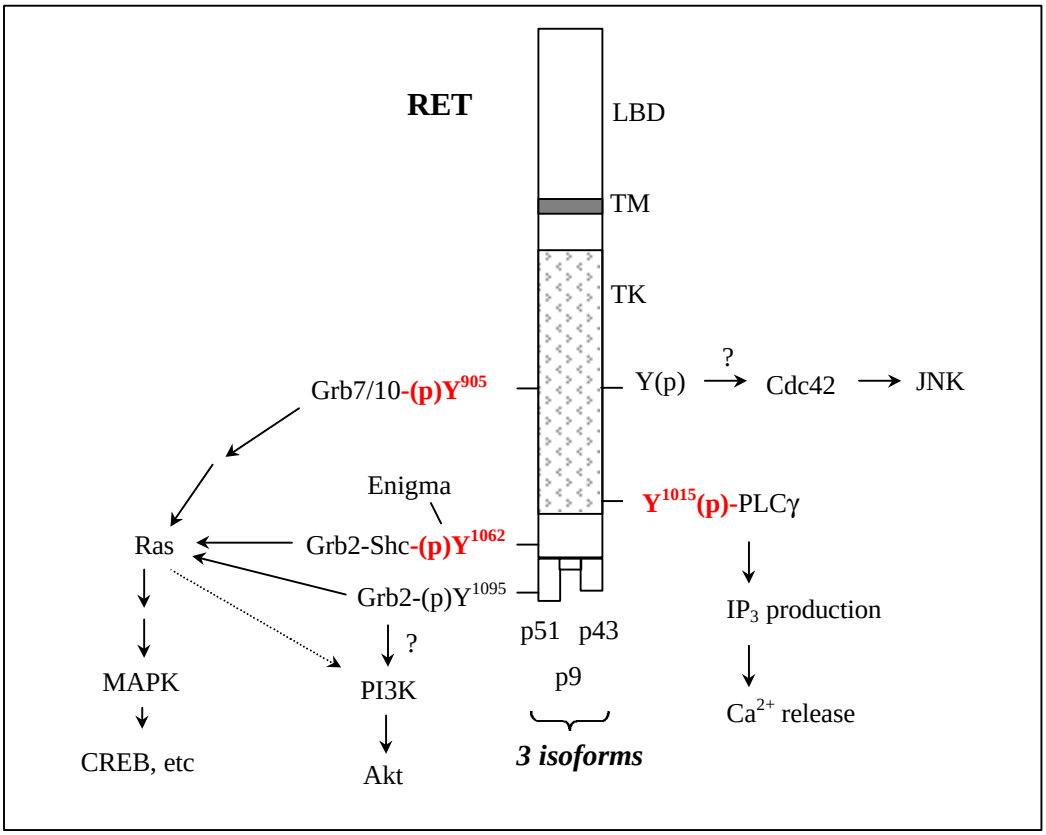

Figure 1.9: Putative RET signaling pathways. The diagram shows the RET phosphotyrosine residues, intracellular binding proteins, and respective signaling pathways found to be critical for RET-mediated cell signaling. LBD: ligand binding domain; TM: transmembrane domain; TK: tyrosine kinase domain. (modified from Airaksinen, 1999)

Signaling molecule	***Phosphotyrosine binding site***		
	RET	PTC1	PTC2
Grb10/7	905	294	429
PLCγ	1015	404	539
Shc/Enigma	1062	451	586

Table 1.1: Tyrosine conversion chart showing the conversion of tyrosine residue numbering between RET and PTC (1 & 2) mutants.

CHAPTER 2

MATERIALS AND METHODS

Site-directed mutagenesis

The *PTC1* cDNA HindIII/XhoI fragment from pBluescript-*TPC1* was subcloned into the MV13amp18 vector (Bio-Rad). Site directed mutagenesis to introduce a tyrosine (Y) to phenylalanine (F) mutation at PTC1 residue 294 (nucleotide change: TAC/TTC), 404 (TAC/TTC), or 451 (TAT/TTT), was performed using an *in vitro* oligonucleotide mutagenesis system (Muta-gene M13 *in vitro* mutagenesis kit, Version 2, Bio-Rad). In brief, mutagenic anti-sense primers containing the desired mutation (indicated in bold lettering; codon underlined) were annealed to the *PTC1* cDNA in the MV13amp18 vector.

Y294F 5'-TCCTCTTCACG**A**AGGAATCCTCT-3'

Y404F 5'-AAGGTCCAAG**A**AGTCTCTCCTC-3'

Y451F 5'-GAAATTCTACCA**A**AGAGTTTGTT-3'

DNA synthesis was performed to produce circular DNA containing the *PTC1-Y/F* cDNA.

Transgene expression studies in cell culture

In order to confirm proper expression and tyrosine phosphorylation of the PTC1 Y/F mutants, mutated *PTC1 Y/F* cDNA was subcloned into the pRC-CMV mammalian expression vector. This allows expression of the *PTC1 Y/F* construct under the control of the CMV promoter. Cos-7 cells (ATCC 1651) were cultured in DMEM, 10% fetal bovine serum, and 1% penicillin-streptomycin (GibcoBRL). $1x10^6$ Cos-7 cells per 100mm plate were transiently transfected with 10 μg of one of the mutant PTC1 Y/F cDNAs, using the calcium phosphate method (GibcoBRL). Growth media was changed 24 hours post-transfection. Cells were harvested 48 hours later, in RIPA lysis buffer (20 mM Tris (pH 7.5), 150 mM NaCl, 20 mM EDTA (pH 8), 1% NP-40, 5 mM sodium vanadate, 1 mM PMSF, 2 μg/ml aprotinin, 2 μg/ml leupeptin). Cells were lysed by sonication on ice, and cellular debris was cleared from the supernate by centrifugation.

Immunoprecipitation of the PTC1 protein from Cos-7 lysates was performed. Cell lysates (500 μg) were incubated with purified anti-RET C-17 polyclonal antibody, recognizing the last 17 amino acids of RET, conjugated to protein-A beads. Immunocomplexes, formed during an overnight incubation at 4^oC on a rocking platform, were precipitated by centrifugation, washed three times with ice cold PBS, resuspended in 20 μl 2X SDS-PAGE loading buffer, and boiled at 100^oC for 10 minutes.

Protein samples were resolved on identical duplicate gels by SDS-PAGE and then transferred to nitrocellulose filter (NCF). The blots were blocked overnight in TBST with 5% milk. Western blot analysis (WB) was then performed by immunobloting with either anti-RET monoclonal antibody (C1) or anti-phosphotyrosine 4G10 monoclonal antibody (Upstate Biotechnology; 1:2000) as primary antibody, anti-mouse IgG-HRP (Transduction Laboratories; 1:3000) as secondary antibody, and ECL substrate reagent (Amersham Pharmacia) for detection of immunoblot signal.

Transgenic mice production and screening

The PTC1-Y/F cDNAs were subcloned (ApaI) into the pRC-CMV-Tg-PTC1 transgene, whose production is described elsewhere (Jhiang, 1996). The Tg-PTC1-Y/F constructs were screened for the desired mutation by sequencing using a modification of the Sanger method (Sequenase 2.0 kit, USB). Transgene isolation was performed by digesting the respective pRC-CMV-Tg-PTC1-Y/F plasmid with KpnI/PvuII, releasing the PTC1-Y/F cDNA under the control of the Tg promoter (Tg-PTC1-Y/F). Each transgene contained within a 3.9 kb KpnI/PvuII fragment was resolved by gel electrophoresis, band isolated, and purified using either the GeneClean DNA purification technique (Bio 101) or the Qiaex II DNA purification kit (Qiagen). The DNA was subsequently injected into fertilized FVB/N mouse eggs which were then implanted into pseudo-pregnant dams.

To determine transgene status of the offspring, PCR amplification across the PTC1 breakpoint was performed using gDNA isolated from ear and tail tissue as template. The thermocycling protocol began with one cycle at 94^{o}C for 3 minutes; 35 cycles of: 94^{o}C for 30 seconds, 56^{o}C for 30 seconds, 72^{o}C for 2 minutes; and ended with an incubation at 72^{o}C, for 8 minutes. The PCR primer pair used was TPC-4 and KD-2, amplifying a 203 bp fragment spanning the breakpoint junction.

TPC-4: 5'-GTCGGGGGGCATTGTCATCT-3'

KD-2: 5'-AGTTCTTCCGAGGGAATTCC-3'

Following separation in a 2% agarose electrophoresis gel containing ethidium bromide, PCR products were visualized by illumination with UV light.

Transgenic mice were mated with non-transgenic mice of the same genetic background. All subsequent offspring were screened using PCR analysis of tail clip gDNA, as described above.

RNA isolation and RT-PCR

Detection of transgene expression within transgenic mice thyroids was performed by RT-PCR analysis of thyroid total RNA pools. Thyroids were isolated from transgenic and non-transgenic control mice, immediately snap frozen, and stored at –80^{o}C until use. Total RNA isolated using the Trizol reagent (GibcoBRL) was subjected to DNase I treatment followed by reverse transcription to produce mouse thyroid cDNA. PCR amplification, using either transgenic or non-transgenic mouse

thyroid cDNA or RNA (control for gDNA contamination) as template, was performed using the same PCR primer set and thermocycling protocol as described above for detection of transgene status. In addition to detection of transgene expression, another PCR reaction was performed in parallel to detect mouse β_2 microglobulin expression, as a marker of RNA integrity for each sample. The primer set MMG-F1/MMG-R1 allows amplification of a 265 bp fragment of mouse β_2 microglobulin.

MMG-F1: 5'-TGTCAGATATGTCCTTCAGC-3'

MMG-R1: 5'-GAAGGTGATGTGTACATTGC-3'

PCR products were resolved by electrophoresis and analyzed as described above.

Low iodide diet

For the single mutant transgenic lines, a group of the mice was fed low iodide diet supplemented with 0.15% propylthiouracil (Harlan Teklad: formula # TD 95125). For a portion of mice from the Tg-PTC1-3Y/F group, a low iodide diet was administered (Harlan Teklad: formula # TD 95007). Regardless of diet, mice were fed the modified diet for a minimum of 2.5 months, in order to induce positive feedback of the hypothalamic-pituitary-thyroid axis and an increase in TSH stimulation of the thyroid.

Histological analysis

Mouse thyroid tissues were isolated, immediately fixed in 10% neutral-buffered formalin, and then embedded in paraffin. To perform histological

characterization, 5 μm thyroid tissue sections were deparaffinized and then stained with hematoxylin and eosin. A grading system was developed with consideration of both gross anatomy and histological features as outlined in the grading system (Table 3.2). Thyroid sections from mice fed either normal diet or an LID/PTU diet were evaluated and classified according to grade 1, 2, or 3.

Iodide accumulation analysis

To analyze *in vivo* iodide accumulation activity, mice were injected intraperitoneally with 0.3 μCi of NaI^{125} (Amersham) per gram of body weight. Following an incubation period (2-6 hr), the thyroid was isolated and immediately fixed in 10% neutral-buffered formalin, in preparation for paraffin embedding. Deparaffinized, 5 μm tissue sections were coated in LM-1 emulsion (Amersham) and allowed to incubate at 4^{o}C for 3-14 days. The micro-autoradiogram emulsions were then developed and counterstained with hematoxylin.

Western blot analysis: Mouse thyroid protein

Harvested mouse thyroid tissues, snap frozen and stored at –80^{o}C, were homogenized in Trizol reagent (GibcoBRL), and protein was extracted following the manufacturer's protocol. Protein concentration was determined using the Bio-Rad protein quantification kit. Total cellular proteins were resolved by SDS-PAGE on a 7.5% acrylamide gel, and then transferred to nitrocellulose filter (NCF). Prior to incubation with antibody, the blots were blocked in TBST with 5% milk.

PTC1 expression was analyzed by Western blot (WB) analysis. The NCF was incubated with primary antibody (anti-RET C-19 pAb: Santa Cruz Biotechnology, 1:200), secondary antibody consisting of either goat anti-rabbit IgG-HRP (Bio-Rad, 1:3000) or goat anti-mouse IgG-AP (Transduction Laboratories, 1: 3000), and lastly, with substrate solution consisting of either ECL substrate (Amersham) or BCIP/NBT alkaline phosphate substrate (GibcoBRL). The blot was then either exposed to x-ray film for various lengths of time in the case of ECL, or incubated with AP substrate solution until immunoblot signal appeared for the colorimetric detection system. In order to detect active phosphorylated MAPK, the NCF was stripped as described elsewhere (Sweetser, 1999), reblocked (1% BSA in TBS, overnight at 4^{o}C) and reprobed with the primary antibody anti-pMAPK pAb (Promega: 1:5000). The secondary antibody and detection conditions were the same as for PTC1 analysis above. The same blots were once again stripped, reblocked (5% dry milk/TBST, overnight at 4^{o}C) and reprobed for detection of total MAPK (Santa Cruz Biotechnology: 1:500 K-23 pAb) with secondary antibody and detection conditions as listed above. Lastly, the blots were once again stripped, blocked and reprobed for detection of β-tubulin (Santa Cruz; 1:200 H-235 pAb) with secondary antibody and detection conditions as listed above.

Following the last WB analysis, the blots were stripped as described elsewhere (Sweetser, 1999) and then washed three times in PBST. The blots were then

incubated in PBST with 0.1% India ink (Higgins) for 3-18 hours on a shaking platform, at room temperature. After the incubation with ink, the blots were rinsed in several washes of PBS, to assist in destaining (Harlow, 1988).

Densitometry analysis

Western blots were subject to densitometry analysis using the NIH image analyzer computer program. The area analyzed was held constant from one lane to the next, specific to the primary antibody used.

Statistical analysis

Statistical analysis was performed by the Ohio State University Biostatistics Core. Chi-squared analysis and Fisher's exact tests were used to compare the frequency distributions of the histological grades among different mouse groups, diets, age groups, and sexes of the animals. Polytomous logistic regression analysis was used to identify differences in frequency distribution among select groups of mice. Analysis of variance was performed upon WB densitometry data. p values ≤ 0.05 were considered statistically significant.

CHAPTER 3

RESULTS

Site-directed mutagenesis

Cell culture studies indicate the significance of PTC1 phosphotyrosine docking sites pY294, pY404 and pY451 for the docking of Grb10/7, PLCγ, Shc and Enigma, respectively, towards the passage of PTC1-specific signal transduction pathways leading to cellular transformation. In order to investigate the role of these three PTC1 residues *in vivo*, site-directed mutagenesis was performed to change each tyrosine residue to phenylalanine. Using PCR in conjunction with mutagenic primers, a single nucleotide point mutation was incorporated into the PTC1 cDNA (p9 isoform), at PTC1 residue 294 (TAC to TTC), 404 (TAC to TTC) or 451 (TAT to TTT) (Fig. 3.1). The triple mutant construct, PTC1 3 Y/F, was produced by subcloning each of the three mutations into one PTC1 construct. The desired mutations were confirmed by sequencing, and subcloned into the construct containing the original Tg-PTC1 transgene, pRC-CMV-Tg-PTC1. In order to isolate the transgene prior to injection, the Tg-PTC1-Y/F fragment was released from the pRC-CMV vector by restriction digest.

PTC1-Y/F expression and tyrosine phosphorylation in cell culture

Expression and tyrosine phosphorylation of the PTC1-Y/F mutants were tested in cell culture. PTC1-Y/F cDNA's were subcloned into the pRC-CMV mammalian expression vector. The resulting plasmids were then transiently transfected into Cos-7 cells. Cell lysates were isolated and immunoprecipitation was performed with anti-RET polyclonal antibody (C-17). The immunoprecipitates were divided into two equal aliquots and resolved separately by SDS-PAGE. PTC1-Y/F mutant protein (~57 KDa) was detected for all three single PTC1-Y/F mutants, as well as the triple PTC1 3 Y/F mutant, by Western blot analysis using anti-RET monoclonal Ab (C1) (Fig. 3.2). Interestingly, immunobloting using anti-phosphotyrosine Ab detected only the three single PTC1 Y/F mutants. The triple mutant PTC1 3 Y/F was undetectable, indicating that the triple mutant is no longer tyrosine phosphorylated. This is significant as tyrosine phosphorylation is believed to be imperative to the function of a tyrosine kinase protein.

Tg-PTC1-Y/F expression studies in vivo

RT-PCR

Following the production of transgenic founder mice carrying one of the four transgenes and development of their respective lineages, expression studies were performed. Total RNA was isolated from both non-transgenic and transgenic mice thyroids. Reverse transcription was performed and the resulting cDNA was screened for the presence of the transgene by PCR (Fig.3.3 A). In a separate but parallel

experiment, PCR was performed in the absence of cDNA template (-RT), to test for gDNA contamination, showing no amplified fragment and thus no contamination. Further, PCR was also performed at the same time to show sufficient RNA integrity by amplifying β_2 microglobulin (MG) within the mouse thyroid RNA population.

RT-PCR analysis showed that, while not all lines were screened, several transgenic mice lines had thyroid-targeted transgene expression (Table 3.1). The Tg-PTC1-Y294F transgenic group, also referred to as "PTC1ΔG" to indicate that the Grb10/7 binding site is abolished by the Y/F mutation, had four RT-PCR (+) lines. The Tg-PTC1-Y404F group ("PTC1ΔP" for the abolished PLCγ binding site) had one RT-PCR (+) line. The Tg-PTC1-Y451F ("PTC1ΔE" for the abolished Enigma and Shc binding site) had eleven transgenic lines with thyroid expression. Lastly, expression of the triple mutant Tg-PTC1-3 Y/F transgene ("PTC1ΔGPE" for abolishing all three binding sites) was only detected in one transgenic line.

Western blot analysis

While expression of the transgene at the RNA level is encouraging, the most important feature is expression of the transgene at the protein level. Mouse thyroid protein samples were resolved by SDS-PAGE and immunobloted using anti-RET polyclonal Ab (C-19). PTC1-Y/F expression was detected at varying levels of signal intensity (Fig. 3.3 B). Summarized in Table 3.1, the majority of transgenic lines have detectable transgene expression by WB analysis. Expression was detected in four

PTC1ΔG lines, three PTC1ΔP lines, nine PTC1ΔE lines, and in the one PTC1ΔGPE line.

Low Iodine diet

While one group of mice was maintained on normal rodent chow, another group was maintained on either a low iodine diet (LID), or a modified LID supplemented with propylthiouracil (LID/PTU). The objective of the special diets was two fold: to increase the thyroid mass to isolate more protein for WB, and to potentially increase the transgene expression level in order to promote any altered phenotype specific to the transgene. As iodine is necessary for thyroid hormone production, LID or LID/PTU diet will result in decreased thyroid hormone production, decreased colloid stored within follicle lumens, and thus collapsed follicles. Also, PTU acts as a competitive inhibitor of TPO-mediated Tg iodination and coupling, thus further preventing colloid production. With the decrease in systemic thyroid hormone, the hypothalamic-pituitary-thyroid axis induces thyroid stimulating hormone (TSH) stimulation of the thyroid follicular cells (Fig. 1.2). TSH stimulation has been shown to increase follicular cell proliferation, resulting in hypertrophy and hyperplasia, as well as expression of thyroglobulin (Tg), sodium iodide symporter (NIS), and thyroid peroxidase (TPO), all in order to increase thyroid hormone production (Kohn, 1995; Ajjan, 1998). Long-term TSH stimulation in rodents has been shown to increase the thyroid mass, similar to goiter in humans (Wynford-Thomas, 1982). Further, in terms of increasing the transgene expression, as TSH stimulation increases Tg expression, it

should also increase the expression of the transgenes under the control of the Tg promoter. Thus, mice were analyzed from both diet groups for changes in histology, and protein profiles in the WB analysis.

Histological analysis showed that both of the two special diets were able to induce goiter equally well. Both special diets were able to induce hyperplasia and hypertrophy of thyroid follicular cells and a reduction in colloid, as described in further detail below. However, WB analysis showed no significant increase in transgene expression, comparing normal diet samples to those treated with the modified diet, as described in the WB analysis results.

Histological analysis

Objectives

Transgenic mice from each of the four PTC1-Y/F groups, as well as the original PTC1 mice and non-transgenic littermates, were evaluated for thyroid histological features. The objective was to determine if the transgenic mice expressing the PTC1-Y/F transgenes have histological features similar to PTC1 transgenic mice, indicating no effect of the loss of the specific tyrosine residue(s), and corresponding pathway(s), towards the development of PTC1-induced tumor formation. If, on the other hand, the PTC1-Y/F mice had histological features similar to their NTG littermates, then that tyrosine residue altered by the Y/F mutation can be assumed to

play a key role in tumor formation. Therefore, an inverse relationship is expected between mutation of the crucial tyrosine residue and frequency of tumor formation.

Grading system

The grading system was developed with consideration of both gross anatomy and histological features as outlined in the grading system (Table 3.2). Thyroid sections from both mice fed a normal diet and mice fed LID/PTU diet were evaluated and classified according to grade 1, 2, or 3. Grade 1 thyroids on normal diet displayed the expected shape, size and color of a mouse thyroid gland, measuring on average 0.4 x 0.4 x 0.2 cm (thyroid and trachea) and displaying a pink-yellow tissue color (Fig. 3.5 A). Each lobe contained cuboidal follicular epithelial cells organized into round follicles (Fig. 3.6 A). Colloid was evident within the lumen of the follicles, and heterogeneous iodide accumulation was detectable (Fig. 3.8 A-B). Grade 1 thyroids treated with LID/PTU diet displayed enlarged thyroids, 0.6 x 0.6 x 0.3 cm in size, which were dark red to purple in color (Fig. 3.5 B; Table 3.2). These thyroid lobes were filled with hyperplastic and hypertrophic masses of columnar follicular epithelial cells (Fig. 3.7 A). As expected in with decreased levels of dietary iodide, colloid was absent. These two grade 1 phenotypes (Table 3.3) were the predominant phenotypes observed in the thyroids of non-transgenic (NTG) mice (Fig. 3.4 A-B, E-F), and Tg-PTC1-3 Y/F mice.

PTC1 transgenic mice, in contrast, developed thyroid tumors with features similar to human papillary thyroid carcinoma (Fig. 3.4 E-F, G-H) and were assigned a grade of 3 (Table 3.3). Grade 3 thyroids on normal diet displayed a change in thyroid lobular architecture, with size variability ranging from 0.4 x 0.4 x 0.2 cm to 0.6 x 0.7 x 0.3 cm (Fig. 3.5 E). The tissue color, in contrast to the yellow-pink color of grade 1 thyroids, was yellow. The histology consisted predominantly of irregular follicle structures, intermixed infrequently with round follicles (Fig. 3.6 D-F). The epithelial structure varied from cuboidal in the round follicle regions, to columnar in regions looking hyperplastic, to spindle shape in a few samples displaying a more anaplastic appearance. Further, there was an overall decrease in colloid observed (10-50% of normal level). Only a minimal amount of radioiodide was accumulated in regions of round follicles within grade 3 normal diet thyroids (Fig. 3.8 E-F).

In grade 3 thyroids treated with LID/PTU, the size of the gland varied from normal to enlarged size, 0.6 x 0.6 x 0.3 to 1.2 x 0.7 x 0.8 cm (Fig. 3.5 F). Further, the color of the gland was altered from the red/purple color seen in grade 1 thyroids, to the same yellow color seen in the grade 3 normal diet thyroids. The follicles within the grade 3 LID/PTU thyroids were either collapsed and consisted of hyperplastic, hypertrophic columnar or spindle cells, or were irregularly shaped and contained a mixture of cuboidal and columnar cells (Fig 3.7 D-F). While the colloid amounts varied, they were greater than that observed in grade 1 thyroids on LID/PTU (10-50% for grade 3 versus 0-5% for grade 1).

A large number of PTC1-Y/F tissue sections presented with histological features classified as neither normal (grade 1) nor tumor (grade 3), but rather displayed distorted or coalescing follicles and was classified as grade 2 (Table 3.2). In terms of gross anatomy, there was no difference in size of the lobes between grades 1 and 2 (Fig. 3.5 A-B versus C-D). However, a difference between grades 1 and 2 was noted in the color of the tissue treated with LID/PTU. Grade 2 thyroids on LID/PTU had multiple small, yellow foci juxtaposed on the expected dark red/purple thyroid gland, as seen in grade 1 thyroids. Histological analysis of normal diet thyroids revealed a portion of the gland consisting of irregularly shaped follicles comprised of cuboidal epithelium (Fig. 3.6 B-C), displaying a decreased level of iodide accumulation (Fig. 3.8 C-D). In tissues treated with LID/PTU, irregularly shaped follicles existed among collapsed follicles, with either cuboidal or columnar epithelium (Fig. 3.7 B-C).

Tg-PTC1-Y294F histological review

In reviewing histological samples from the Tg-PTC1-Y294F lines (PTC1ΔG), a total of 27 thyroids from mice fed normal diet and 22 thyroids from mice fed LID/PTU diet, were graded. Ages ranged from 2.0 to 19.5 months for normal diet studies (average: 6.7 months), and 3.7 to 13.0 months for LID/PTU diet studies (average: 6.3 months). As outlined in Table 3.4, the PTC1-Y294F lines have both intra-line and inter-line variation in histological grades. Intra-line variation is seen, for

example, in line G64. This line has samples in all three grades. Inter-line variation, is seen when comparing, for example, lines G40 versus G64. G40 has an average grade of 1.0 or 1.2, depending on normal or LID/PTU diet. However, G64 has an average grade of 1.9 or 2.0, respectively. Thus, there is a range of histological grades observed within the G lines; a normal diet grade range from 1.0 ± 0.0 to 1.9 ± 0.4, and a LID/PTU diet grade range from 1.0 ± 0.0 to 2.0 ± 0.7 (average ± standard deviation). As indicated in Table 3.7, the average histological grades for the Tg-PTC1-Y294F group are 1.4 ± 0.6 (normal diet) or 1.5 ± 0.7 (LID/PTU diet).

Tg-PTC1-Y404F histological review

There were a total of 39 thyroids graded in the Tg-PTC1-Y404F transgenic group (PTC1ΔP), 19 thyroids per normal diet and 20 thyroids per LID/PTU diet. Ages ranged from 2.0 to 12.8 months in the normal diet group (average: 7.0 months) and 2.5 to 12.9 months in the LID/PTU diet group (average: 7.0 months). Once again, there was both intra-line and inter-line variation (Table 3.5). The histological grades ranged from 1.0 ± 0.0 to 3.0 ± 0.0 for normal diet groups, and 1.5 ± 0.7 to 2.5 ± 1.0 for the LID/PTU diet groups. The average histological grades were 1.9 ± 0.9 and 2.3 ± 0.8 for the normal and LID/PTU diet groups, respectively (Table 3.7).

Tg-PTC1-Y451F histological review

The Tg-PTC1-Y451F transgenic group had the largest number of founder mice and, subsequently, number of mice thyroids characterized histologically: 65 normal

diet tissue sections and 58 LID/PTU sections, from a total of 12 different transgenic PTC1ΔE lines. Ages ranged from embryological day 16.5 to 16.5 months for the normal diet group (average: 8.2 months), and from 4 months to 15.8 months for the LID/PTU diet group (average: 7.3 months). Once again, intra-, and inter-line variations were observed. The histological grades ranged from 1.0 ± 0.0 to 3.0 ± 0.0 for normal diet mice, and 1.0 ± 0.0 to 2.6 ± 0.5 for LID/PTU diet treated mice (Table 3.6). The average grades were 1.8 ± 0.9 and 1.9 ± 0.8, respectively, for normal diet and LID/PTU diet groups (Table 3.7).

Tg-PTC1 3-Y/F histological review

Only one transgenic line was established for the PTC1ΔGPE transgenic group. Twelve mice were characterized by histological analysis: 10 normal diet thyroids and 2 LID thyroids. The age range for these thyroids was E18.0 to 20.0 months for normal diet thyroids (average: 8.0 months), and 6.2 to 6.7 months (average: 6.5 months) for the LID thyroids. The average histological grades were fairly close to that of the NTG thyroids, 1.3 ± 0.5 for normal diet thyroids and 1.0 ± 0.0 for LID thyroids (Tables 3.7).

Comparison of average histological grades among Tg-PTC1-Y/F mice groups

In reviewing the average histological grades among Tg-PTC1-Y/F transgenic groups, the triple mutant line had the lowest values, regardless of diet, with 1.3 for normal diet thyroids and 1.0 for LID/PTU diet thyroids. These values are most similar

to that of NTG (Table 3.7), indicating a lack of oncogenic potential in the Tg-PTC1-3Y/F transgenic group. This would be consistent with a kinase inactive TK domain, suggested by the Cos-7 expression and tyrosine phosphorylation studies.

For the three single mutant groups, average histology grades for normal diet thyroids ranged from 1.4, for Tg-PTC1-Y294F, to 1.8-1.9 for the other two single mutants. This suggests a degree of similarity between Y451F and Y404F, in terms of biological response. Interestingly, Y294F and Y451F average histological grades on LID/PTU remain nearly constant with normal diet values, while the Y404F average grade on LID/PTU increases from 1.9 to 2.3. This may indicate an additive role of TSH stimulation on top of the Tg-PTC1-Y404F signaling, all of which are leading to tumors. Interestingly, studies in cell culture show that TSH signaling can induce activation of both the adenylate cyclase/PKA pathway, as well as PLC/PKC pathway (Dumont, 1989; Berridge, 1989). Perhaps the PTC1-Y404F mutant, unable to activate PLCγ, is able to partially overcome this deficit by the activation of PLC/PKC via the TSH signaling pathway. This could potentially translate into increased oncogenic potential, increased cellular transformation, and subsequently increased histology grade within the LID/PTU treated PTC1-Y404F thyroids.

Statistical analysis of histology data

Transgene, diet, age, and sex compared to the histological grade

Statistical analysis of the histological data, taking into account the transgenic status, the diet, the age and the sex of the tissue section, was able to detect several correlations within the data. When comparing the percentages of mice within each of the three histology grades against their transgenic mutation type (Table 3.8), a significant difference in percentages was detected ($p < 0.0001$). This indicates that within the entire group of mice, there is a correlation between the type of mutation and the histological grade. However, this type of analysis is not able to identify where that significant difference exists. Furthermore, both diet and age differences also correlated with histological differences ($p < 0.05$), as seen in Tables 3.9 and 3.10 respectively. A correlation was found between the LID/PTU diet and an increase in the percentage of grade 2 tissues (data not shown). Interestingly, despite a 2-3:1 ratio of females to males observed in naturally occurring human PC's (Mazzaferri, 1991; Gleich, 1999; Wartofsky, 2000), these mouse models show no significant correlation between sex of the animal and abnormal histology, as outlined in Table 3.11.

Frequency of tumor formation of Tg-PTC1-Y/F mice vs. control groups

Consistent with the correlation between transgene mutation type and histological differences outlined in Table 3.8, differences in the rate of tumor formation have been identified among the 6 different groups of mice (Table 3.12). Rate of tumor formation varied from 0% seen in the Tg-PTC1-3 Y/F group, to 100%

seen in Tg-PTC1 transgenic mice. Among the three single mutants, Tg-PTC1-Y294F had the lowest rate of tumors (6.1%). The next highest were Tg-PTC1-Y451F mice, showing a 4.9 fold increase in the percentage of tumors (30.1%) compared to the Tg-PTC1-Y294F group. Lastly, Tg-PTC1-Y404F had the highest rate of tumor formation among the single mutant groups (41.0%) which resulted in a 6.7 fold increase over Tg-PTC1-Y294F mice and a 1.3 fold increase over Tg-PTC1-Y451F mice.

Statistical analysis shows that there is no significant difference in the rate of tumor formation between NTG and Tg-PTC1-3Y/F, or between Tg-PTC1-Y404F and Tg-PTC1 (Table 3.12). The first relationship is not unexpected, as the Cos-7 expression and tyrosine phosphorylation studies showed that the PTC1 3-Y/F mutant protein was unable to be tyrosine phosphorylated in cell culture (Fig. 3.2). Thus, both the Cos-7 studies and the histology results support the notion that tyrosine phosphorylation is critical for the function of this tyrosine kinase. The correlation between Tg-PTC1 and Tg-PTC1-Y404F is of interest. In light of the inverse relationship expected between the number of tumors and significance towards PTC1 tumor formation, it would appear that Y294 plays the most significant role, and residue Y404 plays the least significant role in PTC1-induced tumor formation. However, as the PTC1-Y404F lines do not display 100 % tumor formation, this respective tyrosine residue may not be completely insignificant in PTC1 signal transduction leading to tumor formation.

Western blot analysis

Objectives

In consideration of the studies implicating the ras/MAPK pathway in RET mutant-induced transforming activity in cell culture, one objective of this study was to determine the impact the PTC1-Y/F transgenes have upon MAPK expression and phosphorylation, *in vivo*. If PTC1 signals through the ras/MAPK pathway at any one of the three tyrosine residues, it is expected that this transgenic group would have lower pMAPK levels. Further, if PTC1 signal is transduced via this same tyrosine through MAPK leading to tumor formation, then potentially a correlation can be made between critical tyrosine residues, a signaling pathway, and tumor formation *in vivo*.

Control studies

Initial control studies were performed to test detection of PTC1 or phosphorylated MAPK (pMAPK) in cell culture. PTC1 signal is readily detected in Cos-7 cells transfected with the *PTC1* cDNA, but not in Cos-7 parental cells (Fig. 3.9.A). Further, PC12 cells were used to test detection of pMAPK. NGF stimulation has been shown to induce MAPK phosphorylation in PC12 cells. Thus, PC12 cell extracts, with or without prior NGF treatment, were analyzed for pMAPK and MAPK immunoblot signal. As is shown in Fig. 3.9 B, the NGF (-) samples show no detectable pMAPK, despite the presence of MAPK. Interestingly, when analyzing the Cos-7 and Cos-7-PTC1 samples for pMAPK signal, a lower level of pMAPK was detected consistently in the PTC1 transfected sample (Fig. 3.9 A). This result is in

contrast to the expectation that PTC1 signal transduction leads to activation of the ras/MAPK pathway in cell cultures. Lastly, WB analysis was performed to analyze differences in transgene expression or pMAPK levels, between normal diet and LID/PTU diet samples. Protein samples from both diets were isolated from the Tg-PTC1-Y451F #68 line. Results show no substantial difference in transgene expression or pMAPK between the two groups. A similar transgene expression pattern was observed among samples treated with each of the two diets from the PTC1-Y294F #55 line (data not shown).

Mouse tissue WB analysis

Following establishment of WB methodologies, mouse thyroid protein samples were analyzed for each of the four proteins of interest: the transgene (PTC1), pMAPK, MAPK, and tubulin. Tubulin was used in an effort to standardize possible discrepancies of protein loading. Further, each blot was finally stained with India ink to evaluate equal total protein loading per lane. Western blot data and India ink data were analyzed from each transgenic group, with the data being subjected to densitometry and statistical analysis.

The WB results for the Tg-PTC1-Y294F group show variable expression patterns (Fig. 3.10 A). When the Tg-PTC1-Y294F group densitometry values are plotted against the average histological grade per line, a relationship emerges between increasing densitometry values for either MAPK, pMAPK or tubulin and the

histological grade (Fig. 3.10 B). In contrast, the transgene expression levels do not follow a similar pattern. This suggests that in this group, PTC1 Y294F-induced signal transduction leads to changes in pMAPK, MAPK, and tubulin that correlate with histological changes. However, the expression level of PTC1-Y294F does not correlate with histological changes.

Tg-PTC1-Y404F samples show a slightly different pattern (Fig. 3.11 A). In this set, PTC1-Y404F expression and pMAPK increase with increasing histological grade (Fig. 3.11 B). However, MAPK expression remains fairly constant. This might indicate a relationship between the expression levels of PTC1-Y404F and phosphorylation levels of MAPK, both of which are proportional to tumor formation.

For Tg-PTC1-Y451F, no significant relationship appears to exist between the proteins profiled and histological grading (Fig. 3.12 A-B), regardless of diet. The data tends to have downward linear regression trendlines (data not shown), indicating that these proteins do not impact upon histology. Considering that pY451 is the docking site for Shc, it would be expected that abolishing the docking site by the Y/F mutation would abolish the ras/MAPK signal pathway. This would also seem to indicate that the increased histological grade seen in these mice is due to signaling via a pathway other than ras/MAPK.

The sole triple mutant Tg-PTC1-3Y/F line was also analyzed. Shown in Fig. 3.13, expression of all four proteins is detected. However, no comparison can be made regarding changes in histology grade, as there is only one line in this group. While pMAPK, MAPK and tubulin are detectable, no tumor formation was observed within this transgenic group.

Statistical analysis

Statistical analysis was performed, comparing the densitometry values for each of the four proteins versus the transgene status, diet and age of the protein sample, and the average histological grade per line from which the protein sample originated. In Table 3.13, the analysis of variance of densitometry values suggest the only significant relationships are between tubulin and diet, as well as between MAPK and the transgene status. Further analysis of the MAPK relationship to transgene status identified a significant difference only between groups 3Y/F and Y451F. However, no significant differences were detected between different transgenic groups, in terms of pMAPK levels. Interestingly, this lack of relationship between a RET-variant transgene, phenotype and pMAPK has been reported before, in a paper looking at MEN2B transgenic mice (Sweetser, 1999). In the MEN2B study, no correlation was observed between transgene expression and pMAPK levels, despite the MEN2B phenotype. Thus, there are now two studies showing a lack of involvement of pMAPK in RET-variant signaling leading to altered phenotype *in vivo*.

A. Tg-PTC1 transgene

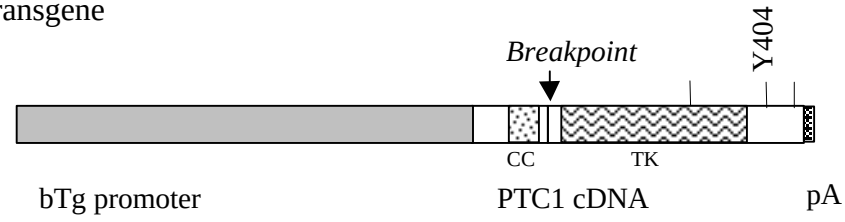

B. Tg-PTC1-Y/F transgenes

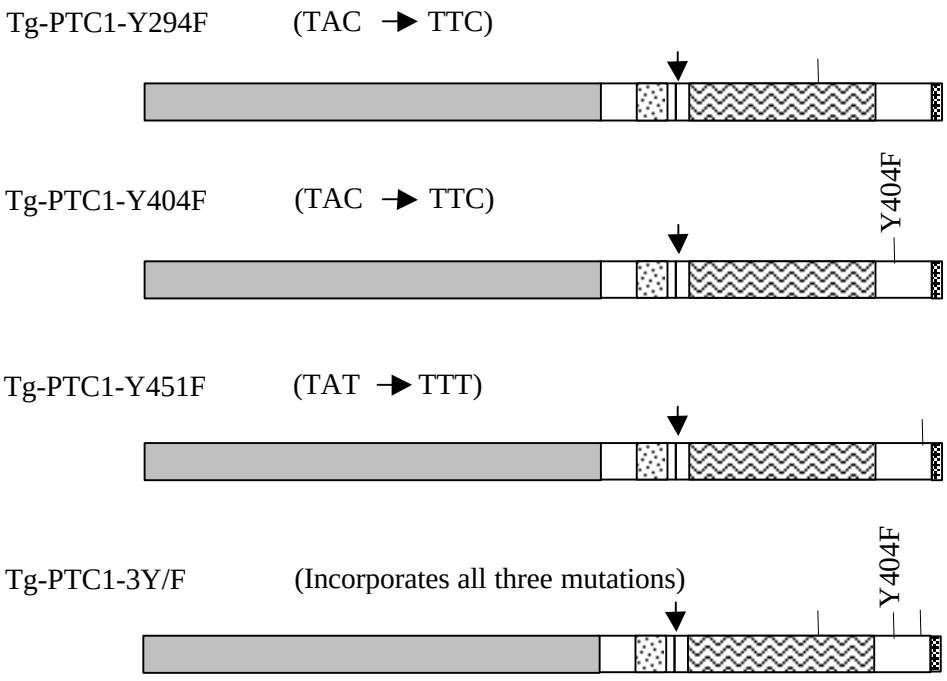

Figure 3.1: Transgene diagrams **A:** Diagram of the original Tg-PTC1 transgene (p9 isoform). **B:** Diagram of Tg-PTC1-Y/F site-directed mutant transgenes and their nucleotide point mutations. (b: bovine, CC: coiled-coil domain, pA: polyadenylation signal sequence, Tg: thyroglobulin, TK: tyrosine kinase domain.)

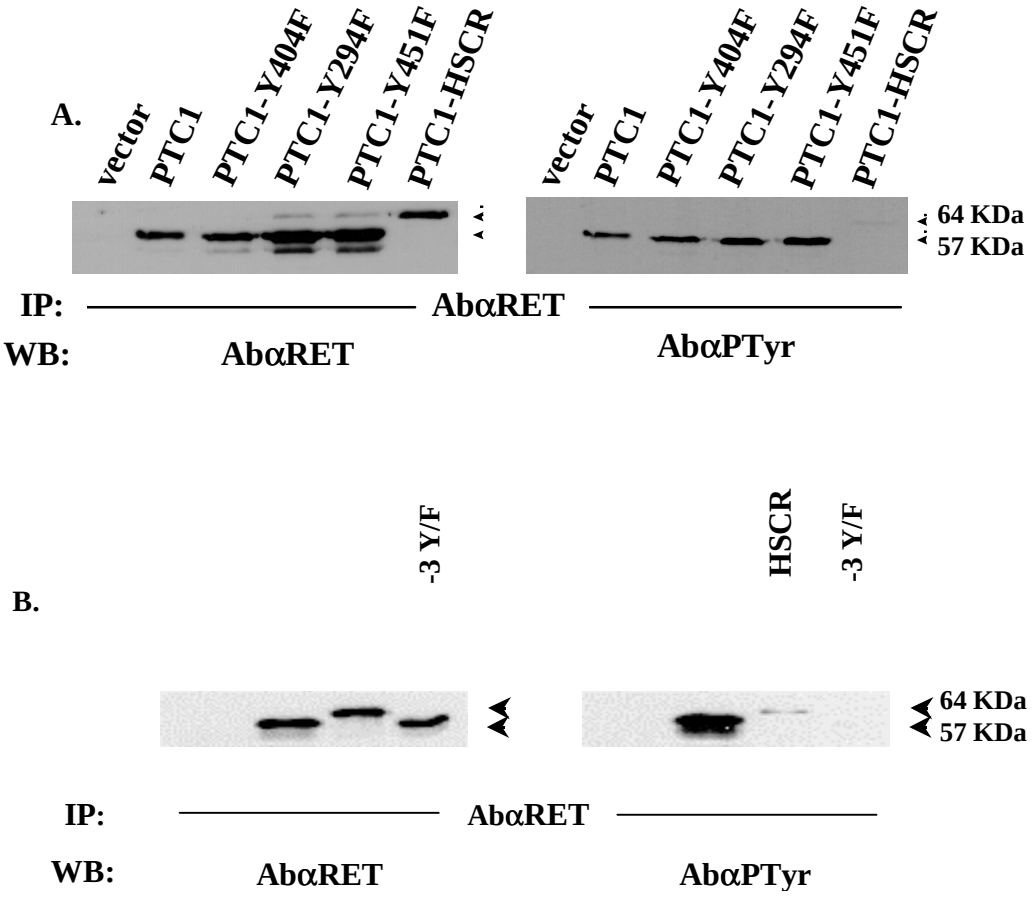

Figure 3.2: Expression and tyrosine phosphorylation of RET/PTC1 (Y294F, Y404F, Y451F, or 3Y/F) in cell culture. COS-7 cells were transiently transfected with the indicated cDNA's (p9: 57 KDa, p51: 64 KDa). Cell lysates were then immunoprecipitated (IP) using antibody against the C-terminus of RET. RET expression and tyrosine phosphorylation were then detected by Western blot analysis (WB) using antibody against either the tyrosine kinase domain of RET (C1 Ab) or against phosphotyrosine (4G10 Ab). **A:** Expression and tyrosine phosphorylation of Tg-PTC1-Y/F single mutants. (Xing, 1998) **B:** Expression and tyrosine phosphorylation of Tg-PTC1-3Y/F triple mutant. (HSCR: RET kinase inactive Hirschsprung disease mutation)

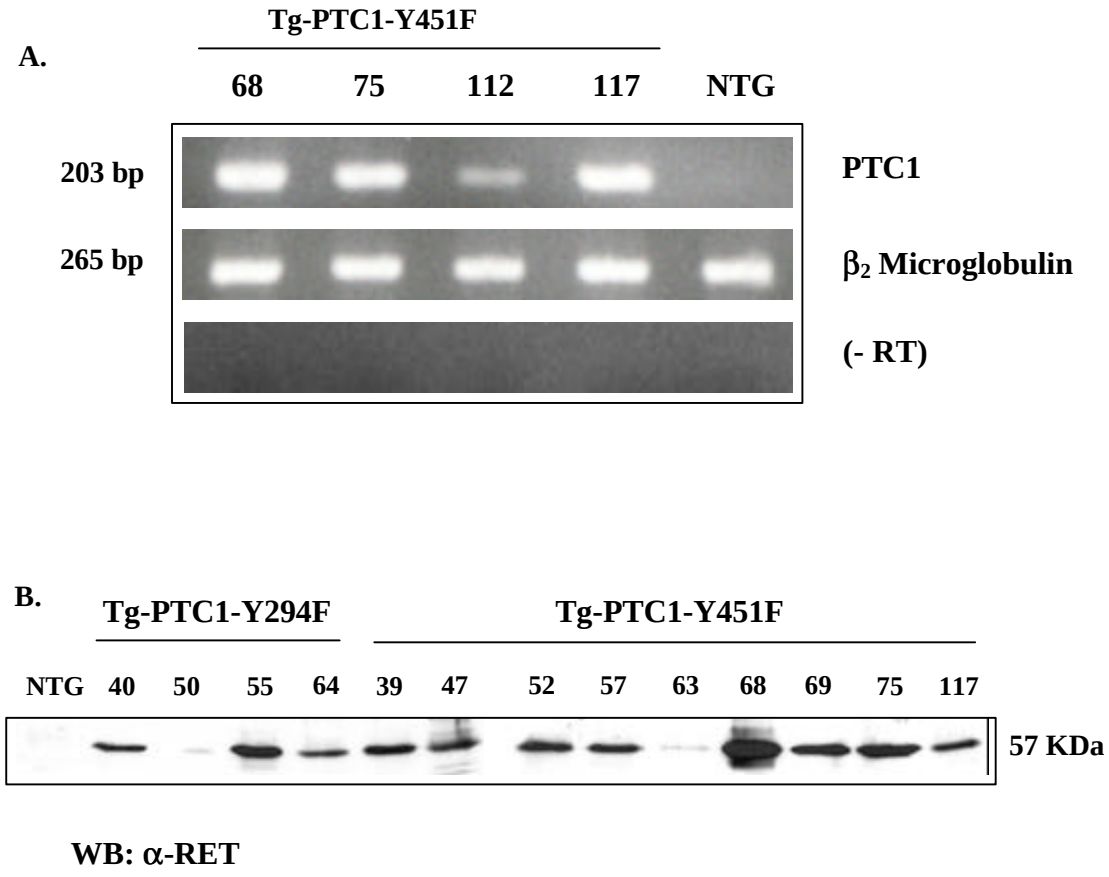

Figure 3.3: Tg-PTC1-Y/F expression in the thyroid gland of transgenic mice: RT-PCR and WB analysis. **A:** A representative RT-PCR analysis of the expression of *ret*/PTC1-Y451F in the thyroids of Tg-PTC1-Y451F transgenic mice. PCR was performed in the presence (+RT) or absence (-RT: without reverse transcription) of cDNA template. To test RNA integrity, PCR amplification of β_2 microglobulin was also performed. **B:** Western blot analysis (WB) showing the various expression levels of RET/PTC1-Y(294 or 451)F in the thyroids of transgenic mice. WB analysis using antibody against the C-terminus of RET (C-19 Ab), detected transgene expression in thyroid protein samples from transgenic mice. (NTG: non-transgenic)

	RT-PCR	WB
Tg-PTC1-Y294F		
40	(+)	(+)
45	ND	ND
50	(+)	(+)
53	(+)	ND
55	(+)	(+)
64	ND	(+)
Tg-PTC1-Y404F		
45	ND	ND
48	ND	(+)
3332	ND	(+)
3341	(+)	(+)
Tg-PTC1-Y451F		
28	(+)	(+)
39	(+)	(+)
47	(+)	(+)
52	(+)	(+)
57	(+)	(+)
59	(+)	ND
61	ND	ND
68	(+)	(+)
69	(+)	(+)
75	(+)	(+)
112	(+)	ND
117	(+)	(+)
Tg-PTC1-3Y/F		
62	(+)	(+)

Table 3.1: Summary of Tg-PTC1-Y/F expression *in vivo*. (ND: not determined.)

A.

Normal diet	*Grade 1*	*Grade 2*	*Grade 3*
Gross anatomy			*(0.4 x 0.4 x 0.2 -*
Size (cm)	0.4 x 0.4 x 0.2	0.4 x 0.4 x 0.2	*0.6 x 0.7 x 0.3)*
Color	Yellow/Pink (Y/p)	Y/p	Yellow (Y)
Histology			
Follicle structure	Round (RD)	RD, Irregular (IR)	IR>>RD
Colloid amount	Normal level (NL)	NL	10-50% NL
Epithelium	Cuboidal (CU)	CU	CU/CO/Spindle
Iodide Uptake	NL	IR:minimal, RD:NL	minimal
Tumor	No	No	Yes

B.

LID/PTU diet	*Grade 1*	*Grade 2*	*Grade 3*
Gross anatomy			*(0.6 x 0.6 x 0.3 -*
Size (cm)	0.6 x 0.6 x 0.3	0.6 x 0.6 x 0.3	*1.2 x 0.7 x 0.8)*
Color	Red/Purple (R/P)	R/P/Yellow (Y)	Y
Histology			
Follicle structure	Collapsed (CL)	CL, Irregular (IR)	CL, IR
Colloid amount	0-5% NL	5-25% NL	10-50% NL
Epithelium	Columnar (CO)	CO/CU	CO/CU/Spindle
Tumor	No	No	Yes

Table 3.2: Thyroid histology grading system. Thyroids were graded both by gross anatomical observations and microscopic histological analysis. Each thyroid received a grade of 1, 2 or 3, depending on severity of alteration from normal thyroid phenotype. **A**: Normal diet samples. **B**: Low iodide diet + propylthiouracil (LID/PTU) diet samples.

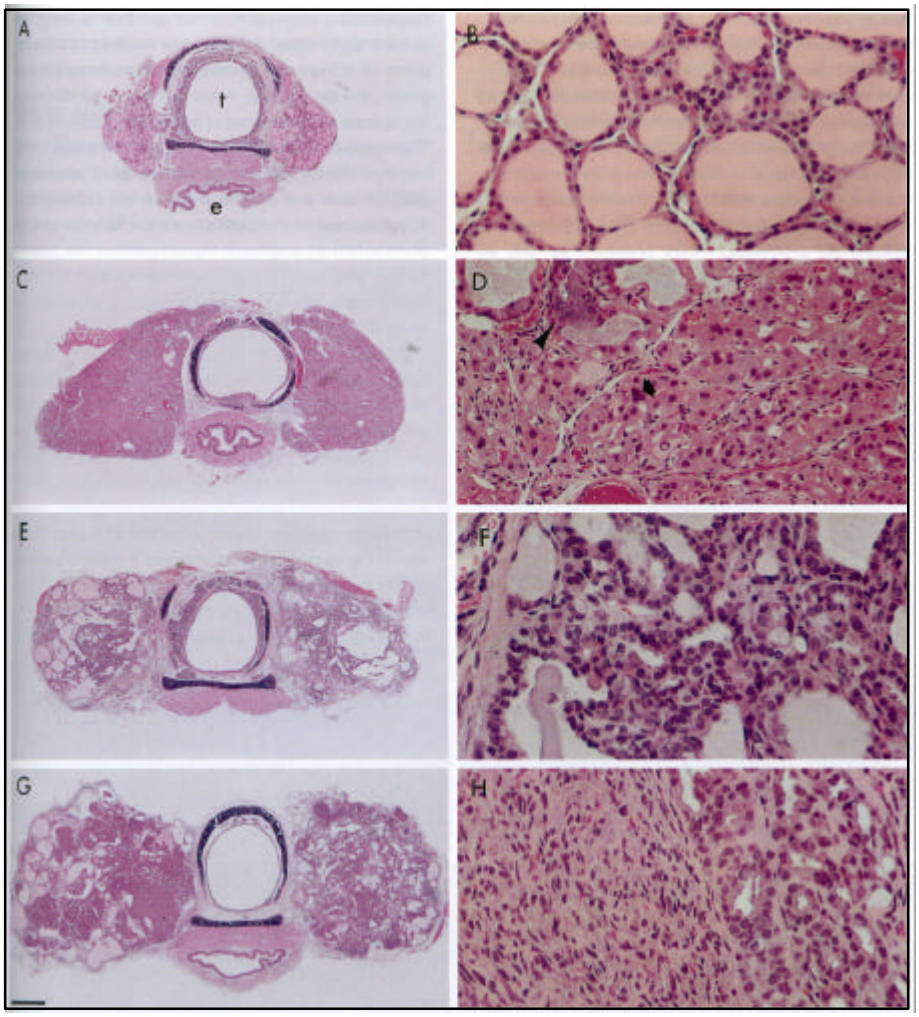

Figure 3.4: H & E stained thyroid glands from non-transgenic mice or Tg-PTC1 transgenic mice. A, B: non-transgenic thyroid (normal diet). C, D: non-transgenic thyroid (LID: low iodine diet). E, F: Tg-PTC1 transgenic thyroid (normal diet). G, H: Tg-PTC1 transgenic thyroid (LID). Bar: 470 µm (A, C, E, G); 42 µm (B, D, F, H). (Sagartz, 1997)

Figure 3.5: H & E staining of thyroid glands from Tg-PTC1-Y/F transgenic mice, showing changes in lobular architecture upon increased histological grade. Normal diet samples: A (grade 1), C (grade 2), E (grade 3). LID/PTU diet samples: B (grade 1), D (grade 2), F (grade 3). (Bar = 3000 μm)

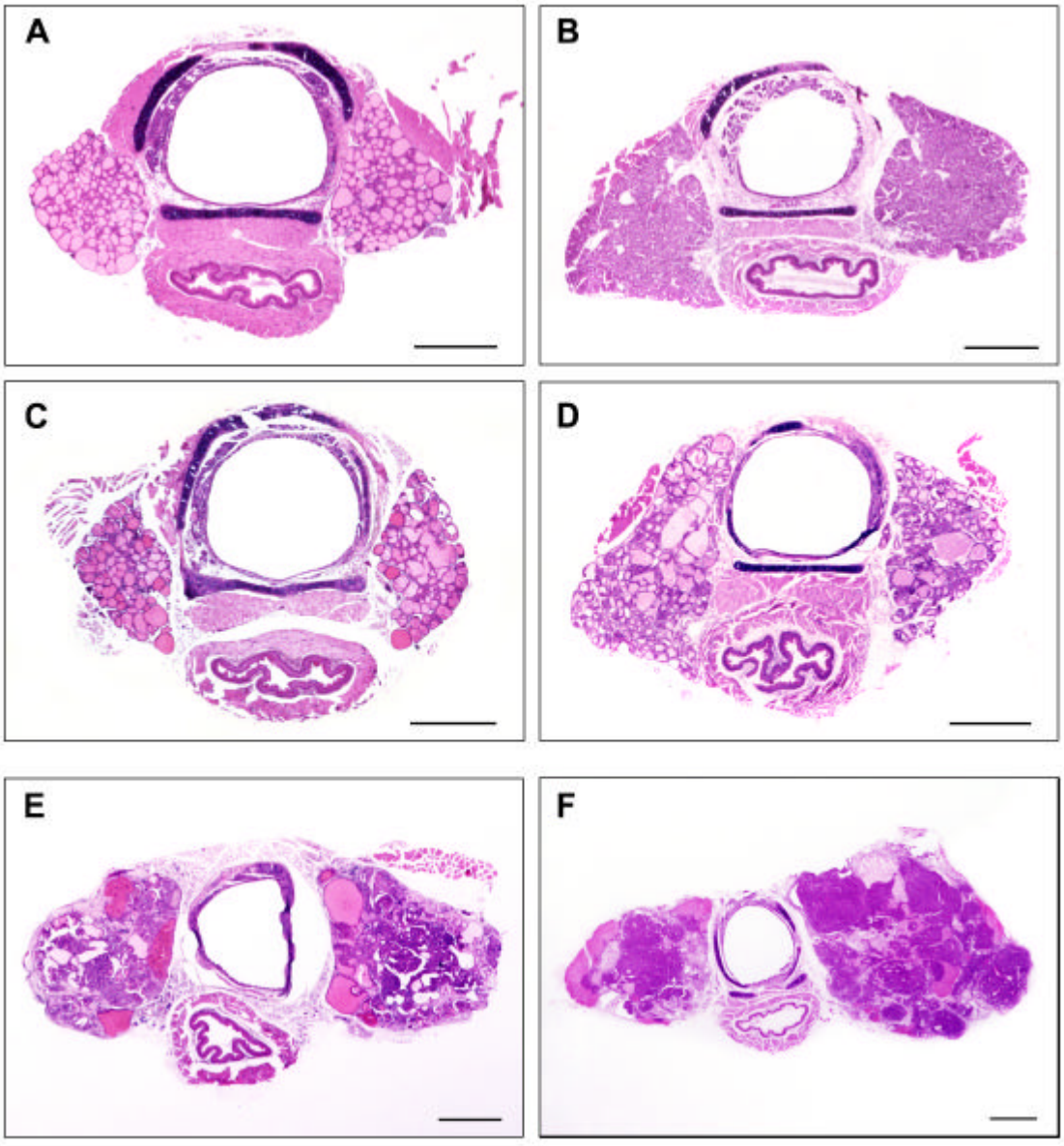

Fig. 3.5

Figure 3.6: H & E staining of thyroid glands from Tg-PTC1-Y/F transgenic mice fed normal diet. Assignment of histological grade corresponded with increased alteration of follicle structure. A: grade 1, B-C: grade 2, D-F: grade 3. (Bar = 1500 μm)

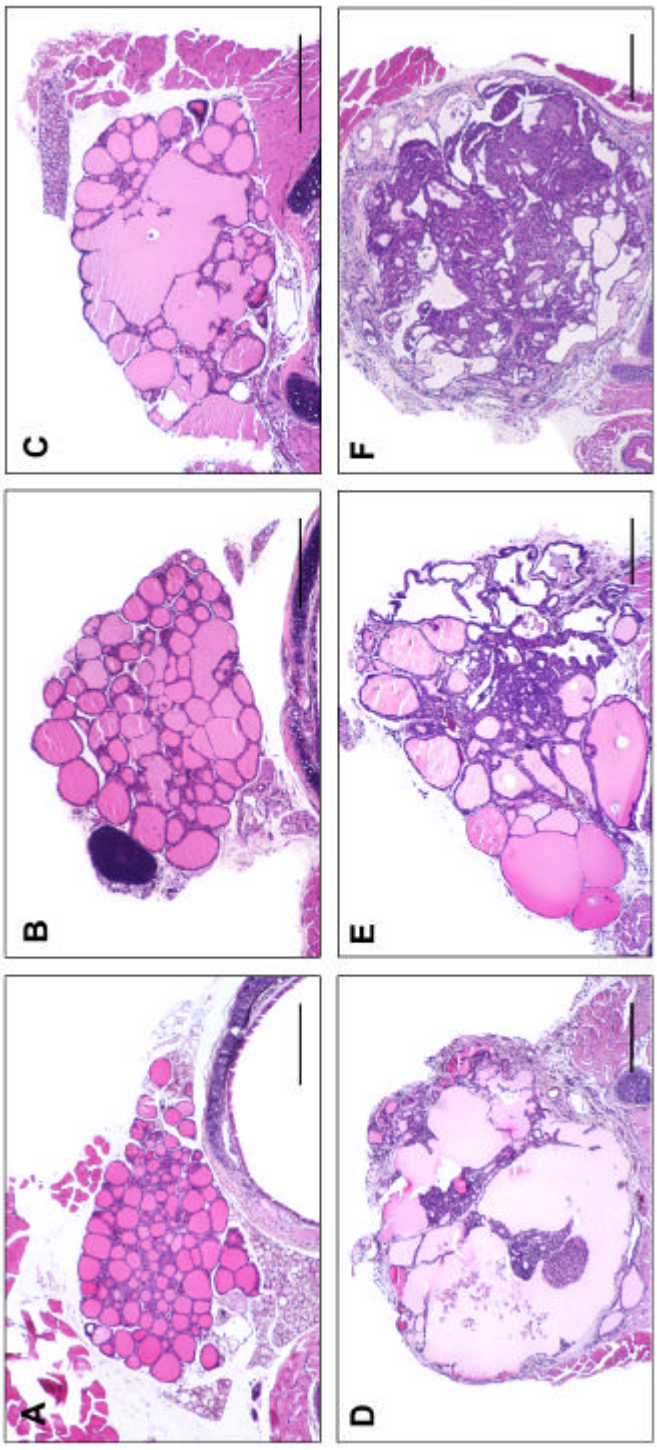

Fig. 3.6

Figure 3.7: H & E staining of thyroid glands from Tg-PTC1-Y/F transgenic mice fed LID/PTU diet. Increasing follicle structure abnormality is seen with increased histological grade. A: grade 1, B-C: grade 2, D-F: grade 3. (Bar = 1500 μm)

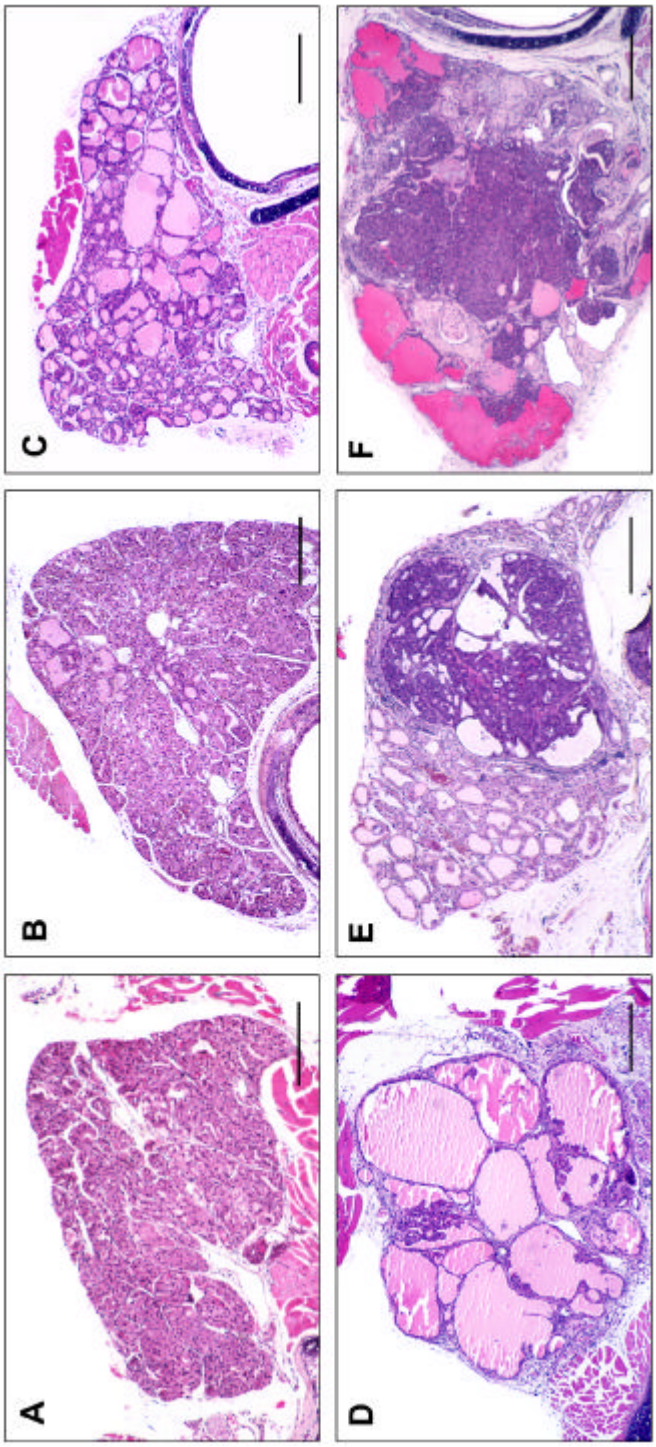

Fig. 3.7

Figure 3.8: Radioiodine accumulation in the thyroid glands of Tg-PTC1-Y/F mice. A decrease in iodide uptake is seen in regions of follicular distortion or tumor formation. Serial sections were used for hematoxylin staining (A, C, E) and autoradiography (B, D, F). A-B: grade 1. C-D: grade 2. E-F: grade 3. (Bar = 1500 μm)

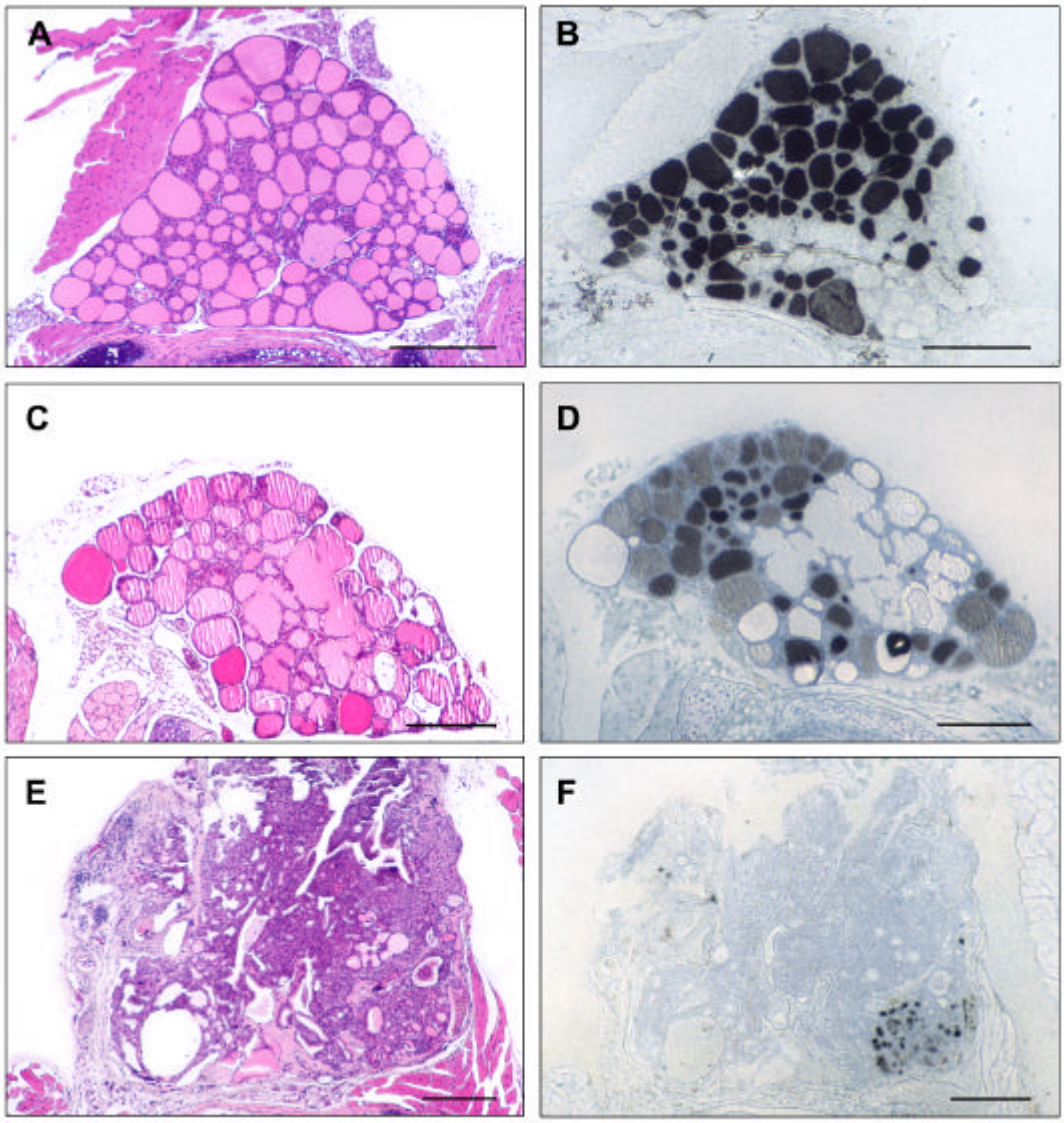

Fig. 3.8

Control groups

	Diet	(n) per grade			(n)	Avg ±SD
		1	2	3		
NTG	***Normal***	32	3		35	1.1 ± 0.3
	L/P	17	3	1	21	1.2 ± 0.5
PTC1	***Normal***			5	5	3.0 ± 0.0
	L/P				0	

Table 3.3: Histological analysis of non-transgenic (NTG) and Tg-PTC1 mice. The table shows the number of mice per transgenic group, per diet, per grade. The average grade is shown with the standard deviation (Avg ± SD). (L/P: Low iodine diet + propylthiouracil)

Tg-PTC1-Y294F

Line #	Diet	(n) per grade			(n)	Avg ± SD
		1	2	3		
40	***Normal***	2			2	1.0 ± 0.0
	L/P	4	1		5	1.2 ± 0.4
45	***Normal***	9	1	1	11	1.3 ± 0.6
	L/P				0	
50	***Normal***	1	1		2	1.5 ± 0.7
	L/P				0	
53	***Normal***	1			1	1.0
	L/P	6			6	1.0 ± 0.0
55	***Normal***	3	1		4	1.3 ± 0.5
	L/P		2		2	2.0 ± 0.0
64	***Normal***	1	6		7	1.9 ± 0.4
	L/P	2	5	2	9	2.0 ± 0.7

Table 3.4: Histological analysis of Tg-PTC1-Y294F transgenic mice. The table shows the number of mice per transgenic line, per diet, per grade. The average grade is shown with the standard deviation (Avg ± SD). (L/P: low iodine diet + propylthiouracil)

Tg-PTC1-Y404F

Line #	Diet	(n) per grade			(n)	Avg ± SD
		1	2	3		
45	***Normal***	3			3	1.0 ± 0.0
	L/P	1	1		2	1.5 ± 0.7
48	***Normal***			6	6	3.0 ± 0.0
	L/P				0	
3332	***Normal***	4	3		7	1.4 ± 0.5
	L/P	2	6	6	14	2.3 ± 0.7
3341	***Normal***	2		1	3	1.7 ± 1.2
	L/P	1		3	4	2.5 ± 1.0

Table 3.5: Histological analysis of Tg-PTC1-Y404F transgenic mice. The table shows the number of mice per transgenic line, per diet, per grade. The average grade is shown with the standard deviation (Avg ± SD). (L/P: low iodine diet + propylthiouracil)

Tg-PTC1-Y451F

Line #	Diet	(n) per grade			(n)	Avg ± SD
		1	2	3		
28	***Normal***	15			15	1.0 ± 0.0
	L/P				0	
39	***Normal***	2			2	1.0 ± 0.0
	L/P	2	2		4	1.5 ± 0.6
47	***Normal***	4			4	1.0 ± 0.0
	L/P	5			5	1.0 ± 0.0
52	***Normal***				0	
	L/P	1	2		3	1.7 ± 0.6
57	***Normal***	5	2		7	1.3 ± 0.5
	L/P		3	2	5	2.4 ± 0.5
59	***Normal***		1		1	2.0
	L/P		2	1	3	2.3 ± 0.6
61	***Normal***		2		2	2.0 ± 0.0
	L/P				0	
68	***Normal***	3	2		5	1.4 ± 0.5
	L/P	1	5	1	7	2.0 ± 0.6
69	***Normal***		1		1	2.0
	L/P	2	1		3	1.3 ± 0.6
75	***Normal***	4			4	1.0 ± 0.0
	L/P	4	1		5	1.2 ± 0.4
112	***Normal***			21	21	3.0 ± 0.0
	L/P	6	3	9	18	2.2 ± 0.9
117	***Normal***		3		3	2.0 ± 0.0
	L/P		2	3	5	2.6 ± 0.5

Table 3.6: Histological analysis of Tg-PTC1-Y451F transgenic mice. The table shows the number of mice per transgenic line, per diet, per grade. The average grade is shown with the standard deviation (Avg ± SD). (L/P: low iodine diet + propylthiouracil)

Summary Chart

	Diet	(n) per grade 1	2	3	(n)	Avg ± SD
NTG	***Normal***	32	3		35	1.1 ± 0.3
	L/P	17	3	1	21	1.2 ± 0.5
Y294F	***Normal***	17	9	1	27	1.4 ± 0.6
(G)	***L/P***	12	8	2	22	1.5 ± 0.7
Y404F	***Normal***	9	3	7	19	1.9 ± 0.9
(P)	***L/P***	4	7	9	20	2.3 ± 0.8
Y451F	***Normal***	33	11	21	65	1.8 ± 0.9
(E)	***L/P***	21	21	16	58	1.9 ± 0.8
3 Y/F	***Normal***	7	3		10	1.3 ± 0.5
(GPE)	***LID***	2			2	1.0 ± 0.0
PTC1	***Normal***			5	5	3.0 ± 0.0
	L/P				0	

Table 3.7: Summary of histological analysis of Tg-PTC1-Y/F mice. The table shows the total number of mice per transgenic group, diet, and histological grade, as well as the average histological grade with standard deviation (Avg ± SD), per transgenic group and diet. (L/P: low iodine diet + propylthiouracil; LID: low iodine diet)

	Percentage of Grade within Mutation (Number)			
Mutation	**1**	**2**	**3**	***Total Number with Mutation***
NTG	87.5 (49)	10.7 (6)	1.8 (1)	56
3 Y/F	75.0 (9)	25.0 (3)	0.0 (0)	12
Y294F	59.2 (29)	34.7 (17)	6.1 (3)	49
Y451F	43.9 (54)	26.0 (32)	30.1 (37)	123
Y404F	33.3 (13)	25.6 (10)	41.0 (16)	39
PTC1	0.0 (0)	0.0 (0)	100.0 (5)	5
Overall Chi-Sq test	$p < 0.0001$			

Table 3.8: Cross-tabulation of the type of mutation and tissue grade. The table shows the percentage of mice per mutation group observed within each histological group. The total number of mice observed per group is shown in brackets, following the percentage amount. The *p* value reflects a significant difference in percentages among the different mutation groups of mice.

	Percentage of Grade within Diet (Number)			*Total Number*
Diet	**1**	**2**	**3**	***on Diet***
LID/PTU	45.9 (57)	31.5 (39)	22.6 (28)	124
Normal	60.6 (97)	18.1 (29)	21.2 (34)	160
Overall Chi-Sq test	$p = 0.018$			

Table 3.9: Cross-Tabulation of diet and tissue grade. The percentage and number of mice (in parentheses) per histology group, per diet is examined. Diet is shown to play a significant role in overall histology grading, as the *p* value is less than 0.05.

	Percentage of Grade within Age group (Number)			
Age group	**1**	**2**	**3**	***Total Number in Age Group***
0-6 months	66.9 (77)	16.5 (19)	16.5 (19)	115
6-12 months	46.4 (64)	28.3 (39)	25.4 (35)	138
12 + months	41.9 (13)	32.2 (10)	25.8 (8)	31
Overall Chi-Sq test	$p = 0.011$			

Table 3.10: Cross-Tabulation of age and tissue grade. The percentage and number of mice (in parentheses) per histology group, per age group is examined. Age is shown to play a significant role in overall histology grading, as the *p* value is less than 0.05.

	Percentage of Grade within Sex (Number)			*Total Number*
Sex	**1**	**2**	**3**	***in Sex***
Female	47.8 (75)	26.1 (41)	26.1 (41)	157
Male	59.3 (70)	22.9 (27)	17.8 (21)	118
Overall Chi-Sq test	$p = 0.132$			

Table 3.11: Cross-tabulation of sex and tissue grade. The percentage and number of mice evaluated (in parentheses) per histological group, per sex, are displayed. Chi-square analysis shows there is no significant relationship between sex and grade, with a p value greater than 0.05.

Comparison of frequency of tumor formation (grade3) of PTC1 Y/F groups versus Controls

Mutation	***Tumor frequency(%)***	**vs NTG***	**vs PTC1****
3 Y/F	0.0	0.383	< 0.001
Y294F	6.1	< 0.004	< 0.001
Y451F	30.1	< 0.0001	0.004
Y404F	41.0	< 0.0001	0.068

*** Chi-Sq test *p* value**
**** Fisher's Exact *p* value**

Table 3.12: Comparison of the frequency of tumor grade of PTC1 Y/F groups versus the control groups (NTG and PTC1). Chi-square analysis shows that the frequency of tumor formation of all groups except PTC1 3Y/F is significantly different from NTG. Comparison against PTC1, by Fisher's exact test, shows that all groups except Y404F are significantly different from PTC1 in terms of tumor formation.

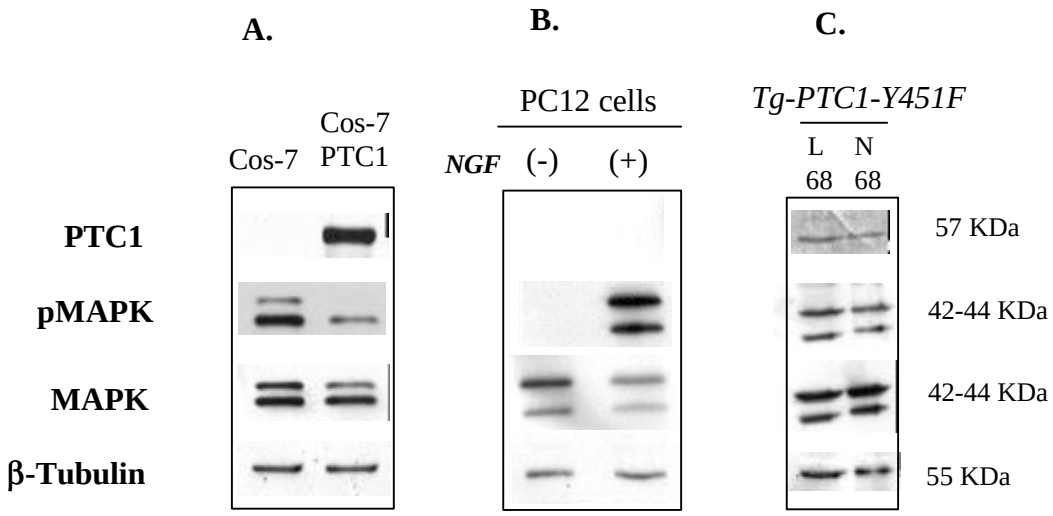

Figure 3.9: Western blot analysis comparing PTC1, phosphorylated MAPK, MAPK, and tubulin expression in cell culture or in mice thyroids (diet comparison). **A:** Cos-7 cells transiently transfected with PTC1 cDNA show specific recognition of PTC1 by anti-RET polyclonal antibody, C-19, in contrast to the Cos-7 parental cells, and thus serve as a positive control for PTC1 detection. **B:** PC12 cell extracts serve as controls for the detection of phosphorylated MAPK (pMAPK). Nerve growth factor (NGF) stimulates MAPK phosphorylation in PC12 cells. Thus, only the cells treated with NGF show pMAPK, despite the presence of MAPK in both sets of extract. **C:** The role of LID/PTU diet upon transgene expression and MAPK phosphorylation was analyzed. Protein samples from two mice from the same line (Tg-PTC1-Y451F, # 68 line), treated with different diets (LID/PTU diet: L; normal diet: N) were analyzed. WB analysis suggests a failure of the LID/PTU diet to significantly boost transgene expression and a minimal impact upon MAPK phosphorylation.

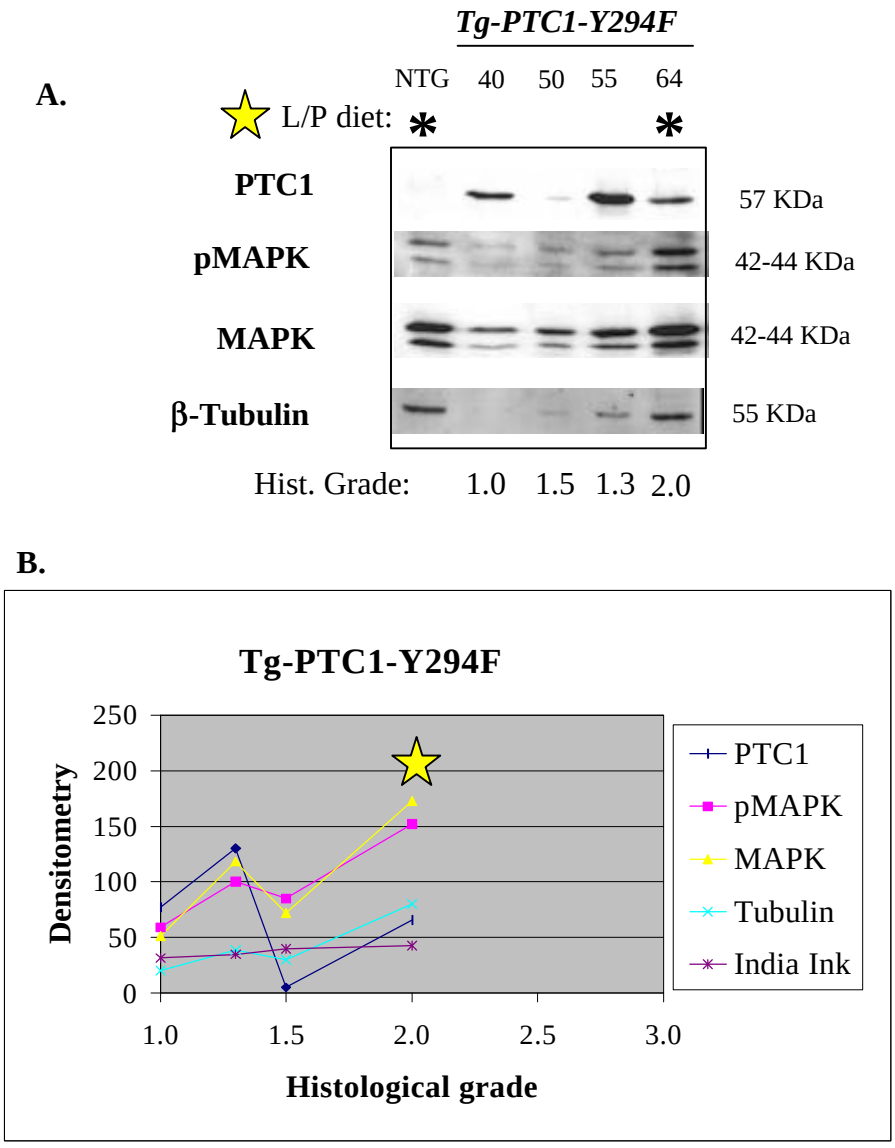

Figure 3.10: Western blot analysis and comparison against average histological grade for the Tg-PTC1-Y294F group. **A:** Western blot analysis of mouse thyroid protein samples from Tg-PTC1-Y294F mice was performed, probing the protein samples with antibody against PTC1, pMAPK, MAPK, and β-tubulin. **B:** Densitometry values from the above WB analysis were plotted against average histological grade of the line of origin of the protein sample.

A.

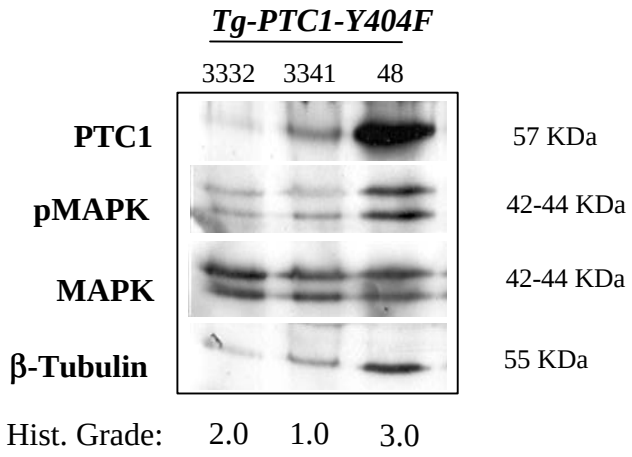

B.

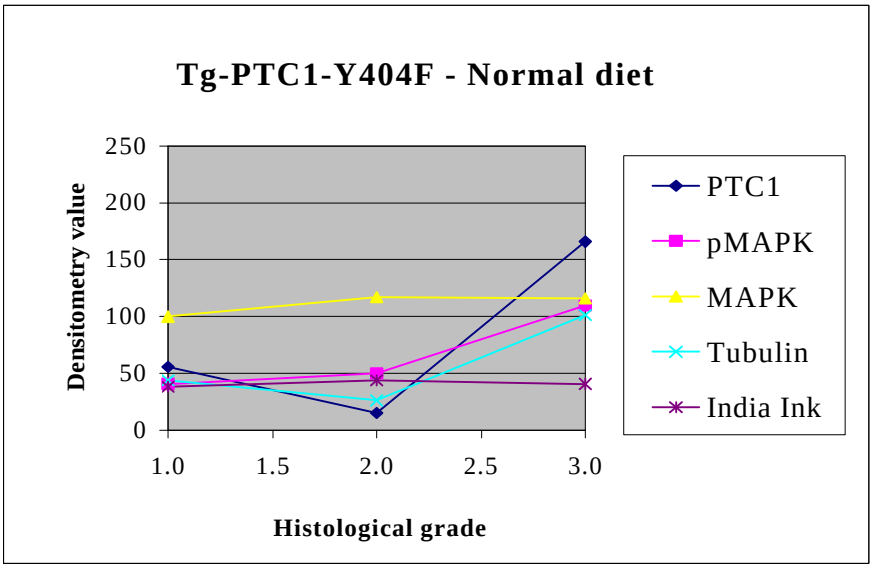

Figure 3.11: Western blot analysis and comparison against average histological grade for the Tg-PTC1-Y404F group. **A:** Western blot analysis of mouse thyroid protein samples from Tg-PTC1-Y404F mice was performed, probing the protein samples with antibody against PTC1, pMAPK, MAPK, and β-tubulin. **B:** Densitometry values from the above WB analysis were plotted against average histological grade of the line of origin of the protein sample.

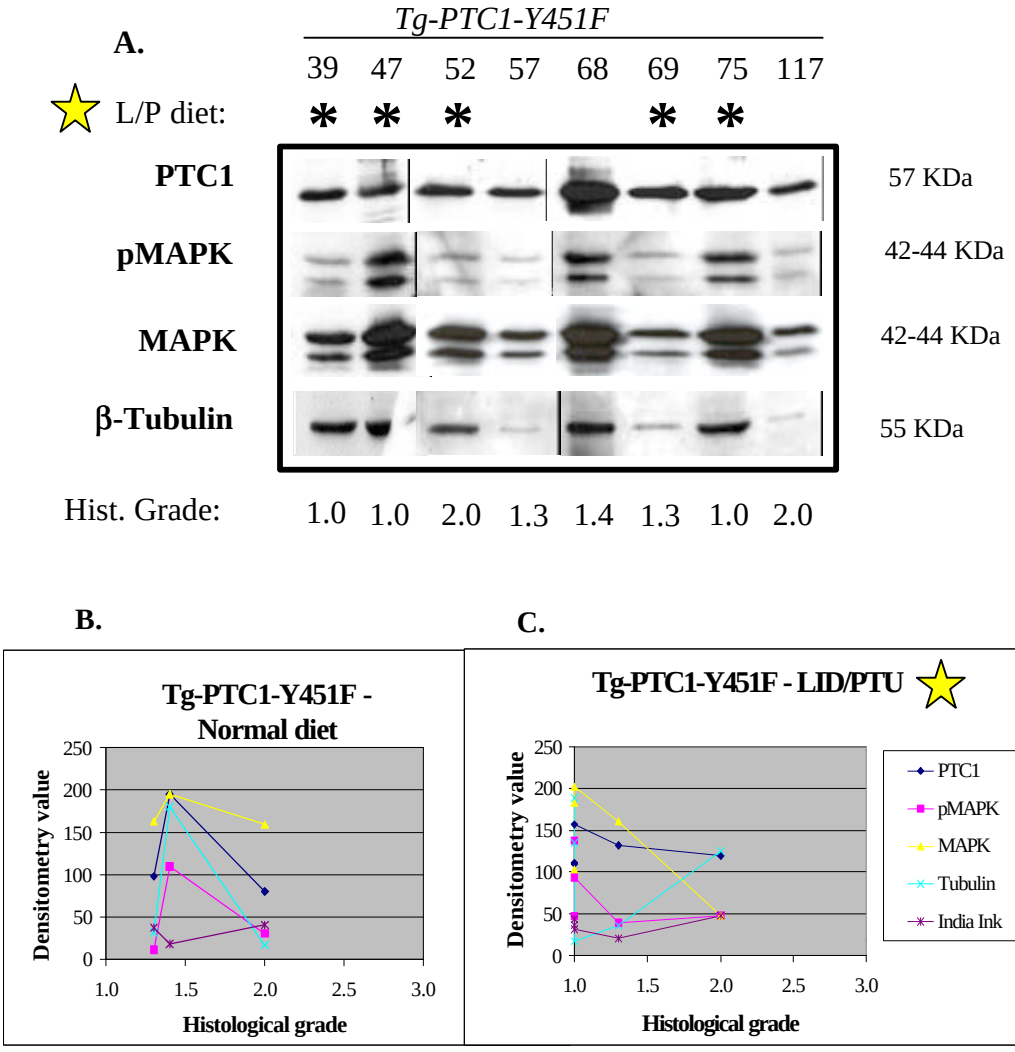

Figure 3.12: Western blot analysis and comparison against average histological grade for Tg-PTC1-Y451F mice. **A:** Western blot analysis of mouse thyroid protein samples from Tg-PTC1-Y451F mice was performed, probing the protein samples with antibody against PTC1, pMAPK, MAPK, and β-tubulin. Densitometry values from the above WB analysis were plotted against average histological grade of the line of origin of the protein sample. **B:** Normal diet samples. **C:** LID/PTU diet samples.

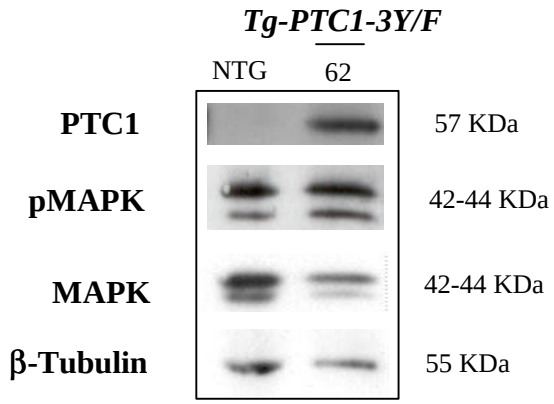

Figure 3.13: Western blot analysis of a mouse thyroid protein sample from the Tg-PTC1-3 Y/F group. Following SDS-PAGE resolution, protein samples were probed with antibody against PTC1, pMAPK, MAPK, and β-tubulin.

Variable	PTC1	pMAPK	MAPK	Tubulin
Mutation	0.5318	0.3501	0.0131	0.5708
Diet	0.4027	0.0845	0.3951	0.0378
Age	0.3243	0.9567	0.7228	0.9689
Hist grade	0.9259	0.1769	0.9675	0.3152

Table 3.13: Analysis of variance of densitometry values. Comparisons were made between type of transgene mutation, diet, age, or histological grade (Hist grade) versus the immunoblot densitometry values for each of the four proteins profiled; PTC1, pMAPK, MAPK and tubulin. The table displays the overall F-test p values. Values of $p < 0.05$ are considered significant.

CHAPTER 4

DISCUSSION AND FUTURE STUDIES

Decreased tumor formation in Tg-PTC1-Y/F transgenic mice

This study has shown an overall decrease in rate of tumor formation in transgenic mice with thyroid-targeted expression of the Tg-PTC1-Y(294, 404 and/or 451)F transgene, compared to the original Tg-PTC1 transgene. Although only one transgenic line was established and investigated for the triple mutant group, the absence of tumor formation in this group is most likely due to kinase inactivation, as PTC1-3Y/F was not tyrosine phosphorylated in Cos-7 studies. It is unlikely that the observed lack of tyrosine phosphorylation is due to a structural change in the protein leading to the complete abolishment of PTC1 autophosphorylation sites, as the tyrosine to phenylalanine mutation is highly conservative resulting in the removal of a single hydroxyl group. Further, it is unlikely that the PTC1-3Y/F mutation will completely abolish PTC1 autophosphorylation, as there are additional PTC1 autophosphorylation sites which are not mutated (pY215 and pY418). Thus, the lack

of tyrosine phosphorylation seen in the PTC1-3Y/F mutant is most likely due to the essential role of these three tyrosine residues towards PTC1 tyrosine kinase activity.

It is of interest to note that while the combination of three mutations did result in inactivation of tyrosine kinase activity in PTC1-3Y/F, a single mutation changing any one of the three tyrosine residues to phenylalanine did not result in inactivation of tyrosine kinase activity. Further, the observed decrease in tumor formation of the single mutant PTC1 transgenic mice indicates that signaling pathways mediated by phosphotyrosines (pY) 294 (Grb10), pY404 (PLCγ), and pY451 (Enigma and Shc), do play a role in PTC1-induced tumor formation in thyroid glands. However, as tumors are still able to form in some transgenic mice from all three single mutant transgenic groups, it would appear that the signaling pathways mediated by one of these three pY can be compensated by alternative pathways and lead to tumor formation. It is not known whether the signaling pathways mediated by these three pY cross-talk with each other or become convergent to a few major signaling pathways. It will be of interest to investigate tumor formation in transgenic mice with thyroid-targeted expression of double mutants involved in two of the three pY residues, Y(294, 404)F, Y(294, 451)F, or Y(404, 451)F.

Distorted follicle formation

Distorted or coalescing follicles were observed in both normal and LID/PTU diet groups. The exact mechanism causing the distorted follicles is unclear. It is

interesting to note that a significant increase in the number of thyroids with distorted follicles was observed in Tg-PTC1-Y404F transgenic mice fed LID/PTU diet. However, the increase in distorted follicles is not observed in non-transgenic (NTG), Tg-PTC1-294F, or Tg-PTC1-Y451F transgenic mice fed with LID/PTU. It is possible that the increase in distorted follicles is due to the ease of detecting distorted follicles in the thyroid glands from mice fed with LID/PTU diet, rather than a direct effect of TSH stimulation to induced distorted follicles. Indeed, when observing the histology samples within the grade 2 LID/PTU group, it appears that the distorted follicles are actually not responding to TSH stimulation, in that they are usually neither hypertrophic nor hyperplastic, and they usually retain a certain amount of colloid.

One possible explanation for distorted follicles would be a de-differentiation effect of PTC1. It appears that the cells are not responding to either internal signals to maintain a certain size follicle structure in the case of normal diet samples, or external signals to respond to TSH stimulation and become hyperplastic in the case of LID/PTU diet samples. Indeed, distorted follicles were observed in the thyroid glands of Tg-PTC1 transgenic embryos as early as embryological day 16, prior to tumor formation (Cho, 1999). Furthermore, the de-differentiation effects of PTC1 have been clearly demonstrated in cultured cells showing that PTC1 activation leads to the loss of expression or function of two transcription factors active in the thyroid (Pax-8 and TTF-1), and reduced expression of Tg and TPO (DeVita, 1998). Further, NIS expression has been shown to be regulated by Pax-8 (Ohno, 1999). De-differentiation

may induce dramatic changes in cytoskeletal proteins, potentially influencing tight junction interactions, membrane stability, or even the rate of phagocytosis, thus influencing the shape of the follicles. Furthermore, this distortion may be an intermediate step toward thyroid tumorigenesis. With the full complement of PTC1 tyrosine residues, the event would perhaps naturally lead much more quickly to tumor formation. However, it is possible that the existence of the Y/F mutations has impeded the natural flow of tumorigenesis, such that the process is stopped or slowed down to the point where the researcher can observe it.

In order to address de-differentiation effect of PTC1 *in vivo*, one could take advantage of a study currently under investigation in our lab, which is to create a thyroid-targeted inducible PTC1 transgenic mouse model. In this model, PTC1 expression can be induced or shut-down at any given time by adding or withdraw doxycyclin. A temporal study could be performed to correlate transgene expression with histological changes, as well as changes in expression and function of several key proteins correlating with differentiated versus de-differentiated status. These proteins could include thyroid transcription factors (Pax-8, TTF-1, etc), proteins involved in follicular cell cytoskeletal structure (actin, tubulin, etc), proteins involved in thyroid function (NIS, Tg, TPO), proteins involved in cellular signaling (MAPK activation), and de-differentiation markers (PCNA, myc, ras, p53, EMA, and CA50) (McDermott, 2000). The interaction between PTC1-induced signaling pathways, leading to distorted follicles, and TSH-stimulated signaling pathways leading to changes in actin

depolimerization (Villione, 1993) can also be investigated. Alternatively, one could look on a broader spectrum using gene array analysis, comparing gene expression patterns within thyroid RNA populations from grade 1, 2 and 3 thyroids, against known controls (RNA from normal thyroid tissue with or without TSH stimulation).

Reduced radioiodine-concentrating activity

Radioiodine-concentrating activity is normally heterogeneous among different follicles in NTG mice with some cells always displaying increased radioiodine accumulation. In contrast, radioiodine-concentrating activity was always severely decreased in regions of the thyroid containing either distorted follicles or tumors in PTC1 or PTC1Y/F transgenic mice. Reduced radioiodine-concentrating activity and distorted follicles have previously been detected in the thyroid glands of Tg-PTC1 transgenic embryos as early as embryological day 16 (Cho, 1999), suggesting that PTC1-induced signaling pathways may have direct effects on reduced radioiodine-concentrating activity and distorted follicles preceding tumor formation. Support for this hypothesis lies in several previous studies. First, PTC1 expression has been shown to decrease expression of Pax-8, Tg, and TPO, and to decrease the function of Pax-8 and TTF-1 in cell culture (De Vita, 1998). Further, a decrease in NIS mRNA levels was detected within tumors seen in Tg-PTC1 mice thyroids (Cho, 1999). However, this study shows that abolishing signaling pathways mediated by pY294, pY404, or pY451 alone does not abolish the signaling pathways induced by PTC1 that lead to reduced radioiodine concentrating activity and distorted follicles.

Intra- and inter-line variation

It is interesting to speculate on the nature of intra- and inter-line variations that exist within each of the single mutant transgenic groups. Inter-line variations could be due to differences between transgenic lines in the transgene copy number or integration sites. Inter-line phenotype differences coinciding with both copy number and protein expression differences have been identified in *ret*/MEN2B transgenic mice (Sweetser, 1999). Thus, copy number differences may play a key role. However, along those same lines, that difference should also be identifiable by WB analysis. Further, copy number differences can sometimes be of secondary concern to integration site differences, as differences in transgene copy number would have a minimal impact upon the transgene expression level when the integration site is a transcriptionally silent region. Integration site differences may impact upon inter-line variation, potentially affecting the expression profile of the transgene in terms of the expression levels, the time of expression onset, and the duration of expression.

However, WB analysis did not show a correlation between the expression levels of transgene and histological grading (for examples, see Table 3.13, PTC1ΔG-40 vs. PTC1ΔG-64, PTC1ΔE-39 vs. PTC1ΔE-117). While it is tempting to conclude that transgene expression levels do not have an impact on histological grades, this issue is complicated by the use of a thyroid-tissue specific and TSH-responsive Tg promoter. It is known that PTC1 does have a de-differentiation effect in thyroid

follicular cells. Therefore, when the thyroid cells express PTC1 to a certain degree, the cells may become de-differentiated to a certain extent, leading to decreased Tg promoter activity which down-regulates PTC1 expression. Therefore, the lack of correlation between transgene expression levels and histological grades can only lead to the conclusion that a high level of transgene expression may play a role in inducing tumor formation, and that it is not required to maintain tumor formation in the thyroid gland.

The onset of transgene expression may also play an important role in determining thyroid morphology. Recently, a study was reported showing a correlation between the increased rate of tumor formation and the earlier expression of the *RET* oncogene under the control of the mouse metallothionein promoter (Kato, 1999). The study hypothesized that when a high level of the transgene is expressed before birth in conjunction with tumor formation, the animal's immune system fails to recognize the tumor expressing the transgene and therefore allows the tumor to continue progressing. In contrast, for transgenic mice with transgene expression levels that peak after birth, the immune system will recognize the transgene product as a foreign protein and prevent the tumor from further developing. Therefore, transgenic mice with a later onset of transgene expression have a decreased rate of tumor formation. The thyroid-targeted inducible PTC1 transgenic mouse model would be able to address the importance of onset of transgene expression in relation to tumor formation.

Lastly, the difference could be due to duration of expression. Expression for a long enough period of time may eventually shift the balance of the cell's fate towards oncogenesis. Interestingly, the statistical results did show that while there was no significant relationship between the expression levels of PTC1-Y/F and age, there was a significant correlation between increasing age of the animal and increasing histological grade. However, with increasing age comes the increased possibility of "second hits", mutations occurring in another gene, which often result in a more aggressive phenotype. The thyroid-targeted inducible PTC1 transgenic mouse model would be able to address the importance of duration of transgene expression in relation to tumor formation.

In contrast to inter-line variation, intra-line variation should not be due to integration site differences. Therefore, intra-line variations may instead be due to the weak oncogenic potential of the mutated PTC1-Y/F transgene. Cell culture studies have shown that mutating these tyrosine residues will reduce PTC transforming activity. Thus PTC-Y/F has less control of the cell culture fate than the fully oncogenic PTC. The challenges of controlling cell fate are, no doubt, more intense in the *in vivo* animal model system. Cells in the animal system are influenced by a vast array of signaling molecules and pathways. As an oncogene, PTC1's signaling presumably takes advantage of a pathway common to several cell fates, exploiting it for the benefit of PTC1 and inducing uncontrolled proliferation. A weakened version

of PTC1 may not be able to completely dominate the signaling trends of the cell, providing an opportunity for a wide array of different cellular microenvironments to affect tumor formation, and thus result in intra-line variation.

Low Iodine Diet supplemented with Propylthiouracil

A portion of mice was fed a low iodine diet (LID) supplemented with propylthiouracil (PTU). The objective was two-fold: to increase the thyroid mass to isolate more protein, as well as to increase the transgene expression level to help enhance any transgene-induced phenotype. By way of the hypothalamic-pituitary-thyroid axis, LID/PTU was expected to promote TSH stimulation of the thyroid, inducing cell proliferation, goiter, and thus an enlarged thyroid. Further, TSH stimulation is known to cause an increase in Tg expression, and therefore, should also result in an increased expression of Tg-PTC1 (Y/F), as the transgene expression is driven by the Tg promoter.

As expected, mice fed with the LID/PTU diet had hyperplastic, hypertrophic, and enlarged thyroids. These results are consistent with that observed by others (Wynford-Thomas, 1982; Sagartz, 1997; Cho, 1999). While Tg levels were not analyzed at the RNA or protein level, WB analysis showed that there is no differences in transgene expression levels in the thyroid glands between transgenic mice fed a normal diet and transgenic mice fed LID/PTU diet. As stated above, PTC1 expression in cultured cells showed decreased expression of Pax-8, Tg and TPO, as well as

decreased function of Pax-8 and TTF-1 (De Vita, 1998). Therefore, TSH-induced increases in Tg and Tg-PTC1-Y/F expression may be negatively regulated by the expression of PTC1-Y/F. The interaction of PTC1-induced de-differentiation and the TSH-stimulated differentiation effects on thyroid follicular cells could be further investigated in cultured thyroid cells, provided the expression of PTC1 was not driven by the TSH-responsive Tg promoter.

In general, mice fed LID/PTU diet had slightly elevated histological grades compared to their normal diet counterparts: 1.5 versus 1.4 for Tg-PTC1-Y294F, 1.9 versus 1.8 for Tg-PTC1-Y451F, and 2.3 versus 1.9 for Tg-PTC1-Y404F. Among all mice investigated, LID/PTU diet has the highest impact on the increase of histological grades in Tg-PTC1-Y404F transgenic mice (Table 3.7). This may reflect the ability of TSHR to activate PLC (Berridge, 1989), potentially compensating to some extent for the loss of PLCγ activation by the Y404F mutation in this PTC1-Y404F mutant. Furthermore, statistical studies comparing the impact of LID/PTU on histological grade showed that the increase in histological grades is mainly contributed by the increase in the frequency of histological grade 2, but not grade 3 (data not shown). Therefore, TSH stimulation of the thyroid glands may facilitate the detection of distorted follicles but rarely promotes tumor formation. However, for transgenic mice genetically predisposed to develop thyroid tumors, TSH stimulation may facilitate the development of more aggressive tumors**,** as shown in tumors developed in Tg-PTC1-Y451F (Line #112), which had a higher amount of spindle cells.

It is noteworthy that while this study showed that the frequency of histological grade 3 (tumor formation) is not significantly increased in mice fed with LID/PTU, Thomas et al (1991) reported a rise in the rate of adenomas and carcinomas in rodents with hypersecretion of TSH. In this study, one of NTG mice fed with LID/PTU diet did develop a thyroid tumor by gross anatomy analysis. Half of the thyroid tissue was analyzed by histology confirming the existence of the thyroid tumor, the other half was analyzed by RT-PCR confirming its NTG status by showing the lack of transgene expression (data not shown). It is known that TSH stimulation leads to increased proliferation of thyroid follicular cells. It is possible that the proliferating thyroid cells may acquire a secondary mutation leading to tumor development. It would be of interest to investigate which genetic mutation leads to tumor formation in this sample.

Western blot analysis

To investigate whether transgene expression levels and the extent of MAPK activation correlate with histological grades in PTC1-Y/F transgenic mice, Western blot analysis was performed to determine the expression levels of transgene, MAPK, and pMAPK. Equal amounts of total protein were loaded for each sample. However, it is known that normal thyroid glands or thyroids with distorted follicles contain significant amounts of extracellular Tg stored in the lumen of follicle in the form of colloid. In contrast, thyroid glands with tumor formation have more cellularity, yet minimal extracellular Tg stored in the lumen of follicles. The equal amount of total

proteins loaded for each sample may have very different cell numbers between samples from thyroid tumors versus samples from normal or distorted follicles. To calibrate the difference in cell numbers among samples, the expression levels of tubulin were determined to serve as an internal control. However, it is not known whether tubulin expression is consistent between normal thyroid cells and tumorigenic thyroid cells. Therefore, it is challenging to compare expression levels of transgene, and the extent of MAPK activation, in samples of normal thyroid glands versus samples of thyroid tumors.

The relationship between the histological grades, the transgene expression levels, and the extent of MAPK activation varies among different transgenic mice. For Tg-PTC1-Y294F transgenic mice, the histological grade appears to correlate with the levels of pMAPK and MAPK, but not with the transgene expression levels. Considering that pMAPK and MAPK patterns were almost identical, it would suggest that the increase in histological grades is correlated with the increase in MAPK expression rather than MAPK activation. Furthermore, the increased expression of MAPK is not due to the increased transgene expression. For Tg-PTC1-Y404F transgenic mice, increasing histological grade was observed with increasing transgene expression, as well as increasing pMAPK levels. Interestingly, the expression levels of MAPK do not increase with the increase of histological grades. This data suggests that increased expression levels of the transgene as well as the associated MAPK activation may play a role in PTC1-induced tumor formation *in vivo*. For Tg-PTC1-

Y451F transgenic mice, no correlation can be found between histological grades and the expression levels of the transgene, or MAPK, or MAPK activation. Taken together, the expression levels of the transgene and the extent of MAPK activation may not serve as general indicators for thyroid tumor formation in these transgenic mice.

It is of interest to note that in both PTC1-Y294F and PTC1-Y451Y transgenic mice, the docking sites that mediate signaling pathways leading to MAPK activation have been abolished. No correlation can be found between MAPK activation and histological grades in these two transgenic groups. In contrast, in the PTC1-Y404F transgenic mice, the docking site that mediates signaling of the PLCγ pathway is abolished. Interestingly, these mice have a higher rate of tumor formation, and a correlation is seen between transgene expression, MAPK activation, and tumor development.

Conclusions

MAPK, PI3K, JNK, PLCγ, or Src have each been determined to be essential for full transforming activity of one of several RET variants, in cell culture. The RET TK tyrosine residues corresponding to PTC1 tyrosine residues 294, 404 or 451 have been shown to bind to Grb10/7, PLCγ, or Enigma and Shc, respectively. The objective of the current study was to determine the role of the 3 tyrosine residues, as intracellular docking sites, in PTC1-induced tumor formation. Our results suggest that

all three tyrosine residues do play a role in PTC1-induced signaling leading to tumor formation, as indicated by a decreased rate of tumor formation in their absence. It appears that pY294 and Grb10 play the most significant role towards PTC1-mediated tumor formation, followed by pY451 (Enigma and Shc), and lastly by pY404, with PLCγ playing perhaps the least significant role towards PTC1-induced tumor formation. However, as tumor formation was not completely abolished in any one of the single Y/F mutant transgenic groups, this suggests that multiple pathways each contribute towards the overall picture of PTC1-mediated thyroid tumor development.

LIST OF REFERENCES

Airaksinen, M., Titievsky, A., and Saarma, M. (1999). GDNF family neurotrophic factor signaling: Four masters, one servant? Molecular and Cellular Neuroscience 13:313-325.

Ajjan, R.A., Kamaruddin, N.A., Crisp, M., Watson, P.F., Ludgate, M., and Weetman, A.P. (1998). Regulation and tissue distribution of the human sodium iodide symporter gene. Clinical Endocrinology 49:517-523.

Alberti, L., Borrello, M.G., Ghizzoni, S., Torriti, F., Rizzetti, M.G., and Pierotti, M.A. (1998). Grb2 binding to the different isoforms of Ret tyrosine kinase. Oncogene 17(9):1079-1087.

Arighi, E., Alberti, L, Torriti, F., Ghizzoni, S., Rizzitti, M.G., Pelicci, G., Pasini, B., Bongarzone, I., Piutti, C., Pierotti, M.A., and Borrello, M.G. (1997). Identification of Shc docking site on Ret tyrosine kinase. Oncogene 14(7):773-782.

Asai, N., Murakami, H., Iwashita, T., and Takahashi, M. (1996). A mutation at tyrosine 1062 in MEN2A-Ret and MEN2B-Ret impairs their transforming activity and association with Shc adaptor proteins. Journal of Biological Chemistry 271(30):17644-17649.

Avantaggiato, V., Dathan, N.A., Grieco, M., Fabien, N., Lazzaro, D., Fusco, A., Simeone, A., and Santoro, M. (1994). Developmental expression of the *RET* proto-oncogene. Cell Growth and Differentiation 5:305-311.

Berridge, M.J., and Irvine, R.F. (1989). Inositol phosphates and cell signaling. Nature 341:197-205.

Bocciardi, R., Mograbi, B., Pasini, B., Borrello, M.G., Pierotti, M.A., Bourget, I., Fischer, S., Romeo, G., and Rossi, B. (1997). The multiple endocrine neoplasia type 2B point mutation switches the specificity of the Ret tyrosine kinase towards cellular

substrates that are susceptible to interact with Crk and Nck. Oncogene 15(19):2257-2265.

Bongarzone, I., Pierotti, M.A., Monzini, N., Mondellini, P., Manenti, G., Donghi, R., Pilotti, S., Grieco, M., Santoro, M., Fusco, A., Vecchio, G., and Della Porta, G. (1989). High frequency of activation of tyrosine kinase oncogenes in human papillary thyroid carcinoma. Oncogene 4(12):1457-1462.

Bongarzone, I., Monzini, N., Borrello, M.G., Carcano, C., Ferraresi, G., Arighi, E., Mondellini, P., Della Porta, G., and Pierotti, M.A. (1993). Molecular characterization of a thyroid tumor-specific transforming sequence formed by the fusion of ret tyrosine kinase and the regulatory subunit RI alpha of cyclic AMP-dependent protein kinase A. Molecular and Cellular Biology 13(1):358-366.

Bongarzone, I., Butti, M.G., Coronelli, S., Borrello, M.G., Santoro, M., Mondellini, P., Pilotti, S., Fusco, A., Della Porta, G., and Pierotti, M.A. (1994). Frequent activation of *ret* proto-oncogene by fusion with a new activating gene in papillary thyroid carcinomas. Cancer Research 54:2979-2985.

Borrello, M.G., Pelicci, G., Arighi, E., De Filippis, L., Greco, A., Bongarzone, I., Rizzetti, M.G., Pelicci P.G., and Pierotti, M.A. (1994). The oncogenic versions of the Ret and Trk tyrosine kinases bind Shc and Grb2 adaptor proteins. Oncogene 9(6):1661-1668.

Borrello, M.G., Alberti, L., Arighi, E., Bongarzone, I., Battistini, C., Bardelli, A., Pasini, B., Piutti, C., Rizzetti, M.G., Mondellini, P., Radice, M.T., and Pierotti, M.A. (1996). The full oncogenic activity of Ret/ptc2 depends on tyrosine 539, a docking site for phospholipase C gamma. Molecular and Cellular Biology 16(5): 2151-2163.

Ceccherini, I., Bocciardi, R., Luo, Y., Pasini, B., Hofstra, R., Takahashi, M., and Romeo, G. (1993). Exon structure and flanking intronic sequences of the human *ret* proto-oncogene. Biochemical and Biophysical Research Communications 196(3):1288-1295.

Chiariello, M., Visconti, R., Carlomagno, F., Melillo, R.M., Bucci, C., de Franciscis, V., Fox, G.M., Jing, S., Coso, O.A., Gutkind, J.S., Fusco, A., and Santoro, M. (1998). Signalling of the Ret receptor tyrosine kinase through the c-Jun NH2-terminal protein kinases (JNKs): evidence for a divergence of the ERKs and JNKs pathways induced by Ret. Oncogene 16(19):2435-2445.

Cho, J.Y., Sagartz, J.E., Capen, C.C., Mazzaferri, E.L., Jhiang, S.M. (1999). Early cellular abnormalities induced by *RET*/PTC1 oncogene in thyroid-targeted transgenic mice. Oncogene 18(24):3659-3665.

Daniels, G.H. (1991). Physical examination of the thyroid gland, in *Werner and Ingbar's The Thyroid* (L.E. Braverman and R.D. Utiger, Eds.), 572-577, J.B. Lippincott Company, New York, NY.

De Lellis, R.A. (1995). Biology of Disease: Multiple endocrine neoplasia syndromes revisited. Laboratory Investigation 72(5):494-505.

De Vita, G., Zannini, M., Cirafici, A.M., Melillo, R.M., Di Lauro, R., Fusco, A., and Santoro, M. Expression of the *RET*/PTC1 oncogene impairs the activity of TTF-1 and Pax-8 thyroid transcription factors. Cell Growth and Differentiation 9(1):97-103.

Donghi, R., Sozzi, G., Pierotti, M.A., Biunno, I., Miozzo, M., Fusco, A., Grieco, M., Santoro, M., Vecchio, G., Spurr, N.K., and Della Porta, G. (1989). The oncogene associated with human papillary thyroid carcinoma (PTC) is assigned to chromosome 10 q11-q12 in the same region as multiple endocrine neoplasia type 2A (MEN2A). Oncogene 4(4):521-523.

Downward, J., Yarden, Y., Meyes, E., Scrace, G., Totty, N., Stockwell, P., Ullrich, A., Schlessinger, J., and Waterfield, M.D. (1984). Close similarity of epidermal growth factor receptor and v-*erb*-B oncogene protein sequences. Nature 307:521-527.

Dumont, J.E., Jauniaux, J.C., and Roger, P.P. (1989). The cyclic AMP-mediated stimulation of cell proliferation. Trends in Biochemical Sciences 14:67-71.

Durick, K., Yao, V.J., Borrello, M.G., Bongarzone, I., Pierotti, M.A., and Taylor, S.S. (1995). Tyrosines outside the kinase core and dimerization are required for the mitogenic activity of RET/PTC2. Journal of Biological Chemistry 270(42):24642-24645.

Durick, K., Wu, R.Y., Gill, G.N., and Taylor, S.S. (1996). Mitogenic signaling by RET/PTC2 requires association with enigma via a LIM domain. Journal of Biological Chemistry 271(22):12691-12694.

Durick, K., Gill, G.N., and Taylor, S.S. (1998). Shc and Enigma are both required for mitogenic signaling by RET/PTC2. Molecular and Cellular Biology 18(4):2298-2308.

Edery, P., Lyonnet, S., Mulligan, L.M., Pelet, A., Dow, E., Abel, L., Holder, S., Nihoul-Fékété, C., Ponder, B.A.J., and Munnich, A. (1994). Mutations of the *RET* proto-oncogene in Hirschsprung's disease. Nature 367:378-380.

Eng, C., Clayton, D., Schuffenecker, I., Lenoir, G., Cote, G., Gagel, R.F., van Amstel, H.K., Lips, C.J., Nishisho, I., Takai, S.I., Marsh, D.J., Robinson, B.G., Frank-Raue,

K., Raue, F., Xue, F., Noll, W.W., Romei, C., Pacini, F., Fink, M., Niederle, B., Zedenius, J., Nordenskjold, M., Komminoth, P., Hendy, G.N., Gharib, H., Thibodeau, S.N., Lacroix, A., Frilling, A., Ponder, B.A.J., and Mulligan, L.M. (1996). The relationship between specific *RET* proto-oncogene mutations and disease phenotype in multiple endocrine neoplasia type 2. International RET mutation consortium analysis. Journal of the American Medicine Association 276:1575-1579.

Fox II, S. (1990). Endocrine Glands: Secretion and Actions of Hormones in *Human Physiology* (E.G. Jaffe, Ed.), Chapter 11, William C. Brown Publishers, Dubuque IA.

Fugazzola, L., Pilotti, S., Pinchera, V., Vorontsova, T.V., Mondellini, P., Bongarzone, I., Greco, A., Astakhova, L., Butti, M.G., Demidchik, E.P., et al. (1995). Oncogenic rearrangements of the *RET* proto-oncogene in papillary thyroid carcinomas from children exposed to the Chernobyl nuclear accident. Cancer Research 55:5617-5620.

Fugazzola, L., Pierotti, M.A., Vigano, E., Pacini, F., Vorontsova, T.V., and Bongarzone, I. (1996). Molecular and biochemical analysis of *RET*/PTC4, a novel oncogenic rearrangement between *RET* and *ELE1* genes, in a post-Chernobyl papillary thyroid cancer. Oncogene 13:1093-1097.

Fusco, A., Grieco, M., Santoro, M., Berlingieri, M.T., Pilotti, S., Pierotti, M.A., Della Porta, G., and Vecchio, G. (1987). A new oncogene in human thyroid papillary carcinomas and their lymph-nodal metastases. Nature. 328:170-172.

Gleich, L.L., and Biddinger, P.W. (1999). Pathology of thyroid tumors, in *Carcinoma of the thyroid* (J.T. Johnson and J.L. Gluckman, Eds.), Chapter 4, Isis Medical Media, Incorporated, Oxford UK.

Gluzman, Y. (1981). SV40-transformed simian cells support the replication of early SV40 mutants. Cell 23:175-182.

Grieco, M., Santoro, M., Berlingieri, M.T., Melillo, R.M., Donghi, R., Bongarzone, I., Pierotti, M.A., Della Porta, G., Fusco, A., and Vecchio, G. (1990). PTC is a novel rearranged form of the *ret* proto-oncogene and is frequently detected *in vivo* in human thyroid papillary carcinomas. Cell 60(4):557-563.

Grieco, D., Santoro, M., Dathan, N.A., and Fusco, A. (1995). Activated *RET* oncogene products induce maturation of xenopus oocytes. Oncogene 11:113-117.

Harlow, E., and Lane, D. (1988). Immunoblotting Protocols: Staining the blot for total protein, in *Antibodies: A laboratory manual*, p. 493-496, Cold Spring Harbor Laboratory, Cold Spring Harbor, NY.

Hofstra, R.M.W., Landsvater, R.M., Ceccherini, I., Stulp, R.P., Stelwagen, T., Luo, Y., Pasini, B., Höppener, J.W.M., van Amstel, H.K.P., Romeo, G., Lips, C.J.M., and Buys, C.H.C.M. (1994). A mutation in the *RET* proto-oncogene associated with multiple endocrine neoplasia type 2B and sporadic medullary thyroid carcinoma. Nature 367:375-376.

Ikeda, H., Ishizaka, Y., Tahira, T., Suzuki, T., Onda, M., Sugimura, T., and Nagao, M. (1990). Specific expression of the *ret* proto-oncogene in human neuroblastoma cell lines. Oncogene 5:1291-1296.

Ishiguro Y., Iwashita, T., Murakami, H., Asai, N., Iida, K.I., Goto, H., Hayakawa, T., and Takahashi, M. (1999). The role of amino acids surrounding tyrosine 1062 in Ret in specific binding of the Shc phosphotyrosine-binding domain. Endocrinology 140(9):3992-3998.

Ishizaka, Y., Ochiai, M., Tahira, T., Sugimura, T., and Nagao, M. (1989). Activation of the *ret*-II oncogene without a sequence encoding a transmembrane domain and transforming activity of two *ret*-II oncogene products differing in carboxyl-termini due to alternative splicing. Oncogene 4:789-794.

Ishizaka, Y., Ushijima, T., Sugimura, T., and Nagao, M., (1990). cDNA cloning and characterization of *ret* activated in a human papillary thyroid carcinoma cell line. Biochemical and Biophysical Research Communications 168(2):402-408.

Ishizaka, Y., Takahashi, M., Ushijima, T., Sugimura, T., and Nagao, M. (1991). A high phosphorylation state and increased activity of the TRE motif in the NIH3T3 cell transformant induced by RET^{TPC}. Biochemical and Biophysical Research Communications 179(3):1331-1336.

Ishizaka, Y., Shima, H., Sugimura, T., and Nagao, M. (1992). Detection of phosphorylated ret^{TPC} oncogene product in cytoplasm. Oncogene 7(7):1441-1444.

Iwamoto, T., Taniguchi, M., Asai, N., Ohkusu, K., Nakashima, I., and Takahashi, M. (1993). cDNA cloning of mouse *ret* proto-oncogene and its sequence similarity to the cadherin superfamily. Oncogene 8:1087-1091.

Iwashita, T., Asai, N., Murakami, H., Matsuyama, M., and Takahashi, M. (1996). Identification of tyrosine residues that are essential for transforming activity of the *ret* proto-oncogene with MEN2A or MEN2B mutations. Oncogene 12:481-487.

Jhiang, S.M., and Mazzaferri, E.L. (1994a). The *ret*/PTC oncogene in papillary thyroid carcinoma. Journal of Laboratory and Clinical Medicine 123(3):331-337.

Jhiang, S.M., Smanik, P.A., and Mazzaferri, E.L. (1994b). Development of a single-step duplex RT-PCR detecting different forms of *ret* activation, and identification of the third form of in vivo *ret* activation in human papillary thyroid carcinoma. Cancer Letters 78:69-76.

Jhiang, S.M., Sagartz, J.E., Tong, Q., Parker-Thornberg, J., Capen, C.C., Cho, J.Y., Xing, S., and Ledent, C. (1996). Targeted expression of the *ret*/PTC1 oncogene induces papillary thyroid carcinomas. Endocrinology 137(1):375-378.

Johnson, J.T. (1999). Applied physiology of the thyroid gland, in *Carcinoma of the thyroid* (J.T. Johnson and J.L. Gluckman, Eds.), Chapter 3, Isis Medical Media, Oxford, UK.

Kato, M., Liu, W., Akhand, A.A., Dai, Y., Ohbayashi, M., Tuzuki, T., Suzuki, H., Isobe, K.I., Takahashi, M., and Nakashima, T. (1999). Linkage between melanocytic tumor development and early burst of RET protein expression for tolerance induction in metallothionein-I/*ret* transgenic mouse lines. Oncogene 18:837-842.

Klugbauer, S., Lengfelder, E., Demidchik, E.P., and Rabes, H.M. (1995). High prevalence of *RET* rearrangement in thyroid tumors of children from Belarus after the Chernobyl reactor accident. Oncogene 11:2459-2467.

Klugbauer, S., Lengfelder, E., Demidchik, E.P., and Rabes, H.M. (1996). A new form of *RET* rearrangement in thyroid carcinomas of children after the Chernobyl reactor accident. Oncogene 13:1099-1102.

Klugbauer, S., Demidchik, E.P., Lengfelder, E., and Rabes, H.M. (1998a). Molecular analysis of new subtypes of *ELE/RET* rearrangements, their reciprocal transcripts and breakpoints in papillary thyroid carcinomas of children after Chernobyl. Oncogene 16:671-675.

Klugbauer, S., Demidchik, E.P., Lengfelder, E., and Rabes, H.M. (1998b). Detection of a novel type of *RET* rearrangement (PTC5) in thyroid carcinomas after Chernobyl and analysis of the involved RET-fused gene *RFG5*. Cancer Research 58:198-203.

Klugbauer, S., and Rabes, H.M. (1999). The transcription coactivator *HTIF1* and a related protein are fused to the RET receptor tyrosine kinase in childhood papillary thyroid carcinomas. Oncogene 18(30):4388-4393.

Kohn, L.D., Shimura, H., Shimura, Y., Hidaka, A., Giuliani, C., Napolitano, G., Ohmori, M., Laglia, G., and Saji, M. (1995). The thyrotropin receptor. Vitamins and Hormones 50:287-384.

Kunieda, T., Matsui, M., Nomura, N., and Ishizaki, R. (1991). Cloning of an activated human *ret* gene with a novel 5' sequence fused by DNA rearrangement. Gene 107:323-328.

Kwok, J.B.J., Gardner, E., Warner, J.P., Ponder, B.A.J., and Mulligan, L.M. (1993). Oncogene 8:2575-2582.

Lanzi, C., Borrello, M.G., Bongarzone, I., Migliazza, A., Fusco, A., Grieco, M., Santoro, M., Gambetta, R.A., Zunino, F., Della Porta, G., and Pierotti, M.A. (1992). Identification of the product of two oncogenic rearranged forms of the *RET* proto-oncogene in papillary thyroid carcinomas. Oncogene 7(11):2189-2194.

Liu, X., Vega, Q.C., Decker, R.A., Pandey, A., Worby, C.A., and Dixon, J.E. (1996). Oncogenic RET receptors display different autophosphorylation sites and substrate binding specificities. Journal of Biological Chemistry 271(10):5309-5312.

Lorenzo, M.J., Eng, C., Mulligan, L.M., Stonehouse, T.J., Healey, C.S., Ponder, B.A., Smith, D.P. (1995). Multiple mRNA isoforms of the human *RET* proto-oncogene generated by alternate splicing. Oncogene 10(7):1377-1383.

Lorenzo, M.J., Gish, G.D., Houghton, C., Stonehouse, T.J., Pawson, T., Ponder, B.A.J., and Smith, D.P. (1997). *RET* alternate splicing influences the interaction of activated RET with the SH2 and PTB domains of Shc, and the SH2 domain of Grb2. Oncogene 14(7):763-771.

Marcos-Gutierrez, C.V., Wilson, S.W., Holder, N., and Pachnis, V. (1997). The zebrafish homologue of the ret receptor and its pattern of expression during embryogenesis. Oncogene 14(8):879-889.

Marshall, G.M., Peaston, A.E., Hocker, J.E., Smith, S.A., Hansford, L.M., Tobias, V., Norris, M.D., Haber, M., Smith, D.P., Lorenzo, M.J., Ponder, B.A.J., and Hancock, J.F. (1997). Expression of multiple endocrine neoplasia 2B RET in neuroblastoma cells alters cell adhesion *in vitro*, enhances metastatic behavior *in vivo*, and activates Jun Kinase. Cancer Research 57(23):5399-5405.

Martin-Zanca, D., Hughes, S.H., and Barbacid, M. (1986). A human oncogene formed by the fusion of truncated tropomyosin and protein tyrosine kinase sequences. Nature 319:743-748.

Mazzaferri, E.L. (1991). Carcinoma of Follicular Epithelium: Radioiodine and other treatments and outcomes, in *Werner and Ingbar's The Thyroid* (L.E. Braverman and R.D. Utiger, Eds.), 1138-1165, J.B. Lippincott Company, New York, NY.

McDermott, M. (2000). Thyroid cancer: DNA ploidy, tumor markers, and cancer-causing genes in *Thyroid Cancer: a Comprehensive Guide to Clinical Management* (Wartofsky, L., Ed.), Chapter 50, Humana Press, Totowa, NJ.

Melillo, R.M., Barone, M.V., Lupoli, G., Cirafici, A.M., Carlomagno, F., Visconti, R., Matoskova, B., Di Fiore, P.P., Vecchio, G., Fusco, A., and Santoro, M. (1999). Ret-mediated mitogenesis requires Src kinase activity. Cancer Research 59(5):1120-1126.

Michiels, F.M., Chappuis, S., Caillou, B., Pasini, A., Talbot, M., Monier, R., Lenoir, G.M., Feunteun, J., and Billaud, M. (1997). Development of medullary thyroid carcinoma in transgenic mice expressing the *RET* protooncogene altered by a multiple endocrine neoplasia type 2A mutation. Proceedings of the National Academy of Science 94:3330-3335.

Minoletti, F., Butti, M.G., Coronelli, S., Miozzo, M., Sozzi, G., Pilotti, S., Tunnacliffe, A., Pierotti, M.A., Bongarzone, I. (1994). The two genes generating RET/PTC3 are localized in chromosomal bands 10q11.2. Genes, Chromosomes, & Cancer 11(1):51-57.

Miyazaki, K., Asai, N., Iwashita, T., Taniguchi, M., Isomura, T., Funahashi, H., Takagi, H., Matsuyama, M., and Takahashi, M. (1993). Tyrosine kinase activity of the *ret* proto-oncogene products in vivo. Biochemical and Biophysical Research Communications 193:565-570.

Mulligan, L., Kwok, J.B.J., Healey, C.S., Elsdon, M.J., Eng, C., Gardner, E., Love, D.R., Mole, S.E., Moore, J.K., Papi, L., Ponder, M.A., Telenius, H., Tunnacliffe, A., and Ponder, B.A.J. (1993). Germ-line mutations of the *RET* proto-oncogene in multiple endocrine neoplasia type 2A. Nature 363:458-460.

Murakami, H., Iwashita, T., Asai, N., Iwata, Y., Narumiya, S., and Takahashi, M. (1999a). Rho-dependent and -independent tyrosine phosphorylation of focal adhesion kinase, paxillin and $p130^{Cas}$ mediated by Ret kinase. Oncogene 18(11):1975-1982.

Murakami, H., Iwashita, T., Asai, N., Shimono, Y., Iwata, Y., Kawai, K., and Takahashi, M. (1999b). Enhanced phosphatidylinositol 3-kinase activity and high phosphorylation state of its downstream signalling molecules mediated by ret with the MEN2B mutation. Biochemical and Biophysical Research Communications 262(1):68-75.

Myers, S.M., Eng, C., Ponder, B.A., and Mulligan, L.M. (1995). Characterization of RET proto-oncogene 3' splicing variants and polyadenylation sites: a novel C-terminus for RET. Oncogene 11:2039-2045.

Nakata, T., Kitamura, Y., Shimizu, K., Tanaka, S., Fujimori, M., Yokoyama, S., Ito, K., and Emi, M. (1999). Fusion of a novel gene, *ELKS*, to *RET* due to translocation t(10:12)(q11;p13) in a papillary thyroid carcinoma. Genes, Chromosomes and Cancer 25:97-103.

Nikiforov, Y.E., Rowland, J.M., Bove, K.E., Monforte-Munoz, H., and Fagin, J.A., (1997). Distinct pattern of *ret* oncogene rearrangements in morphological variants of radiation-induced and sporadic thyroid papillary carcinomas in children. Cancer Research 57:1690-1694.

Ohiwa, M., Murakami, H., Iwashita, T., Asai, N., Iwata, Y., Imai, T., Funahashi, H., Takagi, H., and Takahashi, M. (1997). Characterization of Ret-Shc-Grb2 complex induced by GDNF, MEN2A and MEN2B mutations. Biochemical and Biophysical Research Communications 237(3):747-751.

Ohno, M., Zannini, M., Levy, O., Carrasco, N., and Di Lauro, R. (1999). The paired-domain transcription factor Pax8 binds to the upstream enhancer of the rat sodium/iodide symporter gene and participates in both thyroid-specific and cyclic-AMP-dependent transcription. Molecular and Cellular Biology 19(3):2051-2060.

Pachnis, V., Mankoo, B., and Costantini, F. (1993). Expression of the c-*ret* proto-oncogene during mouse embryogenesis. Development 119:1005-1017.

Pacini, F., Elisei, R., Romei, C., and Pinchera, A. (2000). *RET* proto-oncogene mutations in thyroid carcinomas: clinical relevance. Journal of Endocrinological Investigation 23:328-338.

Park, M., Dean, M., Cooper, C.S., Schmidt, M., O'Brien, S.J., Blair, D.G., and Vande Woude, G.F. (1986). Mechanism of *met* oncogene activation. Cell 45:895-904.

Parker, S.L., Tong, T., Bolder, S., and Wingo, P.A. (1996). Cancer statistics, 1996. CA: A Cancer Journal for Clinicians 46:5-27.

Pasini, B., Hofstra, R.M., Yin, L., Bocciardi, R., Santamaria, G., Grootscholten, P.M., Ceccherini, I., Patrone, G., Priolo, M., Buys, C.H., and Romeo, G. (1995). The physical map of the *RET* proto-oncogene. Oncogene 11:1737-1743.

Pierotti, M.A., Santoro, M., Jenkins, R.B., Sozzi, G., Bongarzone, I., Grieco, M., Monzini, M., Miozzi, M., Herrmann, M.A., Fusco, A., Hay, I.D., Della Porta, G., and Vecchio, G. (1992). Characterization of an inversion on the long arm of chromosome 10 juxtaposing D10S170 and *RET* and creating the oncogenic sequence *RET*/PTC. Proceedings of the National Academy of Science 89(5):1616-1620.

Pierotti, M.A., Vigneri, P., and Bongarzone, I. (1998). Rearrangements of *RET* and *NTRK1* tyrosine kinase receptors in papillary thyroid carcinomas. Recent Results in Cancer Research 154:237-247.

Portella, G., Salvatore, D., Botti, G., Cerrato, A., Zhang, L., Mineo, A., Chiapetta, G., Santelli, G., Pozzi, L., Vecchio, G., Fusco, A., and Santoro, M. (1996). Development of mammary and cutaneous gland tumors in transgenic mice carrying the *RET*/PTC1 oncogene. Oncogene 13(9):2021-2026.

Ries, L.A.G., Kosary, C.L., Hankey, B.F., Miller, B.A., Clegg, L., and Edwards, B.K. (Eds.) (1999). SEER Cancer Statistics Review, 1973-1996, National Cancer Institute, Bethesda, MD.

Robertson, K., and Mason, I. (1997). The GDNF-RET signalling partnership. Trends in Genetics 13(1):1-3.

Romeo, G., Ronchetto, P., Luo, Y., Barone, V., Seri, M., Ceccherini, I., Pasini, B., Bocciardi, R., Lerone, M., Kääriäinen, H., and Martucciello, G. (1994). Point mutations affecting the tyrosine kinase domain of the *RET* proto-oncogene in Hirschsprung's disease. Nature 367:377-378.

Rosenthal, A. (1999). The GDNF protein family: Gene ablation studies reveal what they really do and how. Neuron 22:201-207.

Sagartz, J.E., Jhiang, S.M., Tong, Q., and Capen, C.C. (1997). Thyroid-stimulating hormone promotes growth of thyroid carcinomas in transgenic mice with targeted expression of the *ret*/PTC1 oncogene. Laboratory Investigation 76(3):307-318.

Santoro, M., Melillo, R.M., Grieco, M., Berlingieri, M.T., Vecchio, G., and Fusco, A. (1993). The *TRK* and *RET* tyrosine kinase oncogenes cooperate with *ras* in the neoplastic transformation of a rat thyroid epithelial cell line. Cell Growth and Differentiation. 4:77-84.

Santoro, M., Dathan, N.A., Berlingieri, M.T., Bongarzone, I., Paulin, C., Grieco, M., Pierotti, M.A., Vecchio, G., and Fusco, A. (1994a). Molecular characterization of *RET*/PTC3; a novel rearranged version of the *RET* proto-oncogene in a human thyroid papillary carcinoma. Oncogene 9:509-516.

Santoro, M., Wong, W.T., Aroca, P., Santos, E., Matoskova, B., Grieco, M., Fusco, A., and Di Fiore, P.P. (1994b). An epidermal growth factor receptor/*ret* chimera generates mitogenic and transforming signals: evidence for a *ret*-specific signaling pathway. Molecular and Cellular Biology 14(1):663-675.

Santoro, M., Carlomagno, F. Romano, A., Bottaro, D.P., Dathan, N.A., Grieco, M., Fusco, A., Vecchio, G., Matoskova, B., Kraus, M.H., and Di Fiore, P.P. (1995). Activation of *RET* as a dominant transforming gene by germline mutations of MEN2A and MEN2B. Science 267:381-383.

Santoro, M., Chiappetta, G., Cerrato, A., Salvatore, D., Zhang, L., Manzo, G., Picone, A., Portella, G., Santelli, G., Vecchio, G., and Fusco, A. (1996). Development of thyroid papillary carcinomas secondary to tissue-specific expression of the *RET*/PTC1 oncogene in transgenic mice. Oncogene 12(8):1821-1826.

Schlessinger, J., and Ullrich, A. (1992). Growth factor signaling by receptor tyrosine kinases. Neuron 9:383-391.

Schuchardt, A., D'Agati, V., Larsson-Blomberg, L., Costantini, F., and Pachnis, V. (1994). Defects in the kidney and enteric nervous system of mice lacking the tyrosine kinase receptor Ret. Nature 367:380-383.

Schuchardt, A., Srinivas, S., Pachnis, V., and Costantini, F. (1995). Isolation and characterization of a chicken homolog of the c-*ret* proto-oncogene. Oncogene 10(4):641-649.

Segouffin-Cariou, C., and Billaud, M. (2000). Transforming ability of MEN2A-RET requires activation of the phosphatidylinositol 3-kinase/AKT signaling pathway. Journal of Biological Chemistry 275(5):3568-3576.

Smith, D.P., Houghton, C., and Ponder, B.A.J. (1997). Germline mutation of RET codon 883 in two cases of de novo MEN 2B. Oncogene 15(10):1213-1217.

Smith-Hicks, C.L., Sizer, K.C., Powers, J.F., Tischler, A.S., Costantini, F. (2000). C-cell hyperplasia, pheochromocytoma and sympathoadrenal malformation in a mouse model of multiple endocrine neoplasia type 2B. European Molecular Biology Organization Journal 19(4):612-622.

Songyang, Z., Carraway III, K.L., Eck, M.J., Harrison, S.C., Feldman, R.A., Mohammadi, M., Schlessinger, J., Hubbard, S.R., Smith, D.P., Eng, C., Lorenzo, M.J., Ponder, B.A.J., Mayer, B.J., and Cantley, L.C. (1995). Catalytic specificity of protein-tyrosine kinases is critical for selective signalling. Nature 373:536-539.

Sozzi, G., Pierotti, M.A., Miozzo, M., Donghi, R., Radice, P., De Benedetti, V., Grieco, M., Santoro, M., Fusco, A., Vecchio, G., Mathew, C.G.P., Ponder, B.A.J., Spurr, N.K., and Della Porta, G. (1991). Refined localization to contiguous regions on chromosome 10q of the two genes (*H4* and *RET*) that form the oncogenic sequence *PTC*. Oncogene 6(2):339-342.

Sozzi, G., Bongarzone, I., Miozzo, M., Borrello, M.G., Blutti, M.G., Pilotti, S., Della Porta. G, and Pierotti, M.A. (1994). A t(10;17) translocation creates the *RET*/PTC2 chimeric transforming sequence in papillary thyroid carcinoma. Genes, Chromosomes, and Cancer 9(4):244-250.

Sugaya, R., Ishimaru, S., Hosoya, T., Saigo, K., and Emori, Y. (1994). A Drosophila homolog of human proto-oncogene *ret* transiently expressed in embryonic neuronal precursor cells including neuroblasts and CNS cells. Mechanisms of Development 45(2):139-145.

Sweetser, D.A., Froelick, G.J., Matsumoto, A.M., Kafer, K.E., Marck, B., Palmiter, R.D., and Kapur, R.P. (1999). Ganglioneuromas and renal anomalies are induced by activated RET(MEN2B) in transgenic mice. Oncogene. 18(4):877-886.

Tahira, T., Ishizaka, Y., Itoh, F., Sugimura, T., and Nagao, M. (1990). Characterization of *ret* proto-oncogene mRNAs encoding two isoforms of the protein product in a human neuroblastoma cell line. Oncogene 5(1):97-102.

Takahashi, M., Ritz, J., and Cooper, G.M. (1985). Activation of a novel human transforming gene, *ret*, by DNA rearrangement. Cell 42:581-588.

Takahashi, M., and Cooper, G.M. (1987). *ret* transforming gene encodes a fusion protein homologous to tyrosine kinases. Molecular and Cellular Biology 7(4):1378-1385.

Takahashi, M., Buma, Y., Iwamoto, T., Inaguma, Y., Ikeda, H., and Hiai, H. (1988). Cloning and expression of the *ret* proto-oncogene encoding a tyrosine kinase with two potential transmembrane domains. Oncogene 3(5): 571-578.

Takahashi, M., Buma, Y., and Taniguchi, M. (1991). Identification of the *ret* proto-oncogene products in neuroblastoma and leukemia cells. Oncogene 6:297-301.

Taurog, A. (1991). Hormone synthesis: thyroid iodine metabolism, in *Werner and Ingbar's The Thyroid* (L.E. Braverman and R.D. Utiger, Eds.), 51-97, J.B. Lippincott Company, New York, NY.

Thomas, G.A., and Williams, E.D. (1991). Evidence and possible mechanisms of non-genotoxic carcinogenesis in the rodent thyroid. Mutation Research 248:357-370.

Tong, Q., Li, Y., Smanik, P.A., Fithian, L.J., Xing, S., Mazzaferri, E.L, and Jhiang, S.M. (1995). Characterization of the promoter region and oligomerization domain of

H4 (D10S170), a gene frequently rearranged with the *ret* proto-oncogene. Oncogene 10(9):1781-1787.

Tong, Q., Xing, S., and Jhiang, S.M. (1997). Leucine zipper-mediated dimerization is essential for the PTC1 oncogenic activity. Journal of Biological Chemistry 272(14):9043-9047.

Tsuzuki, T., Takahashi, M., Asai, N., Iwashita, T., Matsuyama, M., and Asai, J. (1995). Spatial and temporal expression of the *ret* proto-oncogene product in embryonic, infant and adult rat tissues. Oncogene 10(1):191-198.

Uchino, S. (2000). Genetic basis of medullary thyroid carcinoma, in *Thyroid Cancer: diagnosis and treatment* (Clark, O.H., and Noguchi, S., Eds.), Chapter 18, Quality Medical Publishing, St. Louis, MS.

van Puijenbroek, A.A.F.L., van Weering, D.H.J., van den Brink, C.E., Bos, J.L., van der Saag, P.T., de Laat, S.W., and den Hertog, J. (1997). Cell scattering of SK-N-MC neuroepithelioma cells in response to Ret and FGF receptor tyrosine kinase activation is correlated with sustained ERK2 activation. Oncogene 14(10):1147-1157.

van Weering, D.H.J., Medema, J.P., van Puijenbroek, A., Burgering, B.M.T., Baas, P.D., and Bos, J.L. (1995). Ret receptor tyrosine kinase activates extracellular signal-regulated kinase 2 in SK-N-MC cells. Oncogene 11(11):2207-2214.

van Weering, D.H.J., and Bos, J.L. (1997). Glial cell line-derived neurotrophic factor induces Ret-mediated lamellipodia formation. Journal of Biological Chemistry 272(1):249-254.

Villione, G., Veneziani, B.M., Picone, R., De Amicis, R., Perrotti, N., and Tramontano, D. (1993). In the thyroid cells proliferation, differentiated and metabolic functions are under the control of different steps of the cyclic AMP cascade. Molecular and Cellular Endocrinology 95:85-93.

Wartofsky, L. (2000). Papillary Carcinoma: Clinical aspects in *Thyroid Cancer: a comprehensive guide to clinical management* (Wartofsky, L., Ed.), Chapter 16, Humana Press, Totowa, NJ.

Widenfalk, J., Widmer, H.R., and Spenger, C. (1999). *GDNF, RET* and *GFR*α1-3 mRNA expression in the developing human spinal cord and ganglia. Neuroreport 10(7):1433-1439.

Worby, C.A., Vega, Q.C., Zhao, Y., Chao, H.H.J., Seasholtz, A.F., Dixon, J.E. (1996). Glial cell line-derived neurotrophic factor signals through the RET receptor and

activates mitogen-activated protein kinase. Journal of Biological Chemistry 271(39):23619-23622.

Wynford-Thomas, D., Stringer, B.M.J., and Williams, E.D. (1982). Dissociation of growth and function in the rat thyroid during prolonged goitrogen administration. Acta Endocrinologica 101:210-216.

Xing, S., Smanik, P.A., Oglesbee, M.J., Trosko, J.E., Mazzaferri, E.L., and Jhiang, S.M. (1996). Characterization of *ret* oncogenic activation in MEN2 inherited cancer syndromes. Endocrinology 137(5):1512-1519.

Xing, S., Furminger, T.L., Tong, Q., and Jhiang, S.M. (1998). Signal transduction pathways activated by RET oncoproteins in PC12 pheochromocytoma cells. Journal of Biological Chemistry 273(9):4909-4914.